INFORMATION TO USERS

This manuscript has been reproduced from the microfilm master. UMI films the text directly from the original or copy submitted. Thus, some thesis and dissertation copies are in typewriter face, while others may be from any type of computer printer.

The quality of this reproduction is dependent upon the quality of the copy submitted. Broken or indistinct print, colored or poor quality illustrations and photographs, print bleedthrough, substandard margins, and improper alignment can adversely affect reproduction.

In the unlikely event that the author did not send UMI a complete manuscript and there are missing pages, these will be noted. Also, if unauthorized copyright material had to be removed, a note will indicate the deletion.

Oversize materials (e.g., maps, drawings, charts) are reproduced by sectioning the original, beginning at the upper left-hand corner and continuing from left to right in equal sections with small overlaps. Each original is also photographed in one exposure and is included in reduced form at the back of the book.

Photographs included in the original manuscript have been reproduced xerographically in this copy. Higher quality 6" x 9" black and white photographic prints are available for any photographs or illustrations appearing in this copy for an additional charge. Contact UMI directly to order.

UMI

A Bell & Howell Information Company
300 North Zeeb Road, Ann Arbor MI 48106-1346 USA
313/761-4700 800/521-0600

VORTEX MOTION AND THE GEOMETRIC PHASE

by

Banavara Narayanamurthy Shashikanth

A Dissertation Presented to the
FACULTY OF THE GRADUATE SCHOOL
UNIVERSITY OF SOUTHERN CALIFORNIA
In Partial Fulfillment of the
Requirements for the Degree
DOCTOR OF PHILOSOPHY
(Aerospace Engineering)

May 1998

UNIVERSITY OF SOUTHERN CALIFORNIA
THE GRADUATE SCHOOL
UNIVERSITY PARK
LOS ANGELES, CALIFORNIA 90007

This dissertation, written by

BANAVARA N. SHASHIKANTH

under the direction of his..... Dissertation Committee, and approved by all its members, has been presented to and accepted by The Graduate School, in partial fulfillment of requirements for the degree of

DOCTOR OF PHILOSOPHY

Dean of Graduate Studies

Date January 30, 1998

DISSERTATION COMMITTEE

Chairperson

To my parents and my brother.

Acknowledgements

I would like to thank my thesis advisor Paul K. Newton for introducing me to geometric phases and for his guidance, enthusiasm and several keen insights during this work. His informal style and friendly personality made working with him a pleasure. His advice and help on several matters, (not all related to phases!), is deeply appreciated. My thanks also go to the the following faculty members: Fred Browand, Eckart Meiburg, Larry Redekopp, Joe Kunc, Mike Gruntman for assistance at various stages of my stay here, the first three for also serving on my committee, and to Firdaus Udwadia for serving as the external member on my committee. Special thanks to Jerry Marsden at Caltech for his interest in this work, in particular for serving as an 'unofficial' member on my qualifying exam committee.

I would also like to thank the AE office staff, past and present, in particular, Alice, Elsie, Marietta, Mai and Connie, for their always helpful and efficient services, Denis Plocher for assistance with computers, my fellow toilers on the Ph.D. path Mark Michaelian, Ching-yao, Peije, Hany, Dave Lim, Paul Taniguchi, Bogdan, Meng, Shari and Fred Lutfy for their support and good cheer, and last, but certainly not the least, Nitin, Ranga, Raju, Ravi, Shudeish, Bud and Deepak for keeping memories of the 'Janmabhoomi' alive and much more.

Contents

List Of Figures

Abstract

This dissertation demonstrates the existense of a non-trivial phase change in adiabatic evolutions of certain vortex configurations in 2-D incompressible, inviscid flows. The phase change is identified with the, by now well-documented, geometric phase (Berry's phase, Hannay angle) occuring in various classical and quantum systems. The calculation of the phase is performed using multi-scale asymptotics. In the geometric interpretation, the phase is shown to be the holonomy of a connection on an appropriately defined fiber bundle. Three canonical point vortex configurations in which the phase appears are first discussed. The planar configurations are a three-vortex (and a canonically similar four-vortex) problem, a vortex in a circle problem, and a model of a mixing layer flow in which an infinite number of vortices undergo subharmonic pairing. The phase appears as an $O(1)$ term in the angle variable of a pair of vortices, one of which could be of zero strength i.e. a passive particle in the flow, at the end of one long time period of an appropriately defined periodic 'slow' motion. The phase term is of the form $\theta_g = f(\Gamma_k, C)\cos 2\theta(0)$, where f is a function of the vortex strengths Γ_k and the periodic vortex orbit C, and $\theta(0)$ is the initial condition. With a view to applications, it is then shown that the length formula for the long time growth of a passive interface in these flows inherits the geometric phase effect and shows the characteristic splitting into a 'dynamic' part and a 'geometric' part. The geometric part depends on the geometric phase θ_g for a particle in the flow and is given by $L_g = -\int_{\xi_A}^{\xi_B} d(\xi\theta_g)$, where ξ parametrizes the interface curve joining particles A and B at $t = 0$. Finally, the phase calculation for a system of two elliptical vortex patches in the Melander, Zabusky and Styczek model is presented. The phase appears in the orientation angle of each elliptical patch and is of the form $\theta_g = f(\Gamma_k, \lambda(0))\cos 2\theta(0)$, where f depends on the patch strengths Γ_k and initial aspect ratio $\lambda(0)$ of the patch.

Chapter 1

Introduction to geometric phases

1.1 History

In 1984, Berry [11] investigated the evolution of a quantum system whose Hamiltonian depends on external parameters which are varied slowly in a closed loop. The adiabatic theorem in quantum mechanics [41] states that for (infinitely) slow changes the system wave function, whose evolution is described by the time-dependent Schrödinger equation is, instantaneously, in an eigenstate of the Hamiltonian (for the values of the external parameters at that instant). Hence, at the end of the cycle when the parameters return to their original values the wave function should return to the eigenstate it started in, except for a possible change in phase. This phase factor was long thought of as being only a dynamic phase factor describing the time effect of the cycle. However, Berry showed that this was not the only phase contribution; there also is a geometric part given by a circuit integral in parameter space and is, thus, independent of the dynamics along the circuit (provided that it is still slow enough for the adiabatic theorem to hold). This phase factor is now commonly referred to as Berry's phase and depends only on the geometry of the closed loop in parameter space.

Hannay [37] subsequently studied the classical analogue of Berry's phase, now commonly referred to as Hannay's angle, by considering the slow evolution of integrable Hamiltonian systems. For such systems there exist, in principle, a set of canonical variables called action and angle variables [27]. The action variables are invariants of the system and in periodic systems represent the area of the closed trajectory of the system in phase space. The conjugate angle variables evolve linearly in time at the system frequencies. Hannay studied integrable systems whose Hamiltonian function depends on certain external parameters. If these parameters do not change in time the Hamiltonian is time-independent and is a conserved quantity along the solutions of the system. He then analysed 'the fate of the angle variables' in the case when the parameters change slowly in a closed loop. Instantaneously, the system evolves at some frequency that depends on the parameter values at that instant. Intuitively, therefore, one would expect that the total angle change at the end of the cycle is just the time integral of the instantaneous evolution over the

period of the cycle. Hannay showed, however, that this need not be true. There could be an extra angle change that, like in the quantum case, depends solely on the circuit in parameter space of the closed loop.

Following this, Berry [12] obtained a semi-classical relationship between his phase and Hannay's angle. Aharonov and Anandan [1] then showed that the geometric phase could be extracted from the total phase change for any general cyclic evolution, not necessarily adiabatic, of a quantum system. Berry and Hannay [16] investigated the classical analogue and found a similar geometric phase for a general non-adiabatic cyclic change. Golin and co-workers wrote a series of papers dealing with different issues related to the Hannay angles in classical Hamiltonian systems--the existense of Hannay angles for smooth systems with one degree-of-freedom [28], Hannay angles in the presence of symmetries [32] and measurement of Hannay angles [33] (see also Golin [29], Golin, Knauf and Marmi [30, 31]).

In a more geometric vein, Simon [90], commenting on Berry's earlier paper, showed that his phase can be interpreted as the holonomy associated with a connection on a line bundle over the parameter space. The adiabatic evolution provides a path (the connection) along which the wave function's initial eigenvector is transported. Anandan and Stodolsky [3] showed that the interpretation can be extended to the holonomy in a vector bundle by considering all the eigenspaces of the wave function. Marsden, Montgomery and Ratiu [52, 53], Marsden and Ratiu [55], Montgomery[64] and Golin, Knauf and Marmi [30] develop these concepts further, especially in the classical case and their extensions to non-integrable systems. They show that averaging defines a connection which can be related to Ehresmann and Cartan connections on fiber bundles [20, 94] and that the Hannay angle is the holonomy of this connection. Non-integrable classical systems have also been examined by Robbins and Berry [78]. Levi [49] examines some simple rigid body motions which have geometric phases and their relation to parallel transport.

In other work, Montgomery examining the rotation of a free rigid body and the gravitational three-body problem [66, 67] has shown how exact formulae for angle changes in these problems can be derived which show the characteristic splitting into a 'dynamic phase' and a 'geometric phase.' Alber and Marsden [2] have shown how the phase shift formula for soliton interactions can be interpreted as a geometric phase. R. Newton [71] derived the Berry phase formula associated with Schrödinger operators with a continuous spectrum and relates it to the well known S matrix from scattering theory. In a series of papers [85, 95, 84], Shapere and Wilczek have shown how a geometric phase arises in the context of self-propulsion of micro-organisms at very low Reynolds number regimes. This point of view is closely related to recent developments of the geometric phase in the context of control theory, which is discussed in [54]. Finally, Marsden and Scheurle [56] use the geometric phase idea on mechanical systems with symmetries to show how symmetric patterns in the phase space of the system can be brought out that would not otherwise be seen (see also [57]). By now, there are several sources where one can get an overview of the various interpretations and applications of the geometric phase in various contexts. A history of the phase

is given by Berry in [15] where he talks about how his phase factor had been 'anticipated' in the works of other scientists--in particular that of S. M. Ryotov, V. V. Vladimirskii, S. Pancharatnam, R. Y. Chiao, A. Tomita and Y. S. Wu in the fields of geometric optics and polarization of light (see also Berry [14]). The collection of papers reprinted in [86] gives a nice introduction to the important papers on the subject before 1989, while [102] gives an overview with the focus on quantum and chemical applications.

1.2 Description

An oft quoted example [12, 37, 53, 55, 28] of a classical system that exhibits a geometric phase is that of the 'rotated rotator' or a particle on a hoop (see Figure 1.1). A bead slides frictionlessly over a closed non-circular hoop of wire whose plane is perpendicular to the local gravitational field. The hoop is made to slowly rotate in its plane in an arbitrary fashion. At the end of one full rotation of the loop the bead is not where it would have been had the loop been stationary, but differs by an amount that *cannot* be made arbitrarily small by slower rotations of the hoop. Moreover, this change can be shown to depend only on the area enclosed by the hoop and its perimeter i.e. purely geometric quantities.

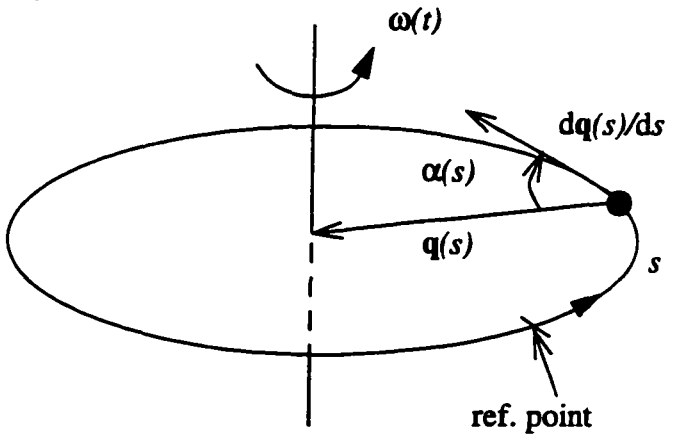

Figure 1.1: A particle sliding frictionlessly around a slowly rotating (horizontal) non-circular hoop of wire experiences a geometric shift in the distance variable s at the end of one period of rotation of the hoop.

To show how this phase arises, we give here a brief version of the treatment by Marsden, Montgomery and Ratiu [55]. Fix a point on the hoop and let the distance of the bead from this point measured along the perimeter of the loop be s. When the hoop is not rotating,

$$\ddot{s} = 0.$$

Now, rotate the hoop slowly around the vertical axis at a rate $\omega(t)$ which need not be a constant. Let $q(s) = \mid \mathbf{q}(s) \mid$, then the equation of the bead (in an inertial frame) is:

$$\ddot{s} = \omega^2 q q' cos(\alpha) - \dot{\omega} q sin(\alpha)$$

(for details see the cited reference), where the prime denotes differentiation with respect to s. If the initial position and velocity of the bead are $s_0, \dot{s_0}$ then integrating the above gives:

$$s(t) = s_0 + \dot{s_0} t + \int_0^t (t-u) \left\{ \omega^2(u) q(s(u)) q'(s(u)) cos(\alpha(s(u))) - \dot{\omega}(u) q(s(u)) sin(\alpha(s(u))) \right\} du.$$

For small ω and $\dot{\omega}$, the bead goes around the hoop many times before there is a significant angular traverse by the hoop; hence, one can replace the s-dependent quantities by their averages around the hoop and get the approximate equation:

$$s(t) \approx s_0 + \dot{s_0} t + \int_0^t (t-u) \left\{ \omega^2(u) \frac{1}{L} \int_0^L q(s) q'(s) cos(\alpha(s)) ds - \dot{\omega}(u) \frac{1}{L} \int_0^L q(s) sin(\alpha(s)) ds \right\} du.$$

where L is the perimeter of the hoop. The first integral within the braces vanishes and the second integral has the value $2A$ where A is the area enclosed by the hoop. The time integral can then be integrated by parts from 0 to T, where T is the time needed for the hoop to make one complete revolution, to give the final result (where we have assumed $\omega(0) = 0$):

$$s(T) \approx s_0 + \dot{s_0} T - \frac{4\pi A}{L}. \tag{1.1}$$

Recognizing the first two terms on the right hand side as the evolution if the hoop were not rotating, the third term is identified as the geometric phase for this problem.[1] Notice that it is independent of T and that it depends on purely geometric quantities, the perimeter and the area enclosed by the hoop.

To understand most simply why the geometric phase, when it arises in the adiabatic limit of a slow change[2] of external parameters, is 'geometric,' it is useful to view it in a general way as follows. Consider the parameter-dependent evolution of some (real) variable $q(t, \mathbf{X}(\epsilon t))$ of any dynamical system, where $\mathbf{X}(\epsilon t)$ denotes the (real) vector of external parameters. Here ϵ measures the rate at which the parameters are varied. The change in the variable value at the end of time

[1] Strictly speaking, the term phase should be reserved for the shift in the Hamiltonian angle variable corresponding to the above shift in s.

[2] In the limit of an infinitely slow change.

$T = 1/\epsilon$ in which one or more of the parameters are varied in a closed loop ($\mathbf{X}(1) = \mathbf{X}(0)$) will be given by :

$$\int_{q(0)}^{q(T)} dq(t, \mathbf{X}(\epsilon t)) = \int_0^T \frac{\partial q(t, \mathbf{X}(\epsilon t))}{\partial t} dt + \oint \frac{\partial q(t, \mathbf{X})}{\partial \mathbf{X}} \cdot d\mathbf{X}. \tag{1.2}$$

The first integral measures the cumulative effect of 'local' changes due to the instantaneous evolution and is identified as the dynamic phase of the system.[3] The second integral is over the closed loop in parameter space. If the integrand is bounded for all time then this integral is finite. In general, it will be a function of T and hence ϵ, and may converge to a non-zero limiting value as $\epsilon \to 0$. To see why the contour integral in parameter space, if it converges, can give rise to a non-zero limit, we can rewrite it as a time integral i.e.

$$\oint \frac{\partial q(t, \mathbf{X})}{\partial \mathbf{X}} \cdot d\mathbf{X} = \int_0^T \dot{\mathbf{X}}(\epsilon t) \cdot \frac{\partial q(t, \mathbf{X}(\epsilon t))}{\partial \mathbf{X}(\epsilon t)} dt, \tag{1.3}$$

where $\dot{\mathbf{X}}(\epsilon t)$ denotes the slow rate at which the parameters are changed. As $\epsilon \to 0$, $\dot{\mathbf{X}}(\epsilon t) \to 0$ and $T \longrightarrow \infty$. If $\frac{\partial q(t, \mathbf{X})}{\partial \mathbf{X}}$ is bounded for all times then the integrand decreases as the range of integration becomes larger. There is no reason, a priori, to believe that in the limit of vanishing ϵ the integral is zero. These quantities can approach their limits in such a way as to give a non-zero result.

The geometric phase is this non-zero limit of the ϵ dependent contour integral. In the adiabatic limit, the ϵ dependency is removed and the integral becomes a function solely of the closed loop in parameter space, i.e. a purely geometric quantity. For small ϵ, the integral can thus be viewed as an $O(1)$ term (the geometric phase), plus $O(\epsilon)$ corrections. Assuming the limit and integration process can be interchanged, the geometric nature of the phase is evident even more clearly by replacing the limit of the contour integral in (1.2) with the contour integral of the integrand as $\epsilon \to 0$. This limit, if it exists, then defines a mapping from the parameter space to the real line. The geometric phase can then be viewed as the contour integral of a 1-form defined on the parameter space. If the contour encloses a region of the parameter manifold then the geometric phase, using Stokes theorem, can also be viewed as the integral of a 2-form defined over the region enclosed by the contour.

This argument is similar to the one given by Hannay in his paper [37] for integrable, parameter-dependent Hamiltonian systems. Hannay looked at integrable Hamiltonians of the form $H(p, q, \mathbf{R})$ where $\mathbf{R}$ is a vector of external parameters. For a fixed or 'frozen' value of the parameters, the phase space of the (n-dimensional) system is diffeomorphic to the n-torus. In principle, there then exists a set of canonical coordinates for this torus called action and angle coordinates: $I(\mathbf{R})$

[3] We stick to the standard terminology and use 'phase' though for the sake of our argument q could be any (real) variable not necessarily an angle variable.

and $\theta(t, \mathbf{R})$, respectively, such that the Hamiltonian $H(I(\mathbf{R}), \mathbf{R})$ depends only on the actions. If the parameters are not varied, then the system equations are

$$\begin{aligned} \dot{I} &= -\frac{\partial H}{\partial \theta} = 0 \\ \dot{\theta} &= \frac{\partial H}{\partial I} = constant. \end{aligned}$$

If the parameters $\mathbf{R}(t)$ are varied, then the actions are, in general, no longer invariant. The equations of motion are

$$\begin{aligned} \dot{I} &= \dot{\mathbf{R}}(t) \cdot \frac{\partial I}{\partial \mathbf{R}(t)} \\ \dot{\theta} &= \frac{\partial H}{\partial I} + \dot{\mathbf{R}}(t) \cdot \frac{\partial \theta}{\partial \mathbf{R}(t)}. \end{aligned} \tag{1.4}$$

Note that the first term on the right hand side of (1.4) is the same as $\frac{\partial \theta}{\partial t}$ i.e. the instantaneous frequency due to the 'frozen' Hamiltonian. If $\dot{\mathbf{R}}(t)$ is small, then one can make estimates of the long term behaviour of the solutions of the above system by considering the alternative system of *averaged* equations [9, 10, 81]. The solutions to the averaged system closely approximate the solutions to the exact system. The averaged system is obtained by replacing the $\frac{\partial \theta}{\partial \mathbf{R}}$, $\frac{\partial I}{\partial \mathbf{R}}$ terms in the above equations by their averages around the torus of the 'frozen' Hamiltonian on which the system instantaneously lies. Denoting averages by $<>$, the averaged system is:

$$\dot{I} = \dot{\mathbf{R}}(t) \cdot < \frac{\partial I}{\partial \mathbf{R}(t)} >, \tag{1.5}$$

$$\dot{\theta} = \frac{\partial H}{\partial I} + \dot{\mathbf{R}}(t) \cdot < \frac{\partial \theta}{\partial \mathbf{R}(t)} > . \tag{1.6}$$

As a consequence of the phase space volume conserving property of Hamiltonian systems, the right hand side of (1.5) vanishes. The angle evolution is given by integrating the right hand side of (1.6) with respect to time. Denoting the contribution of the first term by $\Delta\theta_d$ and of the second by $\Delta\theta_g$, we have:

$$\Delta\theta_d \equiv \int_0^T \frac{\partial H}{\partial I} dt, \tag{1.7}$$

$$\Delta\theta_g \equiv \int_0^T \dot{\mathbf{R}}(t) \cdot < \frac{\partial \theta}{\partial \mathbf{R}(t)} > dt = \oint < \frac{\partial \theta}{\partial \mathbf{R}(t)} > \cdot d\mathbf{R}, \tag{1.8}$$

where the circuit integral is over the closed loop in parameter space. Equation (1.7) gives the familiar dynamic phase. The essence of Hannay's argument is that there is no reason to expect the circuit integral in (1.8) to vanish, even in the limit of infinitely slow change. This is the

geometric phase of the system and, clearly, it depends only on the closed loop in parameter space.

These arguments while suggesting the existense of a geometric drift term do not provide insight into the reason for this drift. Further, such arguments cannot be invoked when considering geometric phases in non-adiabatic processes. It was Simon's paper [90] that first explained the geometric phase as the holonomy associated with parallel transport.[4] The concept of parallel transport has been known to mathematicians since the development of non-Euclidean geometry. It refers to the fact that in spaces different from Euclidean, such as the sphere, there is no concept of 'global parallelism.' Tangent vectors at different points lie in different tangent spaces and there is no canonical way of defining 'parallelism' between vectors.[5] One must be content with a local concept of parallelism defined with respect to the direction in which the tangent vector is transported on the sphere. Thus one talks of parallel transport of a tangent vector along a curve. Intuitively this means transporting the vector along a curve such that its rate of change as it moves along the curve is zero. This reduces to the conventional idea of parallel transport when applied to Euclidean space i.e. a vector with constant coordinates as it moves along the curve. In general this local concept of parallelism does not give rise to a global concept of parallelism due to an important property of parallel transport: *it can be curve dependent.* This is illustrated in Figure 1.2 taken from the book by Schutz [83]. The vectors $\bar{V}'$ and $\bar{V}''$ at point C are both the result of parallel translating vector $\bar{V}$ at point A but along different curves. They end up pointing in different directions and there is clearly no unambigous way of defining which of these vectors is parallel to the initial vector. This property is particularly remarkable when one considers a closed curve. The parallel transported vector returns to the same point but is no longer pointing in the same direction, see Figure 1.3 [35]. The rotation of this vector is an example of the *holonomy associated with parallel transport.*

Holonomy can therefore be intuitively described as 'global change without local change.' The parallel transported vector suffers no local change but yet there is a net change when it returns to its initial point. The net change depends on the topology of the underlying space and, in particular, on the closed curve of traverse. It is independent of the rate at which the curve is traversed. A well-known example of a classical system that exhibits such 'global change without local change' leading to a geometric phase is the Foucault pendulum [74, 14, 15, 93]. Consider a pendulum set into oscillations in a plane at a point on some latitude of the earth (excluding the poles) as in Figure 1.4. Identify the orientation of the plane of oscillations with the (unit) vector along the line of intersection of the plane with the tangent plane to the earth's surface at that point. Neglecting forces due to the earth's rotation the plane of oscillations is unaltered in a laboratory frame i.e. there is no local change. The vector is thus parallel transported as

[4] Simon's work was in the adiabatic setting of Berry's phase.

[5] This is possible in Euclidean spaces since the space itself can be identified with the tangent space at any point. The vector can be translated 'freely' between two points.

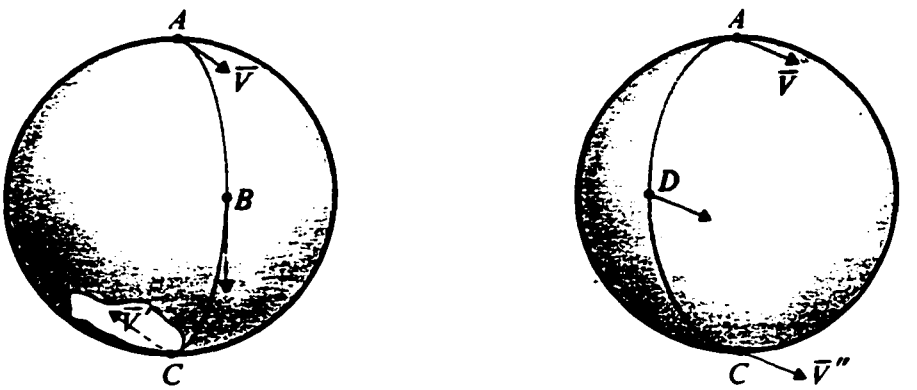

Figure 1.2: Parallel tansport of a vector along two different great circles on the sphere results in different results.

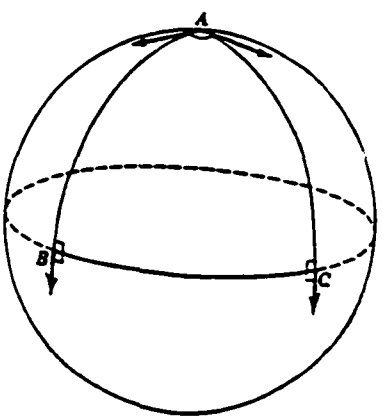

Figure 1.3: The result of parallel transport around a closed curve. The vector has rotated with respect to its initial direction.

the earth rotates. After one complete rotation of the earth, it points in a different direction i.e. there is a shift in the orientation of the oscillating plane. This shift is approximately equal to the rotation of an orthonormal frame when parallel translated along the latitude once around and is given by $2\pi\sin(\beta)$, where β is the degree of the latitude.[6]

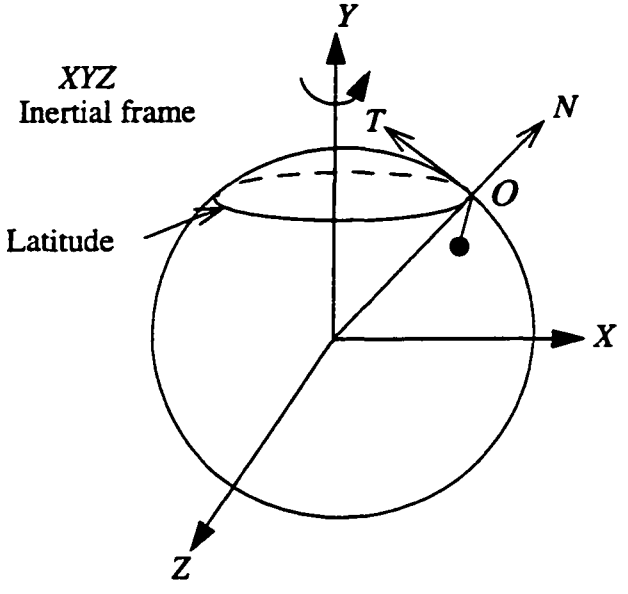

Figure 1.4: The Foucault pendulum: A pendulum at a point O on the earth's surface oscillating in the plane described by ONT. The direction OT is in the tangent plane at O and ON is normal to it. At the end of one rotation of the earth about the Y-axis the plane of the pendulum would have rotated by an amount that depends only on the latitude of O.

The geometric phase of Berry and Hannay measures this holonomy in the dynamical systems in which they occur. To understand this one must generalize the above simple picture of parallel transport of a vector using ideas from differential geometry. Since the ideas involved form a vast mathematical subject of their own, we do not go into details here but attempt to present only a heuristic explanation which may convey some intuitive understanding. Holonomy in the general case is defined for the parallel transport of a 'fiber' over a base 'manifold.' A 'manifold' is a mathematical generalization of our intuitive concept of a surface or a space. It includes the familiar examples of Euclidean space, sphere, torus etc. and many more not obviously fitting into our notions of a surface or a space (such as, for example, the set of lines in $\mathbf{R}^3$ passing through the origin). The 'fiber' can be any set--for our purposes we view it as another abstract manifold. For defining parallel transport in such a general context, one looks at the manifold obtained by 'sticking' a fiber at each point of the base manifold–in other words, 'a fiber bundle,' as depicted in Figure 1.5. For example, in the parameter dependent Hamiltonians considered by

[6] For a nice expository article and simple derivation of this result see Oprea[74].

Hannay, the base manifold is the parameter space, P, and the fiber at each point is the system phase space/configuration space for that value of the parameter, $M_p(p \in P)$. In Berry's context, the base space is again the parameter space and the fiber at each point is the eigenstate of the quantum Hamiltonian for that value of the parameter. A fiber bundle, E, is typically identified with the projection mapping $\pi : E \rightarrow B$, where B is the base. The fiber at a point $b \in B$ is denoted by F_b. A fiber bundle is locally like a product manifold.[7] This means that any point $e \in E$ can be represented as the pair (f, b) where $\pi(e) = b$ and $f \in F_b$. The tangent space of the bundle at any point can thus be viewed as the product space of the tangent space of the fiber at that point and the tangent space of the base point. In mathematical notation, $T_eE \cong T_f F_b \times T_b B$, where $b = \pi(e)$.

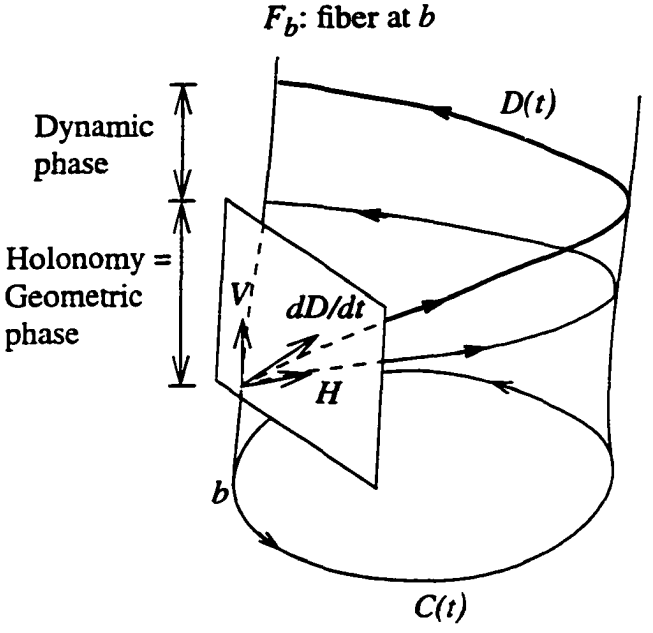

Figure 1.5: A conceptual illustration of a connection and holonomy in a fiber bundle. For explanation, see text.

To define parallel transport on a fiber bundle one defines a *connection* or a way of connecting different fibers. A connection specifies a vector subspace H_e, called the *horizontal* space, of the tangent space T_eE at each point e of the bundle such that $T_eE = H_e \oplus V_e$. V_e, called the *vertical* space, denotes the vector subspace of T_eE which contains all vectors tangent to the fiber at that point. Defining the connection thus implies that at each point every vector in the tangent

[7] A fiber bundle that is globally like a product manifold is called a trivial bundle. Thus in Hannay's case if the system phase space/configuration space is independent of the parameter value then the fiber bundle is trivial and is simply the product manifold $P \times M$.

space of the bundle can be uniquely expressed as the sum of a horizontal vector and a vertical vector. The definition of this distribution of horizontal subspaces determines a way of connecting neighbouring fibers. With any vector η in the tangent space at a point b in the base we can associate a horizontal vector field on F_b. Every element of this field is a horizontal vector. This vector field is called the *horizontal lift* of η. Now consider any curve C on the base, in particular a closed curve, as shown in Figure 1.5. A smooth distribution of horizontal lifts of the tangent vectors to C gives a collection of smooth curves on the bundle all starting from F_b. Each smooth curve is called a horizontal lift of C. For C closed a horizontal lift of C starts and ends on F_b but with a possible shift of the final point with respect to the initial point. Conversely, a given smooth curve on the bundle whose tangent vectors are horizontal at every point and which starts and ends on the same fiber can be viewed as the horizontal lift of a closed curve on the base. The collection of horizontal lifts of C defines a mapping of the fiber onto itself. This defines parallel translation of the fiber around a closed curve on the base. The shift in the points of the fiber under this mapping is the holonomy associated with the parallel transport. Note that this shift is independent of the parametrization of the loop i.e. the rate at which the loop is traversed.

Returning to the context of Berry and Hannay, we now try to understand how their phases can be interpreted in terms of the above holonomy. Any point on the fiber bundle represents their parameter dependent dynamical system at some instant. As time evolves this point traces out a curve $D(t)$ on the bundle, as shown in Figure 1.5, representing the system evolution as the parameters are slowly varied. The tangent vector to this curve at any point represents the rate of evolution of the system. If there is a connection defined on the bundle, then one can split this vector at each point into its horizontal and vertical components (H and V respectively in Figure 1.5). The vertical component, since it is along the fiber, represents the rate at which the system is evolving instantaneously. The path traced by the horizontal vectors with time is the horizontal lift of the closed loop on the base space i.e. the parameter space. This defines parallel translation of the fiber which is the phase space or the eigenstate in this context. Note that the system evolution curve is different from the horizontal lift curve due to the presence of the vertical vectors at each point. At the end of the closed loop, the system curve returns to the same fiber and the shift in the fiber coordinates [8] between the initial and end points is the sum of two parts. The first part is the shift due to the vertical components alone and is the dynamic phase. The second part is the shift due to parallel translation and is the holonomy or the geometric phase.[9]

What defines the connection on the bundle? *The adiabatic evolution of the parameters.* This corresponds to our intuitive understanding of parallel transport since in an adiabatic evolution of the parameters one expects the infinitely slow variation of the parameters *at any instant* to have

[8] The angle variables in Hannay's context and the phase of the wave function in Berry's context.

[9] Note that the first part does depend on the magnitude of the tangent vector and hence on the parametrization of the curve, i.e. the rate of evolution of the system, unlike the second part.

no effect on the system dynamics. In other words, such an evolution implies no local change. The dynamical system is thus parallel transported by the adiabatic evolution and the geometric phase is the holonomy due to this parallel transport. From the fiber bundle construction it is obvious that the phase is independent of the slow rate at which the parameters are varied and is a function of the closed curve on the parameter manifold and the manifold's topology.

This differential geometric viewpoint as mentioned before, allows us to understand the geometric phase in non-adiabatic processes as well, where in general there is no slow time scale. Many of these phases can be described as changes in the configuration of a system brought about by manipulation of internal variables. Thus Shapere and Wilczek's micro-organism [85, 95, 84] achieves locomotion by a continuous deformation of its body shape. The system of hinged rods in Figure 1.6 [55] considered by [46, 98][10] achieves a net rotation of π by a sequence of rotations at each hinge. Another simple example is shown in Figure 1.7 [54]. At the end of the arm movement cycle the arm has rotated by manipulation of the shoulder joint. In the problem of the motion of three point masses first considered by Guichardet [36] and then later by Iwai [39] and Montgomery [67, 65] the triangle defined by the three points undergoes a rigid body rotation about its center of mass at the end of a cycle in which the triangle returns to its original shape.

To understand the phase in terms of holonomy in these problems, one looks at the configuration manifold of the system. Since the phase usually manifests itself as a rotation or translation (or both) of the configuration, one constructs the fiber bundle by 'factoring' the above manifold by the Lie group[11] of these motions. The quotient manifold (or the 'reduced' manifold) is then viewed as the base manifold of the bundle and is usually called the shape space. This is the space of all possible shapes the system could take during a given dynamical evolution. All configurations of the system that have the same shape but differ from each other only by a rigid body rotation or/and translation are represented by the same point in the shape space. A closed loop in the base space thus represents a cycle in which the configuration returns to its original shape but could be rotated or translated. The fibers are the Lie groups and such a bundle is termed a principal fiber bundle. Parallel translation in such problems is usually determined by some dynamical constraint, such as the conservation of angular momentum in the motion of three point masses. The connection is defined by a splitting of the tangent space at each point that is orthogonal in the kinectic energy metric (inner product) on the bundle. Physically the horizontal subspaces correspond to (total) zero angular momentum motions of the three bodies [36, 65]. The vertical directions (which are the group directions) correspond to instantaneous rigid body rotations of the triangle. In other words, the connection implies that at every instant the three body motion can be decoupled into a rigid body rotation with a rotation rate corresponding to the constant initial angular momentum of the configuration and a 'rearranging' motion of zero angular momentum. The shift in the coordinates of the fiber at the end of the closed loop is thus

[10] For more references please see [55].
[11] Also a manifold.

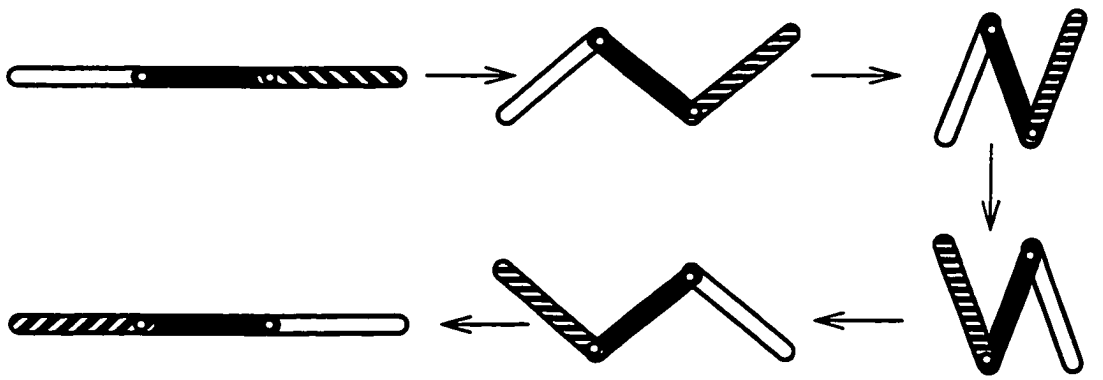

Figure 1.6: The system of hinged rods achieves an overall rotation by a manipulation of its internal hinge angles.

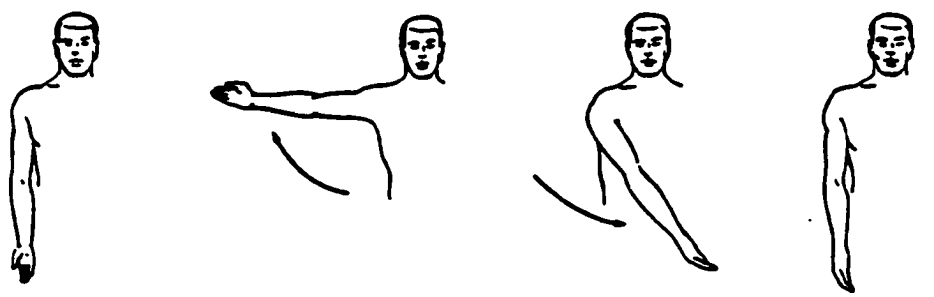

Figure 1.7: An overall rotation in the configuration of the arm without performing a local rotation is achieved by the above sequence.

a rotation angle composed of two parts: the dynamic phase due to the instantaneous rotations and the geometric phase which is the holonomy due to parallel transport. Note again that this result is an example of 'global change without local change.' Indeed, Guichardet's paper sought to answer the following question posed about molecular motions: can rotational motions be separated from vibrational motions ? In the above point mass model where the horizontal directions represent vibrational motions, we see that it cannot. For a thorough mathematical treatment of geometric phases in both adiabatic and non-adiabatic processes and their relation to reduction theory we refer the reader to Marsden, Montgomery and Ratiu [53].

1.3 Techniques

In most systems of mathematical and engineering interest, the variable q with the geometric phase shift typically represents the unknown integral curve of some dynamical system. The problem then is to extract the phase in such systems without knowing exact solutions, or even the action-angle form. The use of elementary techniques as in the particle-in-a-hoop problem is exceptional. The fiber bundle construction yields a set of nonlinear ordinary differential equations for the parallel transport provided a connection can be defined. Integration of these equations will then yield the geometric phase, but obtaining an explicit expression is in general not feasible. In the adiabatic problems, the slow evolution of the parameters introduces a second timescale in the problem. This feature can be exploited to directly calculate the phase by traditional perturbation techniques without resorting to the fiber bundle formalism. For example, in the Hamiltonian systems of the type considered by Hannay, the method of averaging in principle yields the phase. However, as is clear from (1.8) the particular method used by Hannay and Berry [37, 12] requires knowledge of the dependence of the canonical coordinates on the external parameters. In particular one needs to know the partial derivative vector in (1.8) which is the quantity averaged to obtain the integrand. This may not be known *a priori* for most systems. In the absence of such information, it seems natural to ask whether one can calculate the geometric phase by constructing an asymptotic series solution in ϵ for the differential equations governing q. Such a solution would also give information on the ϵ dependency of the total phase. We may mention that asymptotic series solutions have been considered before by Bhattacharjee and Sen [17]. Berry [13] himself has suggested an iterative scheme for calculating the phase, although his procedure is not an asymptotic one.

To construct such a solution, one could use either the method of averaging in its more general form [81] or use the multi-scale technique [42]. In this paper we develop the latter owing to the relative computational ease of calculating the higher order terms in the series. In this technique, one introduces an independent slow time variable $\tau = \epsilon t$ on which the parameters $\mathbf{X}(\tau)$ vary. We

then view the variable $q(t,\tau)$ as a function of these two independent time variables. The formula for the total phase change then reads:

$$\int_{q(0)}^{q(T)} dq(t,\tau) = \int_0^{T=1/\epsilon} \frac{\partial q(t,\tau)}{\partial t} \cdot dt + \int_0^1 \frac{\partial q(t,\tau)}{\partial \tau} \cdot d\tau, \tag{1.9}$$

where the second integral on the right hand side is the same as the contour integral in (1.2). The geometric phase, if it exists, should arise from this integral. The multi-scale technique gives asymptotic series representations for $q(t,\tau)$ and the second integral in the following forms:

$$\begin{aligned} q(t,\tau) &= q_0(t,\tau) + \epsilon q_1(t,\tau) + \epsilon^2 q_2(t,\tau) + ..., \\ \int_0^1 \frac{\partial q}{\partial \tau} \cdot d\tau &= \int_0^1 \frac{\partial q_0}{\partial \tau} \cdot d\tau + \epsilon \int_0^1 \frac{\partial q_1}{\partial \tau} \cdot d\tau + ... \end{aligned} \tag{1.10}$$

The $O(1)$ terms in series (1.10) are then identified as the geometric phase terms.

Chapter 2

Asymptotic construction of the geometric phase

In this chapter we give a general formulation for the calculations to be carried out for obtaining the phase in an adiabatic setting in three canonical point vortex configurations. In §2.1 we describe the basic set-up and highlight the main results for the three canonical configurations to be treated. Since the form of the equations are similar for each configuration, we describe the general form of the equations in §2.2 and show how the multi-scale method leads to the identification of the geometric phase term. §2.3, §2.4, and §2.5 contain the details of the calculations for each of the three canonical configurations that we analyse. The problem described in §2.3 appears to be the simplest point vortex configuration giving rise to a non-trivial phase factor. The configuration analysed in §2.4 shows that a geometric phase can be induced by a solid boundary in the flow. The corresponding problem, without boundaries achieved by using image vortices is related to the three vortex problem discussed in §2.3, although cannot be directly derived from it as a special case. The shear layer model described in §2.5 is the most complex of the three configurations. It is related to the first as well and can be thought of as a restricted three vortex problem in a periodic strip. The geometric interpretation of the phases is given in the next chapter.

2.1 Modus operandi

In this section, we formulate our approach to identifying and computing the 'geometric' or 'Hannay-Berry' phase in three problems in planar, incompressible, inviscid fluid flows involving point vortices. In each of our problems, we track the position of a 'phase object' which for our purposes could be a fluid particle, a passive tracer particle or a point vortex of arbitrary strength. Typically, we are interested in the limiting case where the phase object is close to another point vortex, which we refer to as the 'parent vortex.' The phase object moves under the influence of the parent vortex as well as from the influence of an additional vortex or vortices placed further away, which we refer to as the 'farfield vortices.' Since it is nearby, the parent vortex causes rapid revolution of the phase object with a time period that we denote T_s. It is clear since the velocity field of a planar point vortex scales like $1/r$ that $T_s \sim r^2(0)$, where $r(0)$ denotes

the initial distance between the phase object and its parent vortex. The additional dynamics due to the farfield vortices are such that they induce a periodic motion of the vortices, so that we can define a longer period $T_l \sim D^2(0) >> T_s$, where $D(0)$ is the initial distance between the farfield vortex and the parent vortex. We thus have a natural small parameter at our disposal, which we define as $\epsilon^2 = T_s/T_l \sim r^2(0)/D^2(0)$. We then non-dimensionalize the problem so that $T_s = O(1)$, hence $T_l = O(1/\epsilon^2)$. The time varying periodic coefficients that appear (due to the periodic vortex motion) in the equations of motion of the phase object can then be viewed as varying on the slow timescale $\tau \sim \epsilon^2 t$ and we have an adiabatic process as $\epsilon \to 0$.

The angle change (relative to the parent vortex) of the phase object is then computed at the end of time T_l. In the adiabatic limit, this angle change is shown to split naturally into two parts: a 'fast' part and a 'slow' part. The fast part, which comes from the dynamic phase, is what would be present if the phase object rotated only around the parent vortex, with no farfield vorticity present. We call this the '$\epsilon = 0$,' or 'unperturbed' problem. The slow part is the geometric phase θ_g. As described in Chapter 1, θ_g arises from the limiting adiabatic procedure $\epsilon \to 0$ in the following way.

We view the contribution θ_g as arising from the product of two terms: $\theta_g = \delta\theta \cdot N$. The first term, $\delta\theta$, is defined as the angle difference between the unperturbed and perturbed phase object at any given fixed time t^* (see Figure 2.5), hence:

$$\delta\theta = \theta_\epsilon(t^*) - \theta_0(t^*).$$

Since the perturbed and unperturbed equations approach each other smoothly as $\epsilon \to 0$, we know that $\delta\theta \to 0$ as $\epsilon \to 0$. In all point vortex problems, scaling requires that $\delta\theta \sim C_1\epsilon^2$. The second term, N, is defined to be the number of complete orbits of the phase object during one complete cycle of the farfield vortices. Since the phase object has period T_s and the farfield vortices have period T_l, we have:

$$N \sim T_l/T_s \sim C_2/\epsilon^2.$$

The geometric phase contribution then becomes:

$$\theta_g = \delta\theta \cdot N = (C_1\epsilon^2) \cdot (C_2/\epsilon^2) = C_1C_2 \sim O(1).$$

It arises from the limiting procedure $\epsilon \to 0$ as the balance between one term going to zero, the other to infinity. Notice that in this interpretation the limiting procedure $\epsilon \to 0$ is distinct from the limit $\epsilon = 0$. Such an asymptotic balance is achieved in all of the vortex problems we treat. We now introduce the three problems.

Problem 1: Three point vortices in the plane.

This is the simplest vortex configuration in which a geometric phase occurs and is shown in Figure 2.1. All the point vortex strengths are of the same sign, but can be of arbitrary magnitude $(\Gamma_1, \Gamma_2, \Gamma_3)$. Without loss of generality, we take Γ_1 as the parent vortex,[1] Γ_2 as the phase object, and Γ_3 as the farfield vortex. Our result for the geometric phase induced on the phase object (Γ_2) is:

$$\theta_g = \frac{\Gamma_3}{\Gamma_1 + \Gamma_2 + \Gamma_3} \cdot 2\pi \cdot \cos(2\theta_i),$$

where θ_i is the initial condition for the phase object.

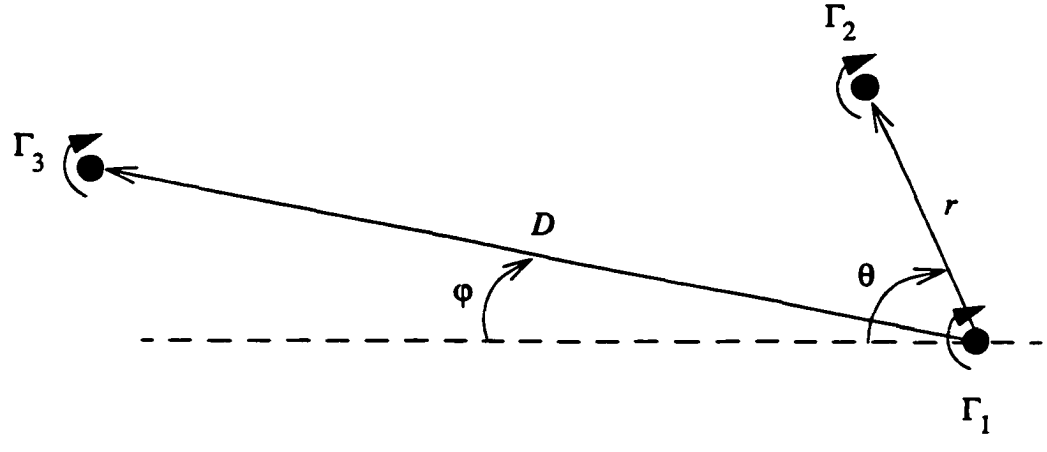

Figure 2.1: Three point vortices (filled circles) of positive strengths in an unbounded plane. The geometric phase is calculated for the variable θ.

Problem 1a: Four point vortices in the plane.

As an extension of Problem 1 we place another vortex $\Gamma_4(> 0)$ in the vicinity of Γ_3. This leads to two phase object-parent vortex pairs, Γ_1, Γ_2 (with angle θ) and Γ_3, Γ_4 (with angle ν), respectively, as shown in Figure 2.2. Each pair also acts as farfield vortices for the other pair. Our result for the geometric phase induced in each pair is:

$$\theta_g = \frac{\Gamma_3 + \Gamma_4}{\Gamma_1 + \Gamma_2 + \Gamma_3 + \Gamma_4} \cdot 2\pi \cdot \cos(2\theta_i),$$
$$\nu_g = \frac{\Gamma_1 + \Gamma_2}{\Gamma_1 + \Gamma_2 + \Gamma_3 + \Gamma_4} \cdot 2\pi \cdot \cos(2\nu_i).$$

[1] Here and elsewhere we refer to vortices by their strengths. We assume positive strengths everywhere. The effect of changing the sign of the strengths in each problem is to merely change the sign of the geometric phase.

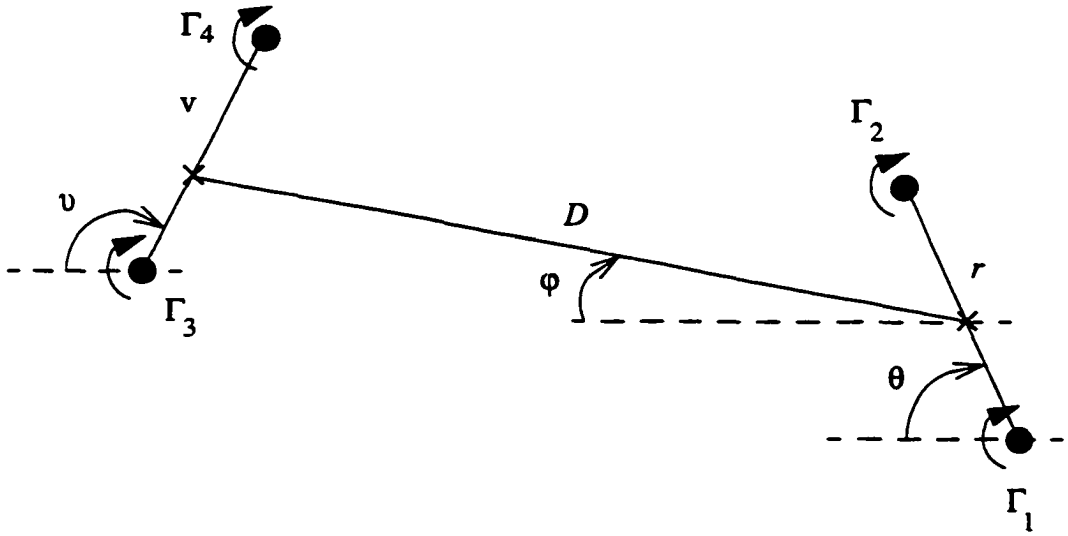

Figure 2.2: Four point vortices (filled circles) of positive strengths in an unbounded plane. The geometric phase is calculated for the variables θ and ν. The Xs mark the centers of vorticity of each pair respectively.

Problem 2: A point vortex and particle in a circle.

In this problem, we show that a geometric phase contribution arises as a result of a boundary effect. Here, the phase object is a passive particle orbiting the parent vortex Γ as shown in Figure 2.3. The parent vortex in any eccentric position moves in a closed circular path with radius R_1 and with constant frequency. The farfield vorticity is due to the circular boundary of radius $R_2 > R_1$. Equivalently, we can think of the farfield vortex as an image vortex $-\Gamma$ placed at its image point R_2^2/R_1 outside the circle [99, 100]. The geometric phase contribution on the phase object is:

$$\theta_g = -\frac{2\pi}{(R_2/R_1)^2 - 1} \cdot \cos(2\theta_i).$$

Note it is independent of the vortex strength.

Problem 3: Pairing in an infinite row of point vortices.

Here, we show that a geometric phase contribution arises during the 'vortex pairing' stage of nonlinear shear layer evolution in a simple two dimensional model for the process thought to be fundamental for the generation of small scale motion and enhanced mixing in a wide range of more complicated real flows [96, 21]. In the model, an infinite row of evenly spaced, equal strength vortices is given a subharmonic perturbation so that neighboring vortices pair up and undergo periodic motion as shown in Figure 2.4. The phase object is a tracer particle near

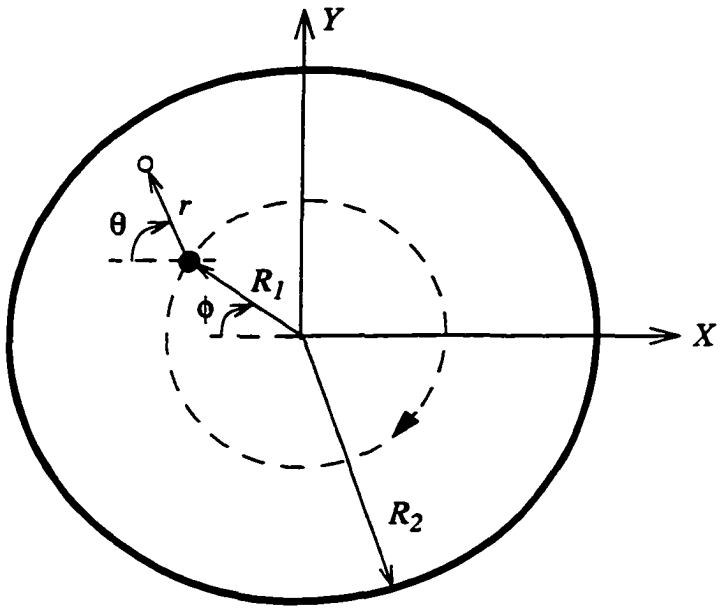

Figure 2.3: A point vortex (filled circle) and a fluid particle (unfilled circle) in a circular domain. Orbit of the vortex is shown by the dashed circle. The cartesian frame X-Y is centered at the center of the circular domain.

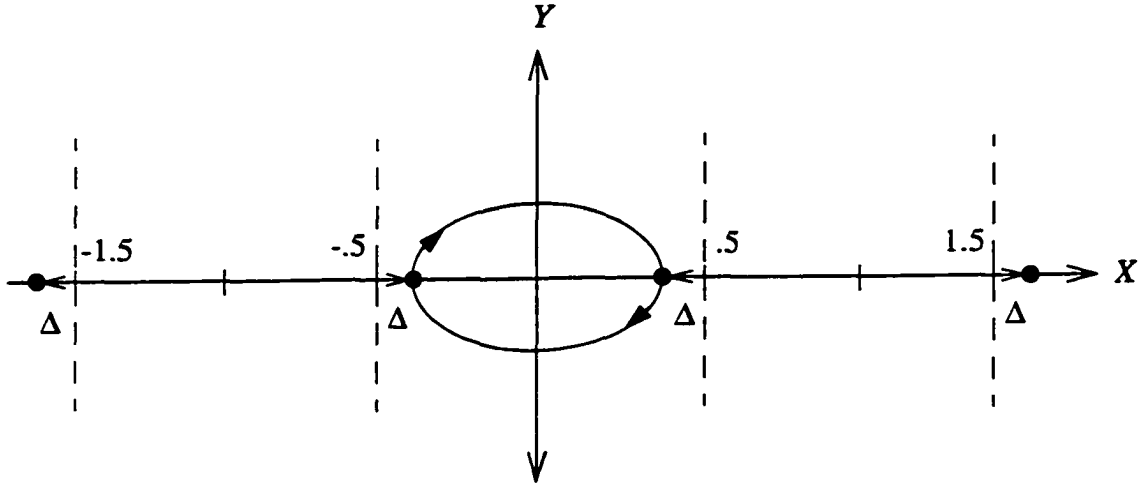

Figure 2.4: The positions of the vortices (filled circles) immediately after the subharmonic perturbations (of magnitude D and direction shown by arrows along X-axis). The subsequent motion of the vortices is shown in the central window. This motion is identical in every other window. The windows are divided by the vertical dashed lines which mark the initial positions of the vortices (here, $a = 1$).

any parent vortex, while the farfield flow is due to the infinite number of other point vortices periodically spaced. Our result for this configuration is:

$$\theta_g = (\frac{2k+6}{3}) \cdot K \cdot \cos(2\theta_i).$$

Here K is the complete Jacobi elliptic integral of the first kind with modulus k [19] arising from the exact solution of the closed vortex orbit.

2.2 Asymptotic procedure.

The three problems we treat, when prepared appropriately, all have the same general form. In this section we outline our asymptotic procedure, based on multi-scale theory [42], for computing the geometric phase θ_g.

Let (r, θ) denote the non-dimensional polar coordinates of the phase object with respect to the parent vortex. The form of the general equations of motion we encounter are:

$$\frac{dr}{dt} = \epsilon^2 f\left(r, \theta, D(\epsilon^2 t), \phi(\epsilon^2 t), \epsilon\right), \tag{2.1}$$

$$\frac{d\theta}{dt} = \frac{\Omega}{r^2} + \epsilon^2 g\left(r, \theta, D(\epsilon^2 t), \phi(\epsilon^2 t), \epsilon\right). \tag{2.2}$$

Here, ϵ is a small dimensionless parameter, f and g are the components of the vector field due to the farfield vortices, and D and ϕ, defined appropriately in each problem, are non-dimensional polar variables representing the periodic vortex motion. These variables provide the periodic time varying coefficients in the above equations, with the angle variable ϕ occuring in the argument of some periodic function:

$$\begin{aligned} D(T_l) - D(0) &= 0, \\ \phi(T_l) - \phi(0) &= 2\pi. \end{aligned}$$

Notice that in the limit $\epsilon = 0$, the equations reduce to those governing a passive particle around an isolated point vortex in an unbounded plane.

Since $T_l = O(1/\epsilon^2)$, there exists a slow timescale $\tau = \epsilon^2 t$ in the superimposed field. By the usual multi-scale 'ansatz', the two timescales (t, τ) are viewed as independent variables. The ordinary differential equations then split into partial differential equations as $\frac{d}{dt} \to \frac{\partial}{\partial t} + \epsilon^2 \frac{\partial}{\partial \tau}$:

$$\frac{\partial r}{\partial t} + \epsilon^2 \frac{\partial r}{\partial \tau} = \epsilon^2 f\left(r, \theta, \tilde{D}, \tilde{\phi}, \epsilon\right), \tag{2.3}$$

$$\frac{\partial \theta}{\partial t} + \epsilon^2 \frac{\partial \theta}{\partial \tau} = \frac{\Omega}{r^2} + \epsilon^2 g\left(r, \theta, \tilde{D}, \tilde{\phi}, \epsilon\right), \tag{2.4}$$

where the $\sim$ overhead denotes dependency on the slow time alone.[2] In order to calculate the geometric phase for such a system, therfore, we seek a two time scale series solution asymptotic in ϵ for given initial conditions $r(0) = 1$ and $\theta(0) = \theta_i$. Thus,

$$\begin{aligned} r(t,\tau) &= r_0(t,\tau) + \epsilon r_1(t,\tau) + \epsilon^2 r_2(t,\tau) + ..., \\ \theta(t,\tau) &= \theta_0(t,\tau) + \epsilon\theta_1(t,\tau) + \epsilon^2\theta_2(t,\tau) + ..., \end{aligned}$$

with $r_0(0) = 1$, $\theta_0(0) = \theta_i$ and $r_j(0) = \theta_j(0) = 0$ for $j = 1, 2, ...$ Substituting in (2.3) and (2.4), we Taylor expand the functions f, g and $1/r^2$ about $\epsilon = 0$, assuming they possess $\epsilon-$derivatives of all orders in a neighborhood of that point. Thus, for example,

$$f\left(r,\theta,\tilde{D},\tilde{\phi},\epsilon\right) = f_0 + \epsilon\left(\frac{df}{d\epsilon}\right)_{\epsilon=0} + \frac{\epsilon^2}{2}\left(\frac{d^2f}{d\epsilon^2}\right)_{\epsilon=0} + ...,$$

where $f_0 = f\left(r_0,\theta_0,\tilde{D},\tilde{\phi},0\right)$ and

$$\begin{aligned} \left(\frac{df}{d\epsilon}\right)_{\epsilon=0} &= \left(\frac{\partial f}{\partial\epsilon}\right)_{\epsilon=0} + \left(\frac{\partial f}{\partial r}\frac{dr}{d\epsilon}\right)_{\epsilon=0} + \left(\frac{\partial f}{\partial\theta}\frac{d\theta}{d\epsilon}\right)_{\epsilon=0}, \\ &= \left(\frac{\partial f}{\partial\epsilon}\right)_{\epsilon=0} + r_1\left(\frac{\partial f}{\partial r}\right)_{\epsilon=0} + \theta_1\left(\frac{\partial f}{\partial\theta}\right)_{\epsilon=0}, \end{aligned}$$

and the higher derivatives in the Taylor expansion are similarly computed. Note that at $\epsilon = 0$, $r = r_0$ and $\theta = \theta_0$. Equating like powers of ϵ gives a pair of first order PDEs at every order and these are solved sequentially from $O(1)$. The solutions contain arbitrary functions of slow time which are determined uniquely by identifying terms that can cause growth on the fast time at higher orders and eliminating them i.e. imposing the so-called 'solvability conditions.'

Consider the first three orders in ϵ:

$$\begin{aligned} O(1): \frac{\partial r_0}{\partial t} &= 0, \\ \frac{\partial\theta_0}{\partial t} &= \frac{\Omega}{\tilde{r}_0^2}, \\ O(\epsilon): \frac{\partial r_1}{\partial t} &= 0, \\ \frac{\partial\theta_1}{\partial t} &= -\frac{2\Omega\tilde{r}_1}{\tilde{r}_0^3}, \\ O(\epsilon^2): \frac{\partial r_2}{\partial t} &= -\frac{d\tilde{r}_0}{d\tau} + f_0, \\ \frac{\partial\theta_2}{\partial t} &= -\frac{\partial\theta_0}{\partial\tau} + \frac{\Omega}{r_0^2}\left(\frac{3r_1^2}{r_0^2} - \frac{2r_2}{r_0}\right) + g_0. \end{aligned}$$

[2] This notation is used throughout the thesis.

Solving the $O(1)$ equation gives:

$$r_0 = \tilde{r}_0(\tau) \quad \tilde{r}_0(0) = 1,$$
$$\theta_0 = \theta_F + \theta_S = \Omega t/\tilde{r}_0^2 + \tilde{\theta}_0(\tau),$$

where $\tilde{\theta}_0(0) = \theta_i$, with $0 \leq \theta_i \leq 2\pi$. Notice:

1. At leading order there is a decompostion of the angle variable into a fast term $\theta_F = \Omega t/\tilde{r}_0^2$, and a slow term $\theta_S = \tilde{\theta}_0(\tau)$.

2. It turns out, as will be shown below, that $\tilde{r}_0 = \text{const}$, and hence the fast term θ_F is the exact angle variable evolution in the $\epsilon = 0$ problem i.e.where the phase object moves about an isolated point vortex with no external slow field. Evaluated at the end of period T_l this gives, as noted earlier, the contribution of the dynamic phase at this order to the angle change.

3. The slow term $\theta_S = \tilde{\theta}_0(\tau)$ evaluated at the end of period T_l gives rise to the geometric phase, θ_g. It is not present in the $\epsilon = 0$ problem. Our goal is to evaluate $\tilde{\theta}_0(\tau)$ by computing its solvability condition at higher order. We call the equation for $\tilde{\theta}_0$ the 'slow phase' equation.

Proceeding to next order, we have:

$$\begin{aligned} O(\epsilon) : r_1 &= \tilde{r}_1(\tau), \\ \tilde{r}_1(0) &= 0, \\ \frac{\partial \theta_1}{\partial t} &= -2\Omega \tilde{r}_1/\tilde{r}_0^3. \end{aligned}$$

In order that θ_1 remain bounded on the fast timescale, we impose the solvability condition: $\tilde{r}_1 = 0$. This then gives: $\theta_1 = \tilde{\theta}_1(\tau)$ with $\tilde{\theta}_1(0) = 0$. Then at $O(\epsilon^2)$ we get:

$$\begin{aligned} \frac{\partial r_2}{\partial t} &= -\frac{d\tilde{r}_0}{d\tau} + f_0, \\ \frac{\partial \theta_2}{\partial t} &= -\frac{\partial \theta_0}{\partial \tau} + g_0 - \frac{2\Omega r_2}{\tilde{r}_0^3}. \end{aligned}$$

Assuming that the terms f_0 and g_0 do not lead to secular growth (which we will verify in our examples), the solvability condition for $\tilde{r}_0$ is: $\frac{d\tilde{r}_0}{d\tau} = 0 \Rightarrow \tilde{r}_0(\tau) = \tilde{r}_0(0) = 1$ and, therefore we can solve for r_2 and θ_2:

$$r_2 = \int f_0 dt + \tilde{r}_2(\tau), \qquad \tilde{r}_2(0) = -\int f_0 dt_{|t=0},$$

and $\theta_2 = \int \left(g_0 - 2\Omega \int f_0 dt\right) dt + \tilde{\theta}_2(\tau)$. The functions f_0 and g_0 now read $f_0 = f(1, \Omega t + \tilde{\theta}_0, \tilde{D}, \tilde{\phi}, 0)$ and $g_0 = g(1, \Omega t + \tilde{\theta}_0, \tilde{D}, \tilde{\phi}, 0)$. The solvability condition for $\tilde{\theta}_0$ then gives the 'slow phase' equation:

$$\boxed{\frac{d\tilde{\theta}_0}{d\tau} = -2\Omega \tilde{r}_2,}$$

which is fundamental in deriving our formula for the Hannay-Berry phase. Notice at this stage:

1. To solve the phase equation for $\tilde{\theta}_0$, we need to derive the governing equation for $\tilde{r}_2$ by imposing the solvability condition at $O(\epsilon^4)$. Therefore to derive the 'slow phase' system for $(\tilde{\theta}_0, \tilde{r}_2)$ we need to go to $O(\epsilon^4)$. This also shows that the leading order phase implicitly depends on higher order amplitude contributions.

2. In all of the examples we treat, it turns out that the equation governing $\tilde{r}_2$ is:

$$\frac{d\tilde{r}_2}{d\tau} = 0 \quad \Rightarrow \tilde{r}_2(\tau) = \tilde{r}_2(0) = -\int f_0 dt_{|t=0}.$$

3. With the above assumptions, the solution for the slow phase is:

$$\begin{aligned} \theta_S \equiv \tilde{\theta}_0(\tau) &= 2\Omega\tau \int f_0 dt_{|t=0} + \theta_i, \\ &= 2\Omega\epsilon^2 t \left(\int f_0 dt_{|t=0}\right) + \theta_i. \end{aligned} \tag{2.5}$$

We now have the solutions (r, θ) through $O(\epsilon^2)$:

$$r(t, \tau) = 1 + \epsilon^2 r_2(t, \tau) + ..., \tag{2.6}$$

$$\theta(t, \tau) = \Omega t + 2\Omega\tau \int f_0 dt_{|t=0} + \theta_i + \epsilon\tilde{\theta}_1(\tau) + \epsilon^2\theta_2(t, \tau) + ..., \tag{2.7}$$

where $r_2(t, \tau)$ and $\theta_2(t, \tau)$ are as derived earlier.

The Hannay-Berry phase can now be calculated by forming the asymptotic series representation of the integral (1.10) using (2.7). It takes the form:

$$\begin{aligned} \int_0^\beta \frac{\partial\theta}{\partial\tau} d\tau = \int_0^\beta \frac{\partial}{\partial\tau}\left(\Omega t + 2\Omega\tau \int f_0 dt_{|t=0} + \theta_i\right) \cdot d\tau \\ + \epsilon \int_0^\beta \frac{d\tilde{\theta}_1}{d\tau} \cdot d\tau + \epsilon^2 \int_0^\beta \frac{\partial\theta_2}{\partial\tau} \cdot d\tau + ..., \end{aligned}$$

where we have assumed the long period $T_l = \beta/\epsilon^2$. In the limit $\epsilon \to 0$ only the first term of the series remains. Due to the decomposition of θ_0 into a fast term and a slow term, we get the Hannay-Berry phase as:

$$\theta_g = 2\Omega\beta \int f_0 dt_{|t=0}, \tag{2.8}$$

$$= \int_0^\beta \frac{d\theta_S}{d\tau} d\tau. \tag{2.9}$$

This is the general formula for the Hannay-Berry phase. An important observation to make about the final formula for θ_g is that *it does not depend on the function g in equation (2.2).*

2.3 A three-vortex problem

In this problem there are 3 point vortices of the same sign in an unbounded plane,[3] two of them close to each other (Γ_1 and Γ_2) and the third (Γ_3) farther away as shown in Figure 2.1. We analyse the angle holonomy for Γ_2 (the phase object) as it moves primarily under the influence of the field of Γ_1 (the parent vortex), with Γ_3 (the farfield vortex) providing the superimposed field.

The equations governing the point vortex motion can be compactly written in complex form as [6, 5]:

$$\dot{z}_\alpha^* = (2\pi i)^{-1} \sum_{\beta=1}^{3} \Gamma_\beta (z_\alpha - z_\beta)^{-1},$$

where $z_\alpha \equiv x_\alpha + iy_\alpha$, $\alpha = 1, 2, 3$ and x_α, y_α are the Cartesian coordinates of the vortices. These equations can be written in real form as:

$$\Gamma_\alpha \dot{x}_\alpha = \frac{\partial \mathcal{H}}{\partial y_\alpha}, \tag{2.10}$$

$$\Gamma_\alpha \dot{y}_\alpha = -\frac{\partial \mathcal{H}}{\partial x_\alpha}, \tag{2.11}$$

with Hamiltonian $\mathcal{H} \equiv -\frac{1}{4\pi} \sum_{\alpha<\beta}^{N} \Gamma_\alpha \Gamma_\beta \log|z_\alpha - z_\beta|$. For more on point vortex motions refer to [72, 7, 101, 43].

For calculating the phase, we use intervortex distances and angles as the vortex variables as shown in Figure 6. r and D denote the distances of Γ_2 and Γ_3 from Γ_1, respectively, and θ and ϕ denote the angles the lines joining Γ_2 and Γ_3 to Γ_1, respectively, make with the horizontal axis. The angles are measured clockwise from the negative x-axis and clockwise circulations

[3] We consider like-signed vortices to prevent the possibility of unbounded motion, see [92].

are assumed to have positive signs.[4] This change of variables from the Cartesian coordinates of the original three degree-of-freedom Hamiltonian system (equations (2.10) and (2.11)) is of the form:[5]

$$y_2 - y_1 = \hat{r}\sin(\theta), \quad x_2 - x_1 = -\hat{r}\cos(\theta),$$

$$y_3 - y_1 = \hat{D}\sin(\phi), \quad x_3 - x_1 = -\hat{D}\cos(\phi),$$

$$y_3 - y_2 = \hat{D}\sin(\phi) - \hat{r}\sin(\theta), \quad x_3 - x_2 = -\hat{D}\cos(\phi) + \hat{r}\cos(\theta).$$

The resulting equations are then non-dimensionalised as follows:

$$r = \frac{\hat{r}}{R_i}, \quad D = \frac{\hat{D}}{D_i}, \quad t = \omega\hat{t}.$$

Here, R_i and D_i are the initial distances of Γ_2 and Γ_3, respectively, from Γ_1. ω is taken as being proportional to the frequency of Γ_1 and Γ_2 orbiting each other in the absence of Γ_3 i.e. to $1/R_i^2$. The ratio of the initial distances is the perturbation parameter:

$$\epsilon = \frac{R_i}{D_i}.$$

The system of non-dimensional equations for r, θ, D, ϕ is :

$$\frac{dr}{dt} = \frac{-\alpha_3\epsilon}{2\pi D}\sin(\phi-\theta)\left[\frac{1}{1-\frac{2\epsilon r}{D}\cos(\phi-\theta)+\frac{\epsilon^2 r^2}{D^2}} - 1\right], \tag{2.12}$$

$$\frac{d\theta}{dt} = \frac{\alpha_1+\alpha_2}{2\pi r^2} + \frac{\alpha_3\epsilon}{2\pi r D}\cos(\phi-\theta)\left[1 - \frac{1}{1-\frac{2\epsilon r}{D}\cos(\phi-\theta)+\frac{\epsilon^2 r^2}{D^2}}\right] + \frac{\alpha_3\epsilon^2}{2\pi D^2}\left[\frac{1}{1-\frac{2\epsilon r}{D}\cos(\phi-\theta)+\frac{\epsilon^2 r^2}{D^2}}\right], \tag{2.13}$$

$$\frac{dD}{dt} = \frac{\alpha_2\epsilon}{2\pi r}\sin(\phi-\theta)\left[1 - \frac{\frac{\epsilon^2 r^2}{D^2}}{1-\frac{2\epsilon r}{D}\cos(\phi-\theta)+\frac{\epsilon^2 r^2}{D^2}}\right], \tag{2.14}$$

$$\frac{d\phi}{dt} = \frac{(\alpha_1+\alpha_3)\epsilon^2}{2\pi D^2} + \frac{\alpha_2\epsilon}{2\pi r D}\cos(\phi-\theta)\left[1 - \frac{\frac{\epsilon^2 r^2}{D^2}}{1-\frac{2\epsilon r}{D}\cos(\phi-\theta)+\frac{\epsilon^2 r^2}{D^2}}\right] + \frac{\alpha_2\epsilon^2}{2\pi D^2}\left[\frac{1}{1-\frac{2\epsilon r}{D}\cos(\phi-\theta)+\frac{\epsilon^2 r^2}{D^2}}\right], \tag{2.15}$$

[4] We follow these conventions in all the problems in this chapter.

[5] Hats denote dimensional variables that will be non-dimensionalized. This notation is followed throughout the thesis. The hats are not marked in the figures.

with initial conditions $r(0) = 1, \theta(0) = \theta_i, D(0) = 1, \phi(0) = 0$ and where $\alpha_k = \Gamma_k/(R_i^2\omega)$ are the non-dimensionalised vortex strengths.

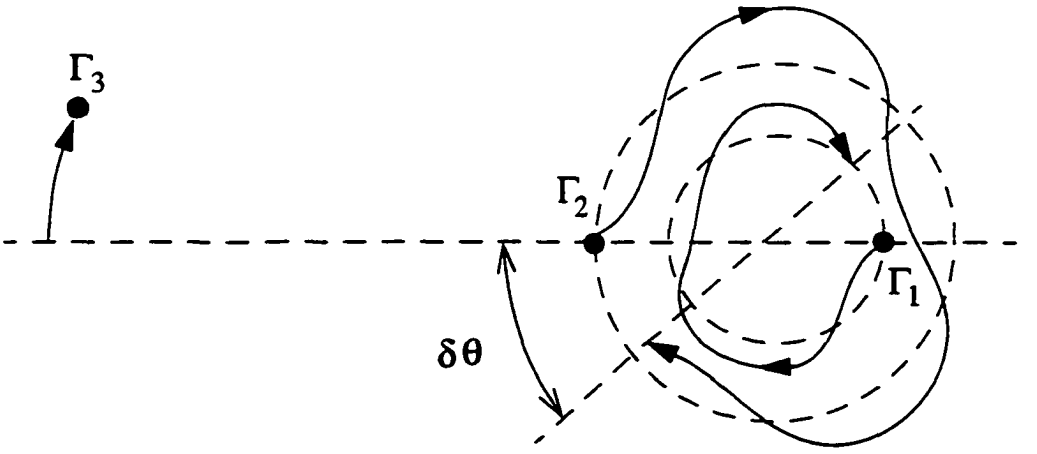

Figure 2.5: A schematic sketch showing the effect of the flow field of Γ_3 on the motion of Γ_2 and Γ_1. In the absence of Γ_3, the constant frequency-constant separation motion of Γ_2 and Γ_1 (about their center of vorticity) is shown by the dashed circles. The presence of Γ_3 distorts these circular orbits in the manner shown (relative to the perturbed center of vorticity of the pair). This causes an angular perturbation of $\delta\theta$ per time period of the unperturbed motion. These perturbations accumulate over Γ_3's time period to give the geometric phase.

We make here several remarks about this system of equations:

1. The equations for (D, ϕ) are coupled to those for (r, θ). In the general formulation described in §2.2, we have made the simplifying assumption that (D, ϕ) are known and thus show up as coefficients in the (r, θ) equations. Here, we derive their evolution in time in an asymptotic form simultaneously from the above equations along with r and θ.

2. For $\epsilon = 0$, the equations reduce to a system in which the farfield vortex is infinitely far away and the two vortices Γ_1 and Γ_2 rotate around their center of vorticity.

3. When $0 < \epsilon << 1$, the farfield vortex Γ_3 is almost equidistant from the other two. The motion of Γ_1 and Γ_2 can be thought of as a small perturbation of the $\epsilon = 0$ problem, see Figure 2.5. As discussed later, the motion of Γ_3 approaches the motion it would have if it were co-orbiting a vortex of strength $\Gamma_1 + \Gamma_2$.

4. We define a (dimensional) time period as the time taken by Γ_3 for an angular change of 2π in ϕ. As a consequence of the previous remark, it is easy to see that for small ϵ this time period varies as $\frac{1}{D_i^2}$. Hence, the nondimensionalised time period T is $O(\frac{1}{\epsilon^2})$ and we can assume the slow time scale $\tau = \epsilon^2 t$

5. Note that with $\alpha_2 = 0$ the last two equations decouple from the rest, D is a constant and ϕ varies linearly with τ. This solution gives the familiar result of two point vortices rotating uniformly about a common (fixed) point. The first two equations then represent the motion of a fluid particle in such a flow (a 'restricted' three-vortex problem) and are of the form represented by (2.1) and (2.2).

Using the multi-scale 'ansatz,' we get a system of four PDEs (with the above initial conditions) and we seek an asymptotic series solution to this system in powers of ϵ:

$$r = \Sigma_{j=0}^{\infty} \epsilon^j r_j(t, \tau),$$

$$\theta = \Sigma_{j=0}^{\infty} \epsilon^j \theta_j(t, \tau),$$

$$D = \Sigma_{j=0}^{\infty} \epsilon^j D_j(t, \tau),$$

$$\phi = \Sigma_{j=0}^{\infty} \epsilon^j \phi_j(t, \tau),$$

where:

$$r_0(0) = 1, \theta_0(0) = \theta_i, D_0(0) = 1, \phi_0(0) = 0,$$

and $r_j(0) = 0, \theta_j(0) = 0, D_j(0) = 0, \phi_j(0) = 0$ for all other j.

Following the method outlined in §2.2 we arrive at the solutions until $O(\epsilon^2)$ as listed below:

$$\begin{aligned}
r_0 &= 1, \\
\theta_0 &= \frac{(\alpha_1 + \alpha_2)}{2\pi} t + \tilde{\theta}_0(\tau), \\
D_0 &= 1, \\
\phi_0 &= \frac{(\alpha_1 + \alpha_2 + \alpha_3)}{2\pi} \tau,
\end{aligned}$$

$$\begin{aligned}
r_1 &= 0, \\
\theta_1 &= \tilde{\theta}_1(\tau), \\
D_1 &= \frac{\alpha_2}{\alpha_1 + \alpha_2} \cos(\phi_0 - \theta_0) + \tilde{D}_1(\tau), \\
\phi_1 &= -\frac{\alpha_2}{\alpha_1 + \alpha_2} \sin(\phi_0 - \theta_0) + \tilde{\phi}_1(\tau),
\end{aligned}$$

$$r_2 = \frac{\alpha_3}{2(\alpha_1 + \alpha_2)} \cos[2(\phi_0 - \theta_0)] + \tilde{r}_2(\tau),$$

$$
\begin{aligned}
\theta_2 &= \frac{\alpha_3}{\alpha_1+\alpha_2}\sin[2(\phi_0-\theta_0)] + \tilde{\theta}_2(\tau), \\
D_2 &= -\frac{\alpha_2}{(\alpha_1+\alpha_2)}(\tilde{\phi}_1-\tilde{\theta}_1)\sin(\phi_0-\theta_0) \\
&\quad -[\frac{\alpha_2}{2(\alpha_1+\alpha_2)}]^2\cos(2(\phi_0-\theta_0)) + \tilde{D}_2(\tau), \\
\phi_2 &= [\frac{\alpha_2}{(\alpha_1+\alpha_2)}]^2\frac{\sin(2(\phi_0-\theta_0))}{2} + \frac{\alpha_2}{(\alpha_1+\alpha_2)}\tilde{D}_1\sin(\phi_0-\theta_0) \\
&\quad -\frac{\alpha_2}{(\alpha_1+\alpha_2)}(\tilde{\phi}_1-\tilde{\theta}_1)\cos(\phi_0-\theta_0) + \tilde{\phi}_2(\tau).
\end{aligned}
$$

The solution for θ_0 displays the characteristic decomposition into a fast term and a slow term. The slow phase equation for $\tilde{\theta}_0(\tau)(\equiv \theta_S)$ comes from imposing the solvability condition in the θ_2 equation. Thus,

$$
\frac{d\tilde{\theta}_0}{d\tau} = -\frac{(\alpha_1+\alpha_2)}{\pi}\tilde{r}_2, \quad \tilde{\theta}_0(0) = \theta_i.
$$

The solutions listed above give all the information necessary[6] to solve for $\tilde{r}_2(\tau)$ by imposing the solvability condition in the $O(\epsilon^4)$ equation in r. Before doing that however we make the following important point.

The leading order terms of D and ϕ do not depend on the fast time. It is clear looking at D_0 and ϕ_0 that Γ_3, to leading order, moves as if co-orbiting a vortex of strength $\Gamma_1+\Gamma_2$. It is only this circular motion of the farfield vortex that is relevant to the geometric phase. As is shown below the phase is determined by the time period of this 2-vortex motion. The higher order terms in D and ϕ (which do depend on the fast time) do not play a role. Indeed, if one were to solve (2.12) and (2.13) with $D = D_0$, $\phi = \phi_0$ for the time period of this 2-vortex motion then one would get the same solutions for r_i, θ_i (i=0,1,2) leading to the same value for the geometric phase. Making the further observation that (2.12) and (2.13) represent, in such a case, the nondimensional equations of motion for a fluid particle in the flow field of two vortices of strengths $\Gamma_1+\Gamma_2$ and Γ_3 leads us to the following:

Proposition 1: *The geometric phase in this 3-vortex problem is the same as the geometric phase in a 'restricted' 3-vortex problem obtained by replacing* Γ_1 *with* $\Gamma_1+\Gamma_2$ *and* Γ_2 *with a fluid particle/passive tracer particle.*

Proceeding with the computations, the equation we finally get for $\tilde{r}_2(\tau)$ is:

$$
\frac{d\tilde{r}_2}{d\tau} = 0, \quad \tilde{r}_2(0) = -\frac{\alpha_3}{2(\alpha_1+\alpha_2)}\cos(2\theta_i).
$$

[6] Note that the explicit form of the other slow functions, for ex. $\tilde{\theta}_1, \tilde{\phi}_1$ etc., need not be known.

Hence, the slow phase for this problem is:

$$\theta_S \equiv \tilde{\theta}_0 = \frac{\alpha_3 \tau}{2\pi}\cos(2\theta_i) + \theta_i. \tag{2.16}$$

Next, we estimate the long time period T as defined in remark 4. Since this is not known exactly, we derive it as an asymptotic series using the asymptotic series solution for ϕ obtained from the above analysis. We are interested in only the leading term[7] for T. Hence, assuming $T \sim T_0/\epsilon^2$ (T_0 is a constant) we do a leading order balance in the equation $2\pi = \phi_0(T_0/\epsilon^2) + \epsilon\phi_1(T_0/\epsilon^2) + ...$ This gives:

$$T \sim \frac{4\pi^2}{(\alpha_1 + \alpha_2 + \alpha_3)\epsilon^2},$$

which is the time period of the 2-vortex motion mentioned above. The Hannay-Berry phase is then obtained from (2.9). Thus,

$$\theta_g = \int_0^{T_0} \frac{d\theta_S}{d\tau} d\tau = \left(\frac{\Gamma_3}{\Gamma_1 + \Gamma_2 + \Gamma_3}\right) 2\pi\cos(2\theta_i). \tag{2.17}$$

We can consider some special cases of the above formula:

Case (i):

If $\Gamma_3 = 0$ then there exists only one time scale in the problem, there is no slowly varying background flow and hence, there is no geometric phase.

Case (ii):

If $\Gamma_1 = \Gamma_2 = \Gamma_3$ then one gets the phase for vortex 2 as

$$\theta_g = \frac{2\pi}{3}\cos 2\theta_i.$$

Case (iii):

If $\Gamma_2 = 0$ then one gets the phase for a fluid particle in the flow field of Γ_1 and Γ_3 as

$$\theta_g = \frac{\Gamma_3}{\Gamma_1 + \Gamma_3} 2\pi\cos 2\theta_i. \tag{2.18}$$

The special case where $\Gamma_3 = \Gamma_1$ was analysed by Newton [69].

[7] Higher order terms in T do not contribute to the phase.

2.3.1 A four-vortex problem

The three-vortex configuration can be extended to a four-vortex configuration by placing a fourth vortex $\Gamma_4(>0)$ in the vicinity of Γ_3 as shown in Figure 2.2. There are now *two* phase object-parent vortex pairs with each pair playing the role of farfield vortices for the other pair. When these two pairs are well separated we expect their slow motion to approach that of two vortices of strengths $\Gamma_1+\Gamma_2$ and $\Gamma_3+\Gamma_4$ respectively. We therefore have an asymptotically defined closed orbit as in the three-vortex problem and we try to see if each pair experiences a geometric phase at the end of one period of this two-vortex motion.

To characterize the slow motion of each pair and to set up the equations of motion of the system we use the following system of variables used by Khanin [43] although in a different context. The equations of motion in Cartesian coordinates follow from (2.10) and (2.11) for $N=4$. We change to intervortex polar variables as before, $(\hat{r},\theta)$ and $(\hat{v},\nu)$ for the pairs Γ_1,Γ_2 and Γ_3,Γ_4 respectively. For the slowly varying variables, following Khanin [43], we choose the distance and angle (with the horizontal) of the line joining the centers of vorticity of each pair respectively. Thus,

$$y_2-y_1=\hat{r}\sin(\theta),\quad x_2-x_1=-\hat{r}\cos(\theta),$$

$$y_4-y_3=\hat{v}\sin(\nu),\quad x_4-x_3=-\hat{v}\cos(\nu),$$

$$\begin{aligned}\frac{\Gamma_3y_3+\Gamma_4y_4}{\Gamma_3+\Gamma_4}-\frac{\Gamma_1y_1+\Gamma_2y_2}{\Gamma_1+\Gamma_2}&=\hat{D}\sin(\phi),\\ \frac{\Gamma_3x_3+\Gamma_4x_4}{\Gamma_3+\Gamma_4}-\frac{\Gamma_1x_1+\Gamma_2x_2}{\Gamma_1+\Gamma_2}&=-\hat{D}\cos(\phi).\end{aligned}$$

Instead of deriving the equations of motion in these polar variables directly from (2.10) and (2.11) we do a further transformation to Khanin's *canonical* variables:

$$\begin{aligned}\hat{R}&=\frac{\hat{r}^2}{2}\left(\frac{\Gamma_1\Gamma_2}{\Gamma_1+\Gamma_2}\right),\\ \hat{V}&=\frac{\hat{v}^2}{2}\left(\frac{\Gamma_3\Gamma_4}{\Gamma_3+\Gamma_4}\right),\\ \hat{P}&=\frac{\hat{D}^2}{2}\frac{(\Gamma_1+\Gamma_2)(\Gamma_3+\Gamma_4)}{\Gamma_1+\Gamma_2+\Gamma_3+\Gamma_4},\end{aligned}$$

the angle variables remaining unchanged. The Hamiltonian in these variables becomes:

$$\begin{aligned}H(\hat{R},\theta,\hat{V},\nu,\hat{P},\phi)&=-\frac{1}{4\pi}[\Gamma_1\Gamma_2\log\left\{2\frac{(\Gamma_1+\Gamma_2)}{\Gamma_1\Gamma_2}\hat{R}\right\}+\Gamma_3\Gamma_4\log\left\{2\frac{(\Gamma_3+\Gamma_4)}{\Gamma_3\Gamma_4}\hat{V}\right\}\\ &\quad+\Gamma_1\Gamma_3\log(l_{13})+\Gamma_1\Gamma_4\log(l_{14})+\Gamma_2\Gamma_3\log(l_{23})+\Gamma_2\Gamma_4\log(l_{24})],\end{aligned}$$

where:

$$
\begin{aligned}
l_{13} &= A^2\hat{P} + B^2\hat{V} + C^2\hat{R} - 2AB\sqrt{\hat{P}\hat{V}}\cos(\phi-\nu) + 2AC\sqrt{\hat{P}\hat{R}}\cos(\phi-\theta) \\
&\qquad -2BC\sqrt{\hat{V}\hat{R}}\cos(\nu-\theta), \\
l_{14} &= A^2\hat{P} + B^2\left(\frac{\Gamma_3}{\Gamma_4}\right)^2\hat{V} + C^2\hat{R} + 2AB\left(\frac{\Gamma_3}{\Gamma_4}\right)\sqrt{\hat{P}\hat{V}}\cos(\phi-\nu) \\
&\qquad +2AC\sqrt{\hat{P}\hat{R}}\cos(\phi-\theta) + 2BC\left(\frac{\Gamma_3}{\Gamma_4}\right)\sqrt{\hat{V}\hat{R}}\cos(\nu-\theta), \\
l_{23} &= A^2\hat{P} + B^2\hat{V} + C^2\left(\frac{\Gamma_1}{\Gamma_2}\right)^2\hat{R} - 2AB\sqrt{\hat{P}\hat{V}}\cos(\phi-\nu) \\
&\qquad -2AC\left(\frac{\Gamma_1}{\Gamma_2}\right)\sqrt{\hat{P}\hat{R}}\cos(\phi-\theta) + 2BC\left(\frac{\Gamma_1}{\Gamma_2}\right)\sqrt{\hat{V}\hat{R}}\cos(\nu-\theta), \\
l_{24} &= A^2\hat{P} + B^2\left(\frac{\Gamma_3}{\Gamma_4}\right)^2\hat{V} + C^2\left(\frac{\Gamma_1}{\Gamma_2}\right)^2\hat{R} + 2AB\left(\frac{\Gamma_3}{\Gamma_4}\right)\sqrt{\hat{P}\hat{V}}\cos(\phi-\nu) \\
&\qquad -2AC\left(\frac{\Gamma_1}{\Gamma_2}\right)\sqrt{\hat{P}\hat{R}}\cos(\phi-\theta) - 2BC\left(\frac{\Gamma_1\Gamma_3}{\Gamma_2\Gamma_4}\right)\sqrt{\hat{V}\hat{R}}\cos(\nu-\theta),
\end{aligned}
$$

and A, B, C are the following functions of the vortex strengths:

$$
A = \sqrt{\frac{2(\Gamma_1+\Gamma_2+\Gamma_3+\Gamma_4)}{(\Gamma_3+\Gamma_4)(\Gamma_1+\Gamma_2)}}, \quad B = \sqrt{\frac{2\Gamma_4}{\Gamma_3(\Gamma_3+\Gamma_4)}}, \quad C = \sqrt{\frac{2\Gamma_2}{\Gamma_1(\Gamma_1+\Gamma_2)}}.
$$

The equations of motion in these variables are then easily obtained from the canonical structure:

$$
\begin{aligned}
\frac{d\hat{R}}{d\hat{t}} &= \frac{\partial H}{\partial\theta}, \qquad \frac{d\hat{V}}{d\hat{t}} = \frac{\partial H}{\partial\nu}, \qquad \frac{d\hat{P}}{d\hat{t}} = \frac{\partial H}{\partial\phi}, \\
\frac{d\theta}{d\hat{t}} &= -\frac{\partial H}{\partial\hat{R}}, \qquad \frac{d\nu}{d\hat{t}} = -\frac{\partial H}{\partial\hat{V}}, \qquad \frac{d\phi}{d\hat{t}} = -\frac{\partial H}{\partial\hat{P}}.
\end{aligned}
$$

We now proceed to nondimensionalize these equations as before:

$$
R = \frac{\hat{R}}{R_i}, \quad , V = \frac{\hat{V}}{V_i}, \quad P = \frac{\hat{P}}{P_i}, \quad t = \omega\hat{t},
$$

where the subscript i denotes initial values. ω is again chosen to be proportional to the unperturbed phase object-parent vortex frequency, but since there are two such pairs we arbitrarily choose the pair Γ_1, Γ_2. Thus $\omega \propto 1/R_i$. We pick the same pair for defining the perturbation parameter:

$$
\epsilon^2 = \frac{R_i}{P_i}.
$$

For notational convenience we also define:

$$\Lambda^2 = \frac{V_i}{R_i} \Rightarrow \epsilon^2\Lambda^2 = \frac{V_i}{P_i}, \quad \alpha_{jk} = \frac{\Gamma_j\Gamma_k}{\omega R_i} \quad (j = 1,2; k = 3,4).$$

This gives the following system of non-dimensional equations:

$$\begin{aligned}
\frac{dR}{dt} &= \frac{\epsilon}{4\pi}\sum_{j=1}^{2}\sum_{k=3}^{4}\frac{\alpha_{jk}M^R_{jk}}{\bar{l}_{jk}},\\
\frac{d\theta}{dt} &= \frac{1}{4\pi}\left[\frac{\alpha_{12}}{R} + \epsilon\sum_{j=1}^{2}\sum_{k=3}^{4}\frac{\alpha_{jk}M^\theta_{jk}}{\bar{l}_{jk}}\right],\\
\frac{dV}{dt} &= \frac{\epsilon}{4\pi\Lambda^2}\sum_{j=1}^{2}\sum_{k=3}^{4}\frac{\alpha_{jk}N^V_{jk}}{\bar{l}_{jk}},\\
\frac{d\nu}{dt} &= \frac{1}{4\pi}\left[\frac{\alpha_{34}}{\Lambda^2 V} + \epsilon\sum_{j=1}^{2}\sum_{k=3}^{4}\frac{\alpha_{jk}N^\nu_{jk}}{\bar{l}_{jk}}\right],\\
\frac{dP}{dt} &= \frac{\epsilon^3}{4\pi}\sum_{j=1}^{2}\sum_{k=3}^{4}\frac{\alpha_{jk}O^P_{jk}}{\bar{l}_{jk}},\\
\frac{d\phi}{dt} &= \frac{\epsilon^2}{4\pi}\sum_{j=1}^{2}\sum_{k=3}^{4}\frac{\alpha_{jk}O^\phi_{jk}}{\bar{l}_{jk}},
\end{aligned}$$

where $\bar{l}_{jk} = l_{jk}/P_i$ and:

$$\begin{aligned}
M^R_{jk} &= f^R_{jk}\sqrt{RP}\sin(\phi-\theta) + \Lambda\epsilon g^R_{jk}\sqrt{RV}\sin(\nu-\theta),\\
M^\theta_{jk} &= \epsilon f^\theta_{jk} + g^\theta_{jk}\sqrt{P/R}\cos(\phi-\theta) + \Lambda\epsilon h^\theta_{jk}\sqrt{V/R}\cos(\nu-\theta),\\
N^V_{jk} &= f^V_{jk}\Lambda\sqrt{PV}\sin(\phi-\nu) + \Lambda\epsilon g^V_{jk}\sqrt{RV}\sin(\nu-\theta),\\
N^\nu_{jk} &= \epsilon f^\nu_{jk} + (g^\nu_{jk}/\Lambda)\sqrt{P/V}\cos(\phi-\nu) + (\epsilon/\Lambda)h^\nu_{jk}\sqrt{R/V}\cos(\nu-\theta),\\
O^P_{jk} &= \Lambda f^P_{jk}\sqrt{PV}\sin(\phi-\nu) + g^P_{jk}\sqrt{RP}\sin(\phi-\theta),\\
O^\phi_{jk} &= f^\phi_{jk} + \epsilon\Lambda g^\phi_{jk}\sqrt{V/P}\cos(\phi-\nu) + \epsilon h^\phi_{jk}\sqrt{R/P}\cos(\phi-\theta),
\end{aligned}$$

where:

$$\begin{aligned}
&-f^R_{13} = -f^R_{14} = 2g^\theta_{13} = 2g^\theta_{14} = g^P_{13} = g^P_{14} = 2h^\phi_{13} = 2h^\phi_{14} = 2AC,\\
&f^R_{23} = f^R_{24} = -2g^\theta_{23} = -2g^\theta_{24} = -g^P_{23} = -g^P_{24} = -2h^\phi_{23} = -2h^\phi_{24} = 2AC(\Gamma_1/\Gamma_2),\\
&f^V_{13} = f^V_{23} = -2g^\nu_{13} = -2g^\nu_{23} = -f^P_{13} = -f^P_{23} = -2g^\phi_{13} = -2g^\phi_{23} = 2AB,\\
&-f^V_{14} = -f^V_{24} = 2g^\nu_{14} = 2g^\nu_{24} = f^P_{14} = f^P_{24} = 2g^\phi_{14} = 2g^\phi_{24} = 2AB(\Gamma_3/\Gamma_4),\\
&g^R_{13} = -2h^\theta_{13} = -g^V_{13} = -2h^\nu_{13} = 2BC,
\end{aligned}$$

$$
\begin{aligned}
&-g^R_{14} = 2h^\theta_{14} = g^V_{14} = 2h^\nu_{14} = 2BC(\Gamma_3/\Gamma_4),\\
&-g^R_{23} = 2h^\theta_{23} = g^V_{23} = 2h^\nu_{23} = 2BC(\Gamma_1/\Gamma_2),\\
&g^R_{24} = -2h^\theta_{24} = -g^V_{24} = -2h^\nu_{24} = 2BC[\Gamma_3\Gamma_1/(\Gamma_4\Gamma_2)],\\
&f^\theta_{13} = f^\theta_{14} = C^2,\\
&f^\theta_{23} = f^\theta_{24} = C^2(\Gamma_1/\Gamma_2)^2,\\
&f^\nu_{13} = f^\nu_{23} = B^2,\\
&f^\nu_{14} = f^\nu_{24} = B^2(\Gamma_3/\Gamma_4)^2,\\
&f^\phi_{13} = f^\phi_{14} = f^\phi_{23} = f^\phi_{24} = A^2.
\end{aligned}
$$

We compare this system of equations to the three-vortex system (2.12), (2.13), (2.14) and (2.15). All the remarks made there apply in an analogous manner here. Note that in addition, dP/dt and $d\phi/dt$ are of higher order terms in ϵ than dD/dt and $d\phi/dt$ in the three-vortex system.

Choosing the slow time $\tau = \epsilon^2 t$, we perform a multi-scale analysis as before and evaluate the changes in θ and ν in the time that ϕ changes through 2π. This time period to leading order is the time period of the two-vortex motion of $\Gamma_1 + \Gamma_2$ and $\Gamma_3 + \Gamma_4$. The initial conditions are $R(0) = 1$, $\theta(0) = \theta_i$, $V(0) = 1$, $\nu(0) = \nu_i$, $P(0) = 1$ and $\phi(0) = 0$. At leading order we get:

$$
\begin{aligned}
R_0 &= 1,\\
\theta_0 &= \frac{\alpha_{12}t}{4\pi} + \theta_S(\tau),\\
V_0 &= 1,\\
\nu_0 &= \frac{\alpha_{34}t}{4\pi\Lambda^2} + \nu_S(\tau),\\
P_0 &= 1,\\
\phi_0 &= \left(\frac{\alpha_{13}+\alpha_{14}+\alpha_{23}+\alpha_{24}}{4\pi}\right)\tau,
\end{aligned}
$$

indicating the characteristic decomposition into a fast and a slow term in θ and ν. As before the slow phase terms θ_S and ν_S are determined by $O(\epsilon^2)$ terms in R and V respectively:

$$
\frac{d\theta_S}{d\tau} = -\frac{\alpha_{12}}{4\pi}\tilde{R}_2, \qquad \frac{d\nu_S}{d\tau} = -\frac{\alpha_{34}}{4\pi\Lambda^2}\tilde{V}_2, \tag{2.19}
$$

with initial conditions $\theta_S(0) = \theta_i$ and $\nu_S(0) = \nu_i$. Proceeding to $O(\epsilon^4)$ we get

$$
\begin{aligned}
\tilde{R}_2(\tau) = \tilde{R}_2(0) &= -\frac{C^2}{\alpha_{12}A^2}\left[\alpha_{13}+\alpha_{14}+(\alpha_{23}+\alpha_{24})\left(\frac{\Gamma_1}{\Gamma_2}\right)^2\right]\cos 2\theta_i,\\
\tilde{V}_2(\tau) = \tilde{V}_2(0) &= -\frac{B^2\Lambda^2}{\alpha_{34}A^2}\left[\alpha_{13}+\alpha_{23}+(\alpha_{14}+\alpha_{24})\left(\frac{\Gamma_3}{\Gamma_4}\right)^2\right]\cos 2\nu_i,
\end{aligned}
$$

From the ϕ_0 equation we get $T \sim 8\pi/(\alpha_{13} + \alpha_{14} + \alpha_{23} + \alpha_{24})$ and this leads to the geometric phase in θ and ν:

$$\theta_g = \frac{\Gamma_3 + \Gamma_4}{\Gamma_1 + \Gamma_2 + \Gamma_3 + \Gamma_4} 2\pi \cos 2\theta_i,$$
$$\nu_g = \frac{\Gamma_1 + \Gamma_2}{\Gamma_1 + \Gamma_2 + \Gamma_3 + \Gamma_4} 2\pi \cos 2\nu_i.$$

For $\Gamma_4 = 0$, θ_g gives the geometric phase derived in §2.3 and ν_g gives the geometric phase for a passive particle in the vicinity of Γ_3 in the three-vortex problem.

2.4 A point vortex in a circle

In this problem we consider the influence of a rigid boundary in a simple problem. We track a fluid particle orbiting a point vortex in a circle as in Figure 2.3. The vortex is stationary when at the center of the circle and moves in a concentric circular orbit with constant speed when displaced from the center. See [99, 100] for some interesting recent work on this flowfield.

The circular motion of the vortex is governed by the Hamiltonian $H_v(p,q) = \frac{\Gamma}{4\pi}\log[R_2^2 - (p^2+q^2)]$, where p, q are the (canonical) coordinates of the vortex of strength Γ in a Cartesian frame centred at the origin of the circle and R_2 is the radius of the circle. If $R_1 (= \sqrt{p^2+q^2})$ denotes the radius of the vortex motion then its speed along its orbit is given by $\frac{\Gamma}{2\pi}\frac{R_1}{R_2^2 - R_1^2}$. From this it follows that the time period of the vortex motion is given by $T = \frac{4\pi^2}{\Gamma}(R_2^2 - R_1^2)$. The motion of the fluid particle is also governed by a Hamiltonian system of equations. For $R_1 = 0$, the vortex remains stationary at the center of the circle and the particle motion is not affected by the boundary since the boundary is a streamline for the time independent flow. It orbits the vortex in circular motion just as in an unbounded flow. If $R_1 \neq 0$, for (canonical) coordinates x, y in the same frame as above, the Hamiltonian is:

$$H(x,y,t) = \frac{\Gamma}{4\pi}\log\left[\frac{(x-p)^2 + (y-q)^2}{(x-ap)^2 + (y-aq)^2}\right], \qquad a = (\frac{R_2}{R_1})^2,$$

where the explicit time dependency of the Hamiltonian is due to the motion of the vortex. It is clear from the form of the Hamiltonian that the equivalent flow without boundary can be achieved by placing an image vortex (the farfield vortex) of strength $-\Gamma$ at radius R_2^2/R_1. The distance between the given vortex and the image vortex is, therefore, $(a-1)R_1 = D$ at all times. The time period of the vortex motion can be rewritten in terms of this distance as $T = \frac{4\pi^2}{\Gamma}(a-1)R_1^2$.

For the phase calculation, we convert to the relative coordinates $\hat{r}, \theta$ as in the previous problem:

$$\begin{aligned} x - p &= -\hat{r}\cos\theta, \qquad x - ap = D\cos\phi - \hat{r}\cos\theta, \\ y - q &= \hat{r}\sin\theta, \qquad y - aq = -D\sin\phi + \hat{r}\sin\theta, \end{aligned}$$

where $\phi = \frac{\Gamma}{2\pi}\frac{\hat{t}}{(R_2^2-R_1^2)} = \frac{\Gamma}{2\pi}\frac{\hat{t}}{(a-1)R_1^2}$ is the angular velocity of the vortex. The small parameter for the adiabatic problem is chosen, as before, as being proportional to the ratio of the initial particle-vortex distance, R_i, to the distance between the parent vortex and farfield vortex D. Specifically,

$$\epsilon = \frac{R_i}{D}.$$

The scheme for non-dimensionalising the variables is the same as before i.e. $\hat{r}$ by R_i and $\hat{t}$ by ω where ω is proportional to the frequency of the particle about an isolated vortex in the absence of the boundary i.e. to $\frac{1}{R_1^2}$. This defines the nondimensional constant α as before. The nondimensional time period of the vortex motion becomes:

$$T = \frac{4\pi^2}{\alpha(a-1)\epsilon^2} = \frac{\beta}{\epsilon^2},$$

and the slowly varying angle coefficient $\phi = \frac{\alpha(a-1)}{2\pi}\epsilon^2 t$. The nondimensional equations of motion for the particle are:

$$\begin{aligned}
\frac{dr}{dt} &= \frac{\alpha}{2\pi}\left[\epsilon\sin(\phi-\theta) - \frac{\epsilon\sin(\phi-\theta)}{1-2\epsilon r\cos(\phi-\theta)+\epsilon^2 r^2}\right], \\
\frac{d\theta}{dt} &= \frac{\alpha}{2\pi}\left[\frac{1}{r^2} + \frac{\frac{\epsilon}{r}\cos(\phi-\theta)-\epsilon^2}{1-2\epsilon r\cos(\phi-\theta)+\epsilon^2 r^2} - \frac{\epsilon\cos(\phi-\theta)}{r}\right],
\end{aligned}$$

with initial conditons $r(0) = 1, \theta(0) = \theta_i$.

These equations have the general structure of equations (2.1) and (2.2) discussed in §2.2. We choose the slow time scale $\tau = \epsilon^2 t$, verify that the assumptions made in that section hold here and make a direct comparison of terms. We have:

$$\begin{aligned}
f &= \frac{\alpha}{2\pi}\frac{\epsilon r^2\sin(\tilde{\phi}-\theta) - r\sin\left[2(\tilde{\phi}-\theta)\right]}{1-2\epsilon r\cos(\tilde{\phi}-\theta)+\epsilon^2 r^2}, \\
\Omega &= \frac{\alpha}{2\pi}.
\end{aligned}$$

Hence,

$$\begin{aligned}
f_0 &= f\left(r=1, \theta = \Omega t + \tilde{\theta}_0, \tilde{\phi}, \epsilon = 0\right), \\
&= -\frac{\alpha}{2\pi}\sin\left[2\left(\tilde{\phi} - \frac{\alpha t}{2\pi} - \tilde{\theta}_0\right)\right].
\end{aligned}$$

Hence,

$$\int f_0 dt_{|t=0} = -\frac{\cos 2\theta_i}{2},$$

and the slow phase term from (2.5) is:

$$\theta_S \equiv \tilde{\theta}_0(\tau) = -\frac{\alpha}{2\pi}\tau\cos 2\theta_i + \theta_i. \tag{2.20}$$

Therefore, the Hannay-Berry phase in this problem using (2.9) is:

$$\begin{aligned}\theta_g &= \int_0^{\beta} \frac{d\theta_S}{d\tau}d\tau, \\ &= -\frac{2\pi}{(a-1)}\cos 2\theta_i = -\frac{2\pi}{(\frac{R_2}{R_1})^2 - 1}\cos 2\theta_i.\end{aligned} \tag{2.21}$$

2.5 A mixing layer model

2.5.1 The model

Consider an infinite number of equally spaced point vortices of the same strength and sign. The vortices in this configuration are all stationary due to the symmetry of the flow field about horizontal and vertical axes passing through any point vortex. If the strength of each vortex is Γ and the spacing between vortices is a, then the complex potential of the flow is given by (see [48], p. 224):[8]

$$w(z) = -\frac{i\Gamma}{2\pi}\log\sin\left[\pi\left(\frac{z - z_{vor}}{a}\right)\right],$$

where $z = x + iy$ is an arbitrary point in the flowfield and $z_{vor} = x_{vor} + iy_{vor}$ denotes the position of any *one* vortex in the row in some chosen x-y coordinate system. (The row is assumed to be parallel to the x-axis). The flow field is given by:

$$\frac{dx}{dt} = \frac{\Gamma}{2a}\frac{\sinh\left[2\pi\left(\frac{y-y_{vor}}{a}\right)\right]}{\cosh\left[2\pi\left(\frac{y-y_{vor}}{a}\right)\right] - \cos\left[2\pi\left(\frac{x-x_{vor}}{a}\right)\right]}, \tag{2.22}$$

$$\frac{dy}{dt} = -\frac{\Gamma}{2a}\frac{\sin\left[2\pi\left(\frac{x-x_{vor}}{a}\right)\right]}{\cosh\left[2\pi\left(\frac{y-y_{vor}}{a}\right)\right] - \cos\left[2\pi\left(\frac{x-x_{vor}}{a}\right)\right]}. \tag{2.23}$$

Note that the equations of motion are invariant with respect to any transformation $z_{vor} \rightarrow z_{vor} \pm na$, $n = 1, 2, \ldots$. If the symmetry about the vertical axis is broken by a perturbation that pushes every adjacent pair of vortices towards each other by an amount Δ, as shown in Figure 2.4, then the vortices start moving in pairs. They move such that each vortex in a pair orbits the other in a closed path. This motion is the same for every pair. The flowfield can be viewed

[8] The complex potential is obtained by adding the complex potential due to each vortex, ignoring constant terms and using the relation $\sin z = \prod_{k=1}^{\infty}\left(1 - \frac{z^2}{k^2\pi^2}\right)$ to simplify.

as the superposition of two infinite evenly spaced rows [59], each with inter-vortex spacing $2a$. The motion of a vortex in row 1 is influenced only by the vortices in row 2 and vice-versa.

We choose an x-y coordinate system in which the x-axis coincides with the direction of the original unperturbed row. Then if (x_{vor}, y_{vor}) are the coordinates of any one vortex in a row, the coordinates of any vortex in the opposite row are of the form:

$$(2na - x_{vor}, -y_{vor}), \qquad n = 0, \pm 1, \pm 2, ... \tag{2.24}$$

Since a point vortex moves like a fluid particle in its place, the equations of motion of any vortex in either row are given by (2.22) and (2.23) with a replaced by $2a$. Thus, the equations of motion for the perturbed vortices are:

$$\frac{dx_{vor}}{dt} = \frac{\Gamma}{4a} \frac{\sinh\left[\frac{2\pi y_{vor}}{a}\right]}{\cosh\left[\frac{2\pi y_{vor}}{a}\right] - \cos\left[\frac{2\pi x_{vor}}{a}\right]}, \tag{2.25}$$

$$\frac{dy_{vor}}{dt} = -\frac{\Gamma}{4a} \frac{\sin\left[\frac{2\pi x_{vor}}{a}\right]}{\cosh\left[\frac{2\pi y_{vor}}{a}\right] - \cos\left[\frac{2\pi x_{vor}}{a}\right]}. \tag{2.26}$$

It is easily checked that the above system (2.25), (2.26) is Hamiltonian with:

$$H = \frac{\Gamma}{8\pi} \log\left[\cosh(\frac{2\pi y_{vor}}{a}) - \cos(\frac{2\pi x_{vor}}{a})\right], \tag{2.27}$$

which is an invariant of the motion. Using this fact, an exact solution can be obtained for initial conditions $x_{vor}(0) = a/2 - \Delta, y_{vor}(0) = 0$ in terms of the Jacobi elliptic functions:

$$\tan(\frac{\pi x_{vor}}{a}) = \cot(\frac{\pi\Delta}{a}) \mathrm{cn}\left(\frac{\pi\Gamma t}{4ka^2}, k\right), \tag{2.28}$$

$$\tanh(\frac{\pi y_{vor}}{a}) = -\frac{\cot(\frac{\pi\Delta}{a})}{1 + \cot^2(\frac{\pi\Delta}{a})} \mathrm{sd}\left(\frac{\pi\Gamma t}{4ka^2}, k\right), \tag{2.29}$$

where $k = \cos^2(\frac{\pi\Delta}{a})$ is the modulus of the associated (incomplete) elliptic integrals of the first kind [19]. Note that when Δ is small, k is close to 1 and when Δ is near $a/2$ i.e. when the vortices in each pair are close to each other, k is close to 0. The time period of the vortex motion, T, is related in a simple manner to the complete elliptic integral, K, as:

$$T = \frac{16ka^2}{\pi\Gamma} K.$$

Since K has infinite series representations in terms of the modulus k, [19] the time period T can also be represented exactly by an infinite series. We choose the following representation for K:

$$K = \frac{\pi}{2} \sum_{m=0}^{\infty} \frac{(\frac{1}{2})_m (\frac{1}{2})_m}{m!m!} k^{2m}, \tag{2.30}$$

where $(\frac{1}{2})_0 = 1$, $(\frac{1}{2})_m = \frac{1}{2}(\frac{1}{2}+1).....(\frac{1}{2}+m-1)$ for $m = 1, 2, ...$ and $m!$ represents factorial of m. Hence:

$$\begin{aligned} T &= \frac{16ka^2}{\pi\Gamma}\left[\frac{\pi}{2}\sum_{m=0}^{\infty}\frac{(\frac{1}{2})_m(\frac{1}{2})_m}{m!m!}k^{2m}\right], \\ &= \frac{8a^2}{\Gamma}\left[\sum_{m=0}^{\infty}\frac{(\frac{1}{2})_m(\frac{1}{2})_m}{m!m!}k^{2m+1}\right]. \end{aligned}$$

The equations of motion, in x-y coordinates, for the particle in the perturbed field are shown below. These equations are obtained from (2.22) and (2.23) using relation (2.24):

$$\begin{aligned} \frac{dx}{dt} &= \frac{\Gamma}{4a}\frac{\sinh\left[\pi\left(\frac{y-y_{vor}}{a}\right)\right]}{\cosh\left[\pi\left(\frac{y-y_{vor}}{a}\right)\right]-\cos\left[\pi\left(\frac{x-x_{vor}}{a}\right)\right]} \\ &\quad +\frac{\Gamma}{4a}\frac{\sinh\left[\pi\left(\frac{y+y_{vor}}{a}\right)\right]}{\cosh\left[\pi\left(\frac{y+y_{vor}}{a}\right)\right]-\cos\left[\pi\left(\frac{x+x_{vor}}{a}\right)\right]}, \end{aligned} \tag{2.31}$$

$$\begin{aligned} \frac{dy}{dt} &= -\frac{\Gamma}{4a}\frac{\sin\left[\pi\left(\frac{x-x_{vor}}{a}\right)\right]}{\cosh\left[\pi\left(\frac{y-y_{vor}}{a}\right)\right]-\cos\left[\pi\left(\frac{x-x_{vor}}{a}\right)\right]} \\ &\quad -\frac{\Gamma}{4a}\frac{\sin\left[\pi\left(\frac{x+x_{vor}}{a}\right)\right]}{\cosh\left[\pi\left(\frac{y+y_{vor}}{a}\right)\right]-\cos\left[\pi\left(\frac{x+x_{vor}}{a}\right)\right]}, \end{aligned} \tag{2.32}$$

where (x_{vor}, y_{vor}) refer to the coordinates of any one vortex in either row.

2.5.2 The geometric phase in the model

For the geometric phase calculation in this model we focus on a pair of nearest vortices from opposite rows as shown in Figure 2.6. We use, as before, $\hat{r}$ for the particle-parent vortex distance[9] and $\hat{D}$ for the parent vortex-farfield vortex distance, and θ and ϕ for their respective angles with the horizontal axis. The origin of the x-y coordinate system (chosen earlier so that the x-axis coincided with the original unperturbed row) is now fixed midway between the two vortices. We thus obtain the transformations:

$$\begin{aligned} x - x_{vor} &= -\hat{r}\cos\theta, \quad 2x_{vor} = \hat{D}\cos\phi, \\ y - y_{vor} &= \hat{r}\sin\theta, \quad 2y_{vor} = -\hat{D}\sin\phi. \end{aligned}$$

[9] The parent vortex could be chosen to be either vortex of the pair.

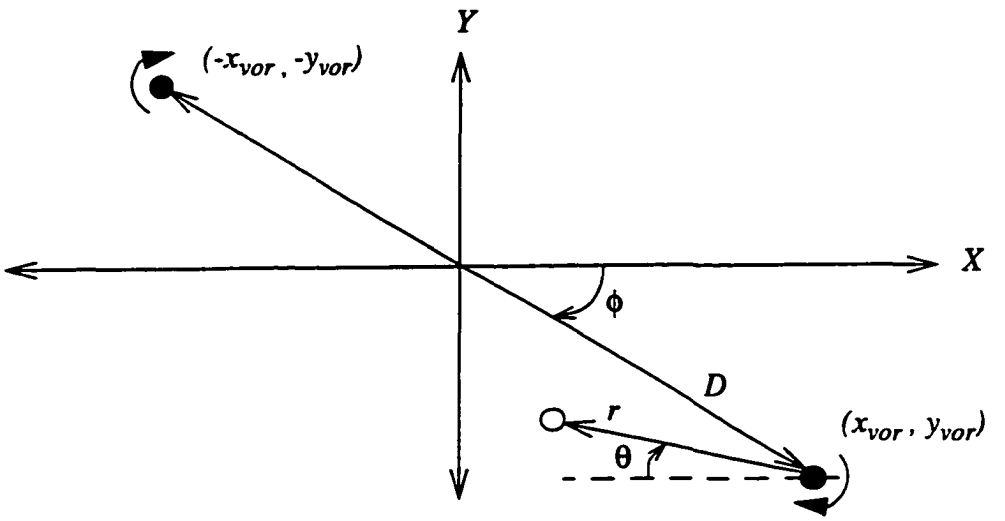

Figure 2.6: An orbiting pair of vortices (filled circles) and a fluid particle (unfilled circle) in the mixing layer model. The cartesian X-Y frame is centered at the midpoint of the line joining the vortices

It follows that

$$\begin{aligned} x + x_{vor} &= \hat{D}\cos\phi - \hat{r}\cos\theta, \\ y + y_{vor} &= -\hat{D}\sin\phi + \hat{r}\sin\theta. \end{aligned}$$

Denoting initial distances by r_i and $\hat{D}_i$ respectively (note that $D_i = a - 2\Delta$), we introduce non-dimensional variables as before:

$$\begin{aligned} r &= \frac{\hat{r}}{r_i}, \\ D &= \frac{\hat{D}}{D_i}. \end{aligned}$$

For notational convenience, we introduce the nondimensional parameter $\delta = \pi\frac{D_i}{a}$. Thus, $k = \sin^2(\delta/2)$. The small parameter ϵ is defined as:

$$\epsilon = \delta\frac{r_i}{D_i}.$$

The time is non-dimensionalised as

$$t = \omega\hat{t},$$

where ω, for fixed δ, is a frequency proportional to that of a particle around an isolated vortex in unbounded flow. We define it as:

$$\begin{aligned} \omega &= \frac{\Gamma}{4\pi k r_i^2}, \\ &= \frac{\pi\Gamma}{4ka^2}\frac{1}{\epsilon^2}. \end{aligned} \tag{2.33}$$

The arguments of the elliptic functions in (2.28) and (2.29), thus, transform as:

$$\frac{\pi\Gamma\hat{t}}{4ka^2} = \epsilon^2\omega\hat{t} = \epsilon^2 t,$$

which is the slow time scale of the motion of the vortices. The nondimensional time period is:

$$T = \frac{4K}{\epsilon^2}.$$

Note that this nondimensional time period depends on δ through K.

With these transformations the nondimensional equations of motion for the particle in (r, θ) become:

$$\begin{aligned} \frac{dr}{dt} = k\epsilon\Bigg[&\frac{S_h\cosh(\epsilon r\sin\theta)\cos\theta - C_h\sinh(\epsilon r\sin\theta)\cos\theta - S_t\cos(\epsilon r\cos\theta)\sin\theta + C_t\sin(\epsilon r\cos\theta)\sin\theta}{-S_h\sinh(\epsilon r\sin\theta) + C_h\cosh(\epsilon r\sin\theta) - S_t\sin(\epsilon r\cos\theta) - C_t\cos(\epsilon r\cos\theta)} \\ &+\frac{\sin(\epsilon r\cos\theta)\sin\theta - \sinh(\epsilon r\sin\theta)\cos\theta}{\cosh(\epsilon r\sin\theta) - \cos(\epsilon r\cos\theta)} + \frac{S_t\sin\theta - S_h\cos\theta}{C_h - C_t}\Bigg], \end{aligned} \tag{2.34}$$

$$\begin{aligned} \frac{d\theta}{dt} = \frac{k\epsilon}{r}\Bigg[&\frac{-S_h\cosh(\epsilon r\sin\theta)\sin\theta + C_h\sinh(\epsilon r\sin\theta)\sin\theta - S_t\cos(\epsilon r\cos\theta)\cos\theta + C_t\sin(\epsilon r\cos\theta)\cos\theta}{-S_h\sinh(\epsilon r sin\theta) + C_h\cosh(\epsilon r\sin\theta) - S_t\sin(\epsilon r\cos\theta) - C_t\cos(\epsilon r\cos\theta)} \\ &+\frac{\sin(\epsilon r\cos\theta)\cos\theta + \sinh(\epsilon r\sin\theta)\sin\theta}{\cosh(\epsilon r\sin\theta) - \cos(\epsilon r\cos\theta)} + \frac{S_t\cos\theta + S_h\sin\theta}{C_h - C_t}\Bigg], \end{aligned} \tag{2.35}$$

where

$$\begin{aligned} S_h(\epsilon^2 t) &= \sinh(\delta D(\epsilon^2 t)\sin\phi(\epsilon^2 t)), \\ C_h(\epsilon^2 t) &= \cosh(\delta D(\epsilon^2 t)\sin\phi(\epsilon^2 t)), \\ S_t(\epsilon^2 t) &= \sin(\delta D(\epsilon^2 t)\cos\phi(\epsilon^2 t)), \\ C_t(\epsilon^2 t) &= \cos(\delta D(\epsilon^2 t)\cos\phi(\epsilon^2 t)), \end{aligned}$$

are functions of the vortex motion and $C_h - C_t = L$ is an invariant. For the chosen initial conditions of the vortex ($D(0) = 1, \phi(0) = 0$), $L = 1 - \cos\delta = 2k$. The initial conditions for the particle are $r(0) = 1, \theta(0) = \theta_i$.

The equations of motion as written above can be brought in the form of (2.1) and (2.2) by expanding (for small ϵ) the trigonometric and hyperbolic functions that appear in them. This enables us to rewrite them as:

$$\begin{aligned} \frac{dr}{dt} &= \epsilon^2 f(r, \theta, D, \phi, \epsilon), \\ \frac{d\theta}{dt} &= \frac{2k}{r^2} + \epsilon^2 g(r, \theta, D, \phi, \epsilon), \end{aligned}$$

where f and g are infinite series obtained from the expansions. The series for f is of the following form:

$$f(r, \theta, D, \phi, \epsilon) = kr\left[\frac{S_h S_t}{L^2}\cos 2\theta + \left(\frac{S_h^2 - S_t^2}{2L^2} - \frac{2}{3}\right)\sin 2\theta\right] + \epsilon f_1(r, \theta, D, \phi) + \ldots\ldots$$

Denoting the slow time by $\tau = \epsilon^2 t$ we apply the multi-scale method as outlined in §2.2. As per our notation we denote functions of τ alone by overhead $\sim$. We verify that the assumptions made in that section hold here and by a direct comparision of terms we get:

$$\begin{aligned} \Omega &= 2k, \\ f_0 &= f(r = 1, \theta = \Omega t + \tilde{\theta}_0, \tilde{D}, \tilde{\phi}, \epsilon = 0), \\ &= k\left[\frac{\tilde{S}_h \tilde{S}_t}{L^2}\cos\left[2\left(2kt + \tilde{\theta}_0\right)\right] + \left(\frac{\tilde{S}_h^2 - \tilde{S}_t^2}{2L^2} - \frac{2}{3}\right)\sin\left[2\left(2kt + \tilde{\theta}_0\right)\right]\right]. \end{aligned}$$

Hence,

$$\begin{aligned} \int f_0 dt_{|t=0} &= \frac{1}{4}\left[\frac{\tilde{S}_h(0)\tilde{S}_t(0)}{L^2}\sin 2\theta_i - \left(\frac{\tilde{S}_h^2(0) - \tilde{S}_t^2(0)}{2L^2} - \frac{2}{3}\right)\cos 2\theta_i\right], \\ &= \left(\frac{k+3}{24k}\right)\cos 2\theta_i. \end{aligned}$$

The slow phase term from (2.5) is:

$$\theta_S \equiv \tilde{\theta}_0(\tau) = \left(\frac{k+3}{6}\right)\tau\cos 2\theta_i + \theta_i. \tag{2.36}$$

Hence, the Hannay-Berry phase in this problem as given by (2.9) is:

$$\theta_g = \int_0^{4K} \frac{d\theta_S}{d\tau} d\tau,$$

$$= \left(\frac{2k+6}{3}\right) K \cos 2\theta_i,$$

where K is given by (2.30). Note that K depends on δ. As $\delta \to 0$ i.e. as $\Delta \to a/2$, we get $k \to 0$ and $K \to \pi/2$ and the above phase approaches the value obtained by Newton [69] as a special case of the 3-vortex problem, i.e. $\pi \cos 2\theta_i$.

Chapter 3

The geometric interpretation

In this chapter we give a geometric interpretation of the phases calculated in the previous point vortex configurations. In §3.1 we present a simple interpretation which shows that the phase can be expressed as an integral in the plane around a closed vortex orbit. In §3.2 we present an interpretation in terms of holonomy and connections. At the end of the section we make some comments on the geometric phase in a non-adiabatic three vortex problem.

3.1 The phase as a contour integral

To develop a geometric interpretation of the Hannay-Berry phase, we seek to express the phase as an integral around a closed path of a *1-form* defined on the parameter space. We identify the parameter space with some open subset U of the physical plane on which the point vortices move. We define U appropriately in each problem later. The closed path is a smooth vortex orbit in U coordinatized by τ. In the second and third problems, such orbits naturally exist in U due to the periodicity of the vortex motion in the physical plane and its dependency on the slow time alone. In the three-vortex and four-vortex problems, such curves do not exist, but as was shown in these problems the geometric phase is determined by the asymptotically defined two-vortex motion in each. This motion is periodic and depends on the slow time alone, we therefore look at their closed orbits in U. The orbits for different initial conditions are non-intersecting[1] and have a well-defined common center. We then make use of the fact that the geometric phase is the integral of a term that depends on the slow time τ alone as given by (2.9). Our goal then is to rewrite this integral, which is in terms of the orbit coordinate τ, in terms of orbit coordinates in U, which transforms the time integral into a contour integral in U. We then show that the integrand defines a 1-form on U and we have our desired result. The details of this procedure are described below.

[1] Each being the unique solution for the given initial conditions of the ODEs governing the vortex motion.

Choose a point in the plane as the origin of a Cartesian X-Y frame. In each case, this point is the common center of the set of closed vortex orbits mentioned above. Note that the parameter space U is not simply connected as it is the union of these concentric closed orbits. We then change the coordinate of our closed orbit from τ to ϕ which, as before, is the angle with the negative X-axis (measured in the clockwise direction). Introduce the real-valued function $\omega_l(\phi) \equiv d\phi/d\tau$ which can be viewed as the angular velocity of the vortex in its orbit. Since the motion of the vortex along the closed path is well-defined at all points so is $\omega_l(\phi)$, and it can, in principle, be obtained from the equations of motion of the vortex. We indicate its dependency on ϕ to show that it can in general vary along the orbit. In all problems $\omega_l(\phi)$ is one-signed for all $\phi \in [0, 2\pi]$. We then rewrite (2.9) as:

$$\begin{aligned} \theta_g &= \int_0^\beta C_l d\tau, \\ &= \int_0^{2\pi} C_l \frac{d\phi}{\omega_l(\phi)}, \end{aligned} \tag{3.1}$$

where $C_l \equiv d\theta_S/d\tau \; (= 2\Omega \int f_0 dt_{|t=0})$ is a constant along the closed orbit. The subscript l denotes the orbit-dependency of these quantities. The next step is to note that $\phi = \tan^{-1}(-Y/X)$ which gives:

$$\theta_g = \oint \frac{C_l}{\omega_l(X,Y)} \left(\frac{Y dX - X dY}{X^2 + Y^2} \right). \tag{3.2}$$

Hence, the geometric phase is expressed as a contour integral in the parameter space. The integrand of (3.2) does not as yet define a 1-form on U since C_l and ω_l are orbit-specific. However since U is the union of such concentric, closed orbits and C_l, ω_l are defined on each orbit, it is possible to define a 1-form on U by smoothly extending C_l and ω_l in (3.2) to all of U. This defines the following 1-form on U:

$$\gamma_u = \frac{C(X,Y)}{\omega(X,Y)} \left(\frac{Y dX - X dY}{X^2 + Y^2} \right), \tag{3.3}$$

where we have now removed the subscript l. Therefore,

$$\theta_g = \oint \gamma_u .$$

We now apply this procedure in each of our problems.

The three-vortex problem:

It is clear from the observations made in §2.3 that there exists well-defined closed paths in the plane associated with the geometric phase in this problem. These closed paths are the concentric circular orbits of Γ_3 and $\Gamma_1 + \Gamma_2$ in a two-vortex motion as shown in Figure 3.1. We define

$U \equiv \mathbf{R}^2 - \{o\}$, where o is the center of vorticity of the two vortices and is the common center of the orbits of both vortices. The motion of each vortex in the Cartesian frame is defined by $\phi(\tau) = \phi_0 = (\alpha_1+\alpha_2+\alpha_3)\tau/2\pi$. Hence $\omega_l = \omega = (\alpha_1+\alpha_2+\alpha_3)/2\pi$ is a constant and is the same for all vortex orbits. Noting that $C_l = C = (\alpha_3/2\pi)\cos 2\theta_i$ from (2.16), we can then rewrite the geometric phase in this problem using (3.2) as:

$$\theta_g = \oint \left(\frac{Y}{X^2+Y^2} dX - \frac{X}{X^2+Y^2} dY \right) \frac{\Gamma_3}{\Gamma_1+\Gamma_2+\Gamma_3} \cos 2\theta_i,$$

where X, Y are the Cartesian coordinates of either of the two vortices and the contour is its closed orbit. This defines the 1-form on U:

$$\gamma_u = \left(\frac{Y}{X^2+Y^2} dX - \frac{X}{X^2+Y^2} dY \right) \frac{\Gamma_3}{\Gamma_1+\Gamma_2+\Gamma_3} \cos 2\theta_i.$$

Let the radius of the circular vortex orbit in V be denoted by R. Since $X^2 + Y^2 = R^2$ and $\int (Y dX - X dY) = 2A_v$ (using Stokes' Theorem) where $A_v = \pi R^2$ is the area swept out by the orbit of the vortex, we get another expression for the geometric phase in this problem which is reminiscent of the geometric phase in the particle on a hoop problem (eqn. (1.1)):

$$\begin{aligned} \theta_g &= \frac{2A_v}{R^2} \frac{\Gamma_3}{\Gamma_1+\Gamma_2+\Gamma_3} \cos 2\theta_i, \\ &= \frac{8\pi^2 A_v}{L^2} \frac{\Gamma_3}{\Gamma_1+\Gamma_2+\Gamma_3} \cos 2\theta_i, \end{aligned}$$

where L is the circumference of the circle swept out by the vortex, i.e. $L = 2\pi R$.

The four-vortex problem:

Analogous to the three-vortex problem, o is the center of vorticity of the two-vortex motion of $\Gamma_1+\Gamma_2$ and $\Gamma_3+\Gamma_4$ and $U \equiv \mathbf{R}^2 - \{o\}$. The closed paths are the concentric circular orbits of these two vortices and they have a common angular velocity about o, $\omega_l = \omega = (\alpha_1+\alpha_2+\alpha_3+\alpha_4)/2\pi$. Noting the two values of $C_l (= C)$ from (2.19), the geometric phases can be written as (using (3.2)):

$$\begin{aligned} \theta_g &= \oint \left(\frac{Y}{X^2+Y^2} dX - \frac{X}{X^2+Y^2} dY \right) \frac{\Gamma_3+\Gamma_4}{\Gamma_1+\Gamma_2+\Gamma_3+\Gamma_4} \cos 2\theta_i, \\ \nu_g &= \oint \left(\frac{Y}{X^2+Y^2} dX - \frac{X}{X^2+Y^2} dY \right) \frac{\Gamma_1+\Gamma_2}{\Gamma_1+\Gamma_2+\Gamma_3+\Gamma_4} \cos 2\nu_i, \end{aligned}$$

and the respective 1-forms on U are:

$$\begin{aligned} \gamma_u^{(\theta)} &= \left(\frac{Y}{X^2+Y^2} dX - \frac{X}{X^2+Y^2} dY \right) \frac{\Gamma_3+\Gamma_4}{\Gamma_1+\Gamma_2+\Gamma_3+\Gamma_4} \cos 2\theta_i, \\ \gamma_u^{(\nu)} &= \left(\frac{Y}{X^2+Y^2} dX - \frac{X}{X^2+Y^2} dY \right) \frac{\Gamma_1+\Gamma_2}{\Gamma_1+\Gamma_2+\Gamma_3+\Gamma_4} \cos 2\nu_i. \end{aligned}$$

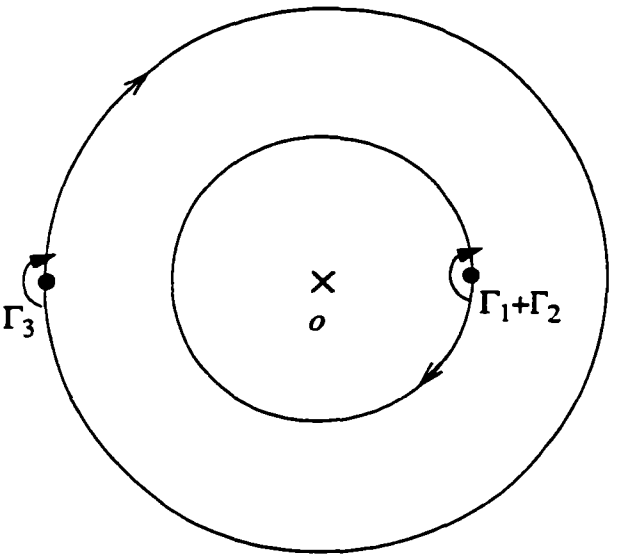

Figure 3.1: For the geometric interpretation in the three-vortex (four-vortex) problem we look at the circular orbits of the two-vortex motion of $\Gamma_1+\Gamma_2$ and $\Gamma_3(\Gamma_3+\Gamma_4)$. The common center of all orbits is the center of vorticity of this two-vortex motion (denoted by o).

In terms of the area and the circumference of the circular vortex orbit, we get:

$$\begin{aligned}
\theta_g &= \frac{2A_v}{R^2}\frac{\Gamma_3+\Gamma_4}{\Gamma_1+\Gamma_2+\Gamma_3+\Gamma_4}\cos 2\theta_i, \\
&= \frac{8\pi^2 A_v}{L^2}\frac{\Gamma_3+\Gamma_4}{\Gamma_1+\Gamma_2+\Gamma_3+\Gamma_4}\cos 2\theta_i, \\
\nu_g &= \frac{2A_v}{R^2}\frac{\Gamma_1+\Gamma_2}{\Gamma_1+\Gamma_2+\Gamma_3+\Gamma_4}\cos 2\nu_i, \\
&= \frac{8\pi^2 A_v}{L^2}\frac{\Gamma_1+\Gamma_2}{\Gamma_1+\Gamma_2+\Gamma_3+\Gamma_4}\cos 2\nu_i,
\end{aligned}$$

where A_v, R and L are the same quantities defined in the three-vortex problem.

The vortex in a circle problem:

Here, the closed paths are the circular vortex orbits with common center at o the center of the physical domain, i.e. the circle. We define $U \equiv \bigcup_r S(r) : 0 < r < R_2$, where $S(r)$ is the circle of radius r centered at o. The vortex motion is defined by $\dot{\phi}(r) = (\alpha/2\pi)(a-1)r$. Hence $\omega_l = (\alpha/2\pi)(a-1)$ is again a constant but varies with the orbits. Referring to §2.4, $a = R_2^2/(p^2+q^2)$ where p, q are the coordinates of the vortex in its circular orbit. We write $X = p/R_2, Y = q/R_2$, hence $\omega = (\alpha/2\pi)(X^2+Y^2)/[1-(X^2+Y^2)]$. Noting that $C_l = C = -(\alpha/2\pi)\cos 2\theta_i$ from (2.20) we can rewrite the geometric phase in this problem using (3.2) as:

$$\theta_g = -\oint \frac{\cos 2\theta_i}{(a-1)}\left(\frac{Y}{X^2+Y^2}dX - \frac{X}{X^2+Y^2}dY\right),$$

where the contour is the closed vortex orbit. The 1-form on U becomes:

$$\gamma_u = -\frac{\cos 2\theta_i}{1-(X^2+Y^2)}(YdX - XdY).$$

Another expression for the phase is obtained in a similiar way as in the 3-vortex problem (using Stokes' Theorem):

$$\begin{aligned}\theta_g &= -\frac{2A_v}{(a-1){R_1}^2}\cos 2\theta_i, \\ &= -\frac{8A_v\pi^2}{(a-1)L^2}\cos 2\theta_i\end{aligned}$$

where $A_v = \pi R_1^2$ is the area of the vortex circle, with circumference $L = 2\pi R_1$.

The mixing layer problem:

As in the previous chapter we focus on a periodic window of adjacent vortices. The vortex orbits are obtained by varying the subharmonic perturbation Δ in the open interval $0 < \Delta < a/2$. These orbits fill a deleted neighbourhood U of their common center o which lies midway between the vortices as shown in Figure 3.2. In other words, $U \equiv \bigcup_\Delta O(\Delta) : 0 < \Delta < a/2$, where $O(\Delta)$ is the orbit corresponding to Δ. Note that $O(\Delta)$ is the same for both vortices. To obtain $\omega_l(\phi) \equiv d\phi/d\tau$, we rewrite (2.25) and (2.26) in D and ϕ coordinates:

$$\omega_l(\phi) \equiv d\phi/d\tau = \frac{2k}{DI}[\sinh(D\sin\phi)\sin\phi + \sin(D\cos\phi)\cos\phi],$$

where, with reference to the variables used in (2.25) and (2.26), $X = 2\pi x_{vor}/a = -D\cos\phi, Y = 2\pi y_{vor}/a = D\sin\phi, \tau = (\pi\Gamma t)/(4ka^2)$ and I is the invariant $\exp(8\pi H/\Gamma)$, where H is given by (2.27). For the initial conditions $x_{vor}(0) = a/2 - \Delta$, $y_{vor}(0) = 0$ we can write $I = 2k$ since $k = \cos^2(\pi\Delta/a)$. Hence $\omega = \omega_l$. Noting that $C_l = (k+3)\cos 2\theta_i/6$ from (2.36) we can then rewrite the geometric phase in this problem using (3.2) as:

$$\theta_g = \oint \frac{(k+3)\cos 2\theta_i}{6}\frac{YdX - XdY}{[Y\sinh Y + X\sin X]}.$$

Noting that $k = (\cosh Y - \cos X)/2$, we get the 1-form on U as:

$$\gamma_u = \frac{(\cosh Y - \cos X + 6)(YdX - XdY)\cos 2\theta_i}{12(Y\sinh Y + X\sin X)}.$$

In the limiting case in which $\Delta \to a/2$ the vortices pair in (approximately) circular orbits. The orbit size becomes smaller and we have $X, Y \to 0$. Noting that $k \to 0$ in this limit we get

$$\theta_g = \oint \frac{\cos 2\theta_i}{2}\frac{YdX - XdY}{Y^2+X^2}$$

$$= \pi \cos 2\theta_i,$$

confirming the result obtained by Newton [69].

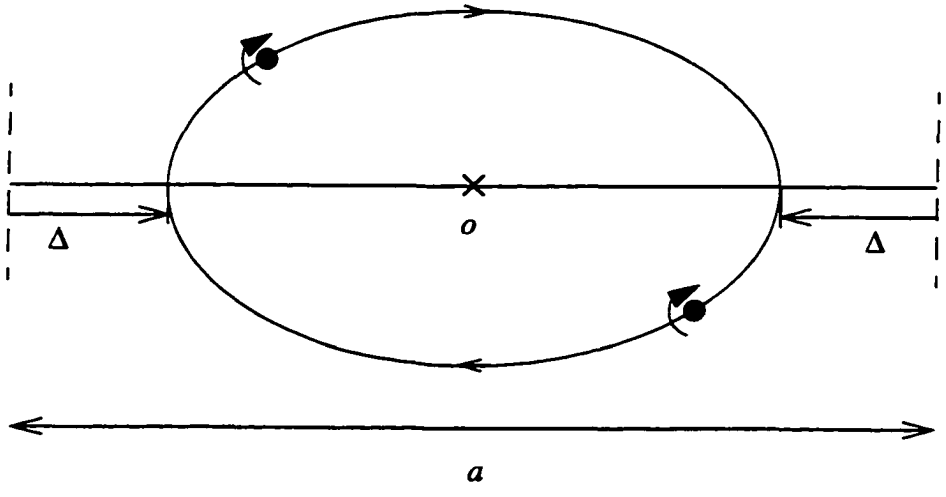

Figure 3.2: For the geometric interpretation in the mixing layer problem we look at the closed orbits of the vortex pair (in a periodic window). These orbits are defined for all values of the subharmonic perturbation D lying between zero and $a/2$. The common center of these orbits, corresponding to $D = a/2$, is denoted by o. The position of the vortices in the unperturbed configuration is shown by the vertical dashed lines

3.2 The phase as the holonomy of a connection

In this section we show how the geometric phases of the previous chapter can also be viewed as the holonomy of appropriately defined connections on a principal fiber bundle. In each problem the connection which defines the parallel translation is determined by the ratio of two angular velocities: the slow phase term angular velocity $d\theta_S/d\tau$ induced on the phase object by the farfield vortices, and the angular velocity, $\omega_l(\phi)$, of the periodic vortex in its closed orbit, as defined in the last section. The principal fiber bundle is a family of 'unperturbed' systems (the fibers) over the domain U (the base space) defined in the previous section. The unperturbed system is the product of the configuration spaces of each phase object-parent vortex system in the absence of the farfield vortices. In all problems, except the four-vortex problem, this space, for any initial condition, is diffeomorphic to the unit circle S^1. In the four-vortex problem, since there are two phase object-parent vortex pairs, this space is diffeomorphic to $S^1 \times S^1$. The base space in all problems can be viewed as the open domain $U \subset \mathbf{R}^2$ defined in the previous section as the union of non-intersecting, concentric closed vortex orbits. However since each of these orbits is again diffeomorphic to the unit circle and since our attention is focussed only on such closed loops in U, we can also identify the base space with S^1. We therefore formulate **Theorem 1**

for the trivial principal bundle $\pi : S^1 \times S^1 \to S^1$. We then extend this to **Theorem 1a** for the bundle $\pi : (S^1 \times S^1) \times S^1 \to S^1$ in the four-vortex problem and then finally to **Theorem 2** for the bundle $\pi : S^1 \times U \to U$.

First consider the trivial principal fiber bundle $\pi : E = S^1 \times S^1 \to S^1$. Since E is a product space, any point $e \in E$ can be represented by $e = (f, b)$, where $b = \pi(e)$, $f \in F_b$, and $F_b (\equiv S^1)$ is the fiber at b. Choose coordinates (θ, ϕ) on E, with $\pi(\theta, \phi) = \phi$, and denote the tangent space at $e \in E$ as T_eE. Note that $T_eE \equiv T_e(S^1 \times S^1) \cong T_fS^1 \times T_bS^1 \cong \mathbf{R} \times \mathbf{R}$, where $\cong$ denotes vector space isomorphism, T_bS^1 is the tangent space to the base at b and T_fS^1 is the tangent space to F_b at f. Choosing the naturally defined coordinate basis on T_eE we can identify any vector $\eta \in T_eE$ by its components $(\eta_\theta, \eta_\phi) \in \mathbf{R} \times \mathbf{R}$.

To show the existense of a connection, recall that in the previous section we showed that there is defined a 1-form γ_u on U in each problem. However the fact that we could express the geometric phase as an integral around each closed vortex orbit implies that there is also defined a 1-form on each orbit and hence on S^1. Indeed going back to equation (3.1), which defines the following equation between differentials:

$$d\theta_S = C_l \frac{d\phi}{\omega_l(\phi)}, \tag{3.4}$$

we see that the right hand side of the above equation defines a 1-form γ on the base manifold S^1:

$$\gamma = C_l \frac{d\phi}{\omega_l(\phi)} \equiv v(\phi) d\phi, \tag{3.5}$$

(where, to simplify notation, we have removed the subscript l in $v(\phi)$). In other words, γ defines a real-valued linear map on T_bS^1 at each point b (with coordinate ϕ) of the base.[2] Thus, if $\eta_\phi \in T_bS^1$, then $\gamma(\eta_\phi) = v(\phi)\eta_\phi$. However since $T_fS^1 \cong \mathbf{R}$ for all $f \in F_b$, we can view the form as associating a vector field on the fiber F_b at each $b \in T_bS^1$. Thus $v(\phi)\eta_\phi \in T_fS^1$ for each $f \in F_b$. This vector field can be trivially extended to a vector field on E as $(v(\phi)\eta_\phi, 0) \in T_eE$ at each $f \in F_b$. The elements of this vector field are still tangent to F_b. Recall that we said in §1.2 that the horizontal lift associates a vector field on E along (but not necessarily tangent to) the fiber at b. To extend our vector field to such a vector field and thereby obtain a horizontal lift, we add the base vector (viewed as an element of T_eE) at each point. This gives the vector field along F_b whose elements are $(v(\phi)\eta_\phi, 0) + (0, \eta_\phi) = (v(\phi)\eta_\phi, \eta_\phi) \in T_eE$. Such a construction can be done at every b on the base. It is trivial to show that this defines a horizontal lift. Associated

[2] In general a 1-form on a manifold defines a multi-linear skew-symmetric map on the tangent space at each point on the manifold. On a 1-dimensional manifold this reduces to a linear map on the tangent space at each point.

with this horizontal lift is a direct sum decomposition of T_eE. Any vector $(\eta_\theta, \eta_\phi) \in T_eE$ can be written uniquely as:

$$(\eta_\theta, \eta_\phi) = (\eta_\theta - v(\phi)\eta_\phi, 0) + (v(\phi)\eta_\phi, \eta_\phi), \tag{3.6}$$

where $(\eta_\theta - v(\phi)\eta_\phi, 0) \in T_fS^1 \equiv V_e$ is the *vertical* part and $(v(\phi)\eta_\phi, \eta_\phi) \in H_e$ is the *horizontal* part. H_e (the span of all vectors $(v(\phi)\eta_\phi, \eta_\phi)$) is a 1-dimensional subspace of T_eE at each e. Thus $T_eE = H_e \oplus V_e$ and this construction defines a *connection* on E.

If we now look at the constant-frequency constant-separation motion of the unperturbed phase object-parent vortex pair then it is represented by a circular orbit on E with coordinates $(\theta_F(t), \phi$ =constant). The leading order perturbation term due to the farfield vortices is θ_S (remember that there is no leading order change in the separation). This perturbation causes the circular orbit on E to drift and thus wind around the torus. It is now defined by

$$(\theta(t) = \theta_F(t) + \theta_S(t), \phi(t)) \,. \tag{3.7}$$

The tangent vector to this orbit lies in T_eE at each e. According to (3.6) we can write it as:

$$\left(\frac{d\theta}{dt}, \frac{d\phi}{dt}\right) \equiv \left(\frac{d\theta}{dt} - v(\phi)\frac{d\phi}{dt}, 0\right) + \left(v(\phi)\frac{d\phi}{dt}, \frac{d\phi}{dt}\right).$$

Using (3.4) and (3.7), we can rewrite this as:

$$\begin{aligned}\left(\frac{d\theta}{dt}, \frac{d\phi}{dt}\right) &\equiv \left(\frac{d\theta}{dt} - \frac{d\theta_S}{dt}, 0\right) + \left(\frac{d\theta_S}{dt}, \frac{d\phi}{dt}\right), \\ &\equiv \left(\frac{d\theta_F}{dt}, 0\right) + \left(\frac{d\theta_S}{dt}, \frac{d\phi}{dt}\right).\end{aligned}$$

This clearly shows, as discussed in §1.2, that the vertical part of the tangent vector is the rate of evolution at the unperturbed frequency leading to the dynamic phase and the vertical drift due to the horizontal part gives the geometric phase at the end of one circuit around the base circle representing the closed vortex orbit in U. The geometric interpretation can be summarized as:

Theorem 1: *The geometric phase in each of the three point vortex configurations can be viewed as the holonomy of a flat connection*[3] *on the trivial principal bundle* $\pi : E = S^1 \times S^1 \to S^1$. *E (the 2-torus) is diffeomorphic to the product space of the unperturbed phase object-parent vortex*

[3] For the definition of a flat connection, see remark at the end of this section.

configuration space and the closed vortex orbit in U, the fiber at each point being diffeomorphic to the configuration space. The connection 1-form is given by

$$\delta = d\theta - v(\phi)d\phi, \tag{3.8}$$

where (θ, ϕ) are the torus coordinates and $v(\phi)$ is the ratio of the constant slow phase 'angular velocity', $d\theta_S/d\tau$, induced by the farfield vortices, and the angular velocity of the vortex in the closed orbit, $\omega_l(\phi)$.

For the four-vortex problem, we consider the trivial principal bundle $\pi : E = S^1 \times S^1 \times S^1 \to S^1$. In coordinates $\pi(\theta, \nu, \phi) = \phi$, we have two *1-forms* defined on the base manifold S^1 associated with the geometric phase of each pair:

$$\gamma_\theta = \frac{d\theta_S/d\tau}{\omega_l(\phi)}d\phi \equiv v(\phi)d\phi, \qquad \gamma_\nu = \frac{d\nu_S/d\tau}{\omega_l(\phi)}d\phi \equiv w(\phi)d\phi. \tag{3.9}$$

Thus $\gamma_\theta(\eta_\phi) = v(\phi)\eta_\phi$ and $\gamma_\nu(\eta_\phi) = w(\phi)\eta_\phi$ for $\eta_\phi \in T_bS^1$. Now define the vector-valued 1-form γ:

$$\gamma(\eta_\phi) \equiv (\gamma_\theta(\eta_\phi), \gamma_\nu(\eta_\phi)) \equiv (v(\phi)\eta_\phi, w(\phi)\eta_\phi),$$

which again due to the isomorphism $T_f(S^1 \times S^1) \cong \mathbf{R} \times \mathbf{R}\ \forall f \in F_b$ can be viewed as the linear map $\gamma : T_bS^1 \to X_{F_b}$, where X_{F_b} is the space of vector fields on the fiber F_b. Proceeding in the same way as before leads to the definition of a horizontal lift and a direct sum decomposition of T_eE:

$$(\eta_\theta, \eta_\nu, \eta_\phi) = (\eta_\theta - v(\phi)\eta_\phi, \eta_\nu - w(\phi)\eta_\phi, 0) + (v(\phi)\eta_\phi, w(\phi)\eta_\phi, \eta_\phi),$$

for $(\eta_\theta, \eta_\nu, \eta_\phi) \in T_eE$. The first component on the right clearly belongs to the 2-dimensional *vertical* space and the span of the second component defines a 1-dimensional *horizontal* subspace $H_e \subset T_eE$ at each e. This again defines a *connection* on E.

Again we look at the orbit on E which represents the leading order perturbed motion of both pairs. It is defined by coordinates:

$$(\theta(t) = \theta_F(t) + \theta_S(t), \nu(t) = \nu_F(t) + \nu_S(t), \phi(t)).$$

The tangent vector to this orbit at each $e \in E$ can be written as:

$$\left(\frac{d\theta}{dt}, \frac{d\nu}{dt}, \frac{d\phi}{dt}\right) \equiv \left(\frac{d\theta}{dt} - v(\phi)\frac{d\phi}{dt}, \frac{d\nu}{dt} - w(\phi)\frac{d\phi}{dt}, 0\right) + \left(v(\phi)\frac{d\phi}{dt}, w(\phi)\frac{d\phi}{dt}, \frac{d\phi}{dt}\right),$$

showing that the vertical part represents the evolution of the two pairs at their unperturbed frequencies leading to the dynamic phase for each and the geometric phase for each is due to the

vertical drift of the horizontal part. We thus have:

Theorem 1a: *The geometric phase in the four-vortex configuration can be viewed as the holonomy of a flat connection on the trivial principal bundle* $\pi : E = S^1 \times S^1 \times S^1 \to S^1$. *E (the 3-torus) is diffeomorphic to the product space of each unperturbed phase object-parent vortex configuration space and the closed vortex orbit (for a given initial condition) in V, the fiber at each point being diffeomorphic to the product of the two configuration spaces. The vector-valued connection 1-form is given by*

$$\delta = (d\theta - v(\phi)d\phi, d\nu - w(\phi)d\phi)\,, \tag{3.10}$$

where (θ, ν, ϕ) *are the torus coordinates and* $v(\phi), w(\phi)$ *are the ratios of the constant slow phase 'angular velocities',* $d\theta_S/d\tau, d\nu_S/d\tau$, *induced by the farfield vortices on each pair, and the angular velocity of the vortex in the closed orbit,* $\omega_l(\phi)$, *respectively.*

We now extend **Theorem 1** by considering the domain U of all the closed vortex orbits. Consider the trivial principal fiber bundle $\pi : E = S^1 \times U \to U$. Choose coordinates (θ, X, Y), where X, Y were defined for each problem in the last section. Thus $\pi(\theta, X, Y) = (X, Y)$. We again have the identification $T_eE \equiv T_e(S^1 \times U) \cong T_fS^1 \times T_bU \cong \mathbf{R} \times \mathbf{R} \times \mathbf{R}$, where $b \in U$ and $f \in F_b$. Choosing the naturally defined coordinate basis on T_eE identify any vector $\eta \in T_eE$ by its components $(\eta_\theta, \eta_X, \eta_Y) \in \mathbf{R} \times \mathbf{R} \times \mathbf{R}$. Now pick the 1-form γ_u defined on U from the last section. As in the previous two theorems, due to the isomorphism $T_fS^1 \cong \mathbf{R}\ \forall f \in F_b$, γ_u can be viewed as associating a vector field tangent to F_b at each $b \in U$. Thus, we have the linear map $\gamma_u : T_bU \to X_{F_b}$, where X_{F_b} is the space of vector fields on F_b. In coordinates, from (3.3), $\gamma_u((\eta_X, \eta_Y)) = (C/\omega)(Y\eta_X - X\eta_Y)/(X^2 + Y^2)$. Extending the image to a vector field on E and adding the field $(0, \eta_X, \eta_Y)$ defines a *connection* as before. Thus any vector $(\eta_\theta, \eta_X, \eta_Y) \in T_eE$ can be written uniquely as the sum of a *vertical* part and a *horizontal* part:

$$(\eta_\theta, \eta_X, \eta_Y) = \left(\eta_\theta - v(X,Y)\frac{\eta_X Y - \eta_Y X}{X^2+Y^2}, 0, 0\right) + \left(v(X,Y)\frac{\eta_X Y - \eta_Y X}{X^2+Y^2}, \eta_X, \eta_Y\right), \tag{3.11}$$

where $v(X,Y) = C/\omega$. The *horizontal* subspace $H_e \subset T_e$ is the span of all vectors of the form $(v(X,Y)(\eta_X Y - \eta_Y X/X^2+Y^2), \eta_X, \eta_Y)$ (for $(\eta_X, \eta_Y) \in T_bU$) and this is clearly a 2-dimensional vector space.

The leading order perturbed motion of the phase object-parent vortex pair can be represented on E by the orbit:

$$(\theta(t) = \theta_F(t) + \theta_S(t), X(t), Y(t)).$$

According to (3.11) the tangent vector to this orbit at any point can be written as:

$$\left(\frac{d\theta}{dt}, \frac{dX}{dt}, \frac{dY}{dt}\right) = \left(\frac{d\theta}{dt} - \frac{v(X,Y)}{X^2+Y^2}\left(Y\frac{dX}{dt} - X\frac{dY}{dt}\right), 0, 0\right) + \left(\frac{v(X,Y)}{X^2+Y^2}\left(Y\frac{dX}{dt} - X\frac{dY}{dt}\right), \frac{dX}{dt}, \frac{dY}{dt}\right).$$

Clearly, the vertical component gives rise to the dynamic phase and the vertical drift of the horizontal component gives the geometric phase at the end of one closed loop in the base space representing the closed vortex orbit in U. Thus, **Theorem 1** with U as the base space becomes:

Theorem 2: *The geometric phase in each of the three point vortex configurations can be viewed as the holonomy of a connection on the trivial principal bundle $\pi : E = S^1 \times U \to U$. E is diffeomorphic to the product space of the unperturbed phase object-parent vortex configuration space and U. The connection 1-form is given by:*

$$\delta = d\theta - v(X,Y)\left(\frac{YdX - XdY}{X^2+Y^2}\right), \tag{3.12}$$

where (θ, X, Y) are the bundle coordinates, X, Y being coordinates on U. The function $v(X,Y)$ is the ratio of the two functions $C(X,Y)$ and $\omega(X,Y)$ defined in obtaining (3.3). These two functions are the smooth extensions to U of the orbit-specific functions $d\theta_S/d\tau$ and $\omega_l(X,Y)$ (respectively) of the previous two theorems.

The analogous extension of **Theorem 1a** is obvious and we do not state it here.

Comments:

1. The word 'flat' describing the connection in **Theorem 1** and **Theorem 1a** refers to the fact that the connection has zero *curvature*. The curvature of a connection δ is defined [53] as a 2-form on E, $\Theta(\eta,\zeta) \equiv d\delta(\eta^{hor}, \zeta^{hor})$, where $\eta, \zeta \in T_eE$, the superscript *hor* refers to the horizontal components of these vectors, and d denotes the exterior derivative. In both (3.8) and (3.10) we get $d\delta = 0$. This is not true in general for the connection in **Theorem 2**.

2. The 1-forms in (3.3) and (3.5) are examples of forms that are closed but not exact [23].

3. Analogous to the geometric phase in the planar three-body problem [67], [36], [39] it is of interest to ask if there is a geometric phase in a **non-adiabatic three-vortex problem** when all vortices have the same signs. To be precise: *In the evolution of the vortex triangle,*

if at any instant the triangle returns to its original shape[4] *then can the angle by which the final triangle may have possibly rotated with respect to the initial triangle be decomposed into a 'dynamic' part and a 'geometric' part ?* Our attempt to answer this question will be primarily through a comparision with the three-body problem. This suggests that the same geometric construction leading to a geometric phase can be applied here simply by replacing the masses m_k with the vortex strengths $\Gamma_k(>0)$. Thus following the procedure in the cited references we choose an orthogonal frame ($\in \mathbf{R}^2$) centered at the fixed center of vorticity of the system. Let $q = (q_1, q_2, q_3)$ be position vectors, in this frame, of the three point vortices $\Gamma_1, \Gamma_2, \Gamma_3$ respectively, where $q_k = (x_k, y_k) \in \mathbf{R}^2$. Since $\sum_1^3 \Gamma_k q_k = 0$, the span of all such vectors q is a four-dimensional linear subspace $Q \subset \mathbf{R}^6$. Let $Q^* \equiv Q - \{q_i = q_j\}$, where $\{q_i = q_j\}$ is the set of all collisions of the configuration. Q^* is a manifold and we denote the four-dimensional tangent space at each $q \in Q^*$ by T_qQ^*. Consider now the action of the circle group $SO(2)$ or S^1 on Q^*. The action of any element $\theta \in SO(2)$ on Q^* is a rigid body rotation of the triangle about its center of vorticity (origin of the position vectors). Since the action is free and proper, the quotient space $Q^*/SO(2)$ is also a manifold. It can then be shown that on the principal fiber bundle $\pi : Q^* \to Q^*/SO(2)$ a connection can be defined as follows. Define the *vortex kinetic energy inner product* on Q^*: $K_q(\eta, \zeta) = \sum_1^3 \Gamma_k < \eta_k, \zeta_k >$ where $\eta_k, \zeta_k \in \mathbf{R}^2$, $\eta = (\eta_1, \eta_2, \eta_3)$ and $\zeta = (\zeta_1, \zeta_2, \zeta_3) \in T_qQ^*$ and $< >$ is the standard inner product on $\mathbf{R}^2$. Then the horizontal space at each point can be defined to be the subspace $H_q \subset T_qQ^*$ which is the *orthogonal complement*, in the above inner product, to the vertical space V_q (the subspace of vectors tangent to the fiber $\equiv$ group). Since a vector subspace (of an inner product space) and its orthogonal complement define a direct sum decomposition it follows that $T_qQ^* = H_q \oplus V_q$. The total angle change by which the vortex triangle has rotated at the end of the cyclic shape change is then the sum of a dynamic phase and a geometric phase. The geometric phase is the holonomy of this connection. Note the purely geometric nature of the above construction where the form of the Hamiltonian function plays no explicit role. Physically, the horizontal directions represent the evolution of a configuration with a zero value of $J = \sum_1^3 \Gamma_k(x_k dy_k/dt - y_k dx_k/dt)$. J is the analogue of the angular momentum in the point mass problem and is an invariant of (N) point vortex motion.[5] A heuristic comparision of this nature thus leads us to infer the existense of a geometric phase in the three vortex problem analogous to the phase in the planar three body problem. One way in which the geometric construction in the vortex problem does differ from that in the mass problem is in the existense of the invariant $I = \sum_1^3 \Gamma_k(x_k^2 + y_k^2)$. This implies that the orbits in Q^* (for a specified value of this invariant) are restricted to

[4] The existense of such dynamical evolutions for like-signed vortices has been shown by [92, 4]. There also exists a subset of such evolutions which do not pass through collinear states.

[5] It can be shown [47] that $J = (\Gamma_1\Gamma_2 + \Gamma_2\Gamma_3 + \Gamma_1\Gamma_3)/2\pi$ which implies that J is also independent of the initial positions.

lie on the smooth compact surface $\sum_1^3 \Gamma_k(x_k^2 + y_k^2) =$ constant, which is diffeomorphic to S^3.

4. Writing the invariant J in the variables of Figure 2.1 gives:

$$J = \Gamma_3 D^2 \frac{d\phi}{dt} + \Gamma_2 r^2 \frac{d\theta}{dt}.$$

It seems tempting to try to derive (3.4) from the above relation and thereby derive the adiabatic phase in the three vortex problem in a different way. If possible this would also suggest a relation between the adiabatic and the non-adiabatic phase and thereby show the role of the invariant J in the generation of the adiabatic phases. However, it should be noted that when comparing the adiabatic and non-adiabatic phases, one is comparing the geometric drifts in different quantities. In the adiabatic problem the quantity is the configuration space variable of the unperturbed *two*-vortex (Γ_1 and Γ_2) motion whereas in the non-adiabatic problem the quantity is the *three*-vortex-triangle rotation angle. In the absence of any canonical or natural way in which these quantities could be related it would seem reasonable to expect no such relation between their geometric phases.

Chapter 4

An application to slowly varying spiral structures

In this chapter, with a view to applications, we derive formulas for the long time evolution of passive interfaces in the three canonical point vortex configurations of Chapter 2. We show how the formula for the evolution of the interface driven by the dynamics of the vortices inherits the geometric phase effect. We begin by a brief literature survey, in §4.1, of work done on spiral structures and evolving interfaces in a general fluid mechanics context. In §4.2 we define the interface problem and describe it for the three vortex configurations of Chapter 2. §4.3 contains a description of our asymptotic procedure for the general equations of motion. The calculation is divided into three main steps whose details are outlined. In §4.4 we implement the procedure on the first two of our vortex configurations: (a) a restricted three-vortex setup and (b) the vortex in a circular domain. In §4.5 we perform the calculations on the mixing layer model.

4.1 Introduction

A frequently recurring theme in the fluid dynamics literature is the focus on 'spiral structures' as important dynamical states in both two-dimensional and three-dimensional flows. These structures are especially prominent in vortex dominated flows [24] where they appear in the evolution of vorticity regions or interfaces of passive scalars (ex. concentration, temperature). They form for several reasons, depending on the flow configuration in question. Coherent vortices can acquire spiral-like structures near their vorticity maximum due to the winding up of variations in the initial vorticity distribution. As the flow evolves, further spirals are created through instabilities or collisions. This idea has been used more than once as the basis for phenomenological models for turbulent flows–see, for example, Lundgren [50], Gilbert [26], Moffat [63].

In an influential paper by Lundgren [50] a three-dimensional spiral vortex model is introduced in which vorticity is not axially symmetric as in the Burger's vortex (see Marcu, Meiburg and Newton [51]), but has a characteristic spiral structure. In this model, these structures arise dynamically from the interaction of two regions of constant vorticity. As the vortices coalesce into a single vortex core, spiral arms are thrown out in an effort to conserve energy and angular

momentum. Because of the differential rotation caused by the dominant vortex core, the spiral arms stretch and deform into thin vortex sheets which then dissipate out due to viscous diffusion. In Gilbert [26], the focus is on the winding up of a weak vortex patch by a strong vortex core, in two dimensions, where the patch is so weak that it can be treated as being passively advected. The winding is due to the differential rotation rates inherent to the vortex structures. Essentially, the model considered by Gilbert [26] is kinematic as opposed to dynamic.

In a different context, the nonlinear evolution of an incompressible shear layer has been extensively studied. In Corcos and Sherman [21] and in Pozrikidis and Higdon [77], one goal is to determine the growth rate of interfacial area between two separated fluid regions. This quantity is of great interest to chemical engineers who study reacting streams. If the reaction rate is fast, hence diffusion limited, the generation of products is proportional to the growth rate of the interfacial area. In Pozrikidis and Higdon [77] a vortex dynamics (inviscid) simulation of a 2-D shear layer is carried out. One of the conclusions of this work is that the growth rate of interfacial area approaches a constant value for all shear layers they consider, a fact consistent with the experiments of Breidenthal [18] who found constant reaction rates as long as the mixing layer maintains its two-dimensional structure. This paper should be read in conjunction with Corcos and Sherman [21] who perform a finite difference calculation on the corresponding viscous problem. In their relatively low Reynolds number simulation, there is a rapid diffusion of vorticity in contrast to the inviscid calculation of Pozrikidis and Higdon [77]. On the one hand, the inviscid calculations are capable of showing fine details (small-scales) of the flow that are obscured by viscous effects. On the other hand, the inviscid calculations are more difficult to compare with experiment since they represent an idealised limit. The work of Corcos and Sherman [21] goes further in identifying clearly the two distinct stages of the nonlinear evolution of a 2-D shear layer. The first stage is the roll-up of the interface around a local vorticity maximum. The interface evolves into a spiral formation where the marker particles migrate inward along the arms and accumulate near their center. The second stage is the by now well documented [96] vortex pairing process in which, due to a dominant subharmonic instability, neighbouring vortices pair and orbit each other as the spiral arms continue to wrap locally and evolve globally (see for example figure 4 of Corcos and Sherman [21]). In general, the process is complex and well studied--see for example the review of Ho and Huerre [38].

It is not our intention in this thesis to comment on the merits of the spiral vortex models as far as their relevance to turbulence theory is concerned. Rather we focus more narrowly on a particular dynamical question associated with the evolution of spiral structures in flowfields populated with point vortices. We are interested in the long time growth of a passively advected interface in such flows under the influence of two processes. On the one hand, there is a 'fast' wrapping of the interface into a spiral around a nearby vorticity maximum (point vortex). On the other hand, there is a slow evolution of the spiral interface due to the farfield vorticity. We

thus have two widely separated timescales in the dynamics of the interface and we consider the evolution of such a slowly varying spiral structure.

The flowfields that we consider were introduced in Chapter 2. We examine a passively evolving, smooth interface in these flows in a similar adiabatic setting i.e. in the vicinity of the parent vortex. We find that the effect of the slowly moving farfield vortices on the dynamics of the interface, though weak, accumulates over long times, and at the end of one farfield time period T gives an $O(1)$ contribution. In particular, we show that a simple formula emerges for the long time growth of the interface length. The formula shows that the growth decomposes into two distinct parts. The first, due to the rapid local wrapping about the parent vortex, is the growth in the absence of the farfield vortices, while the second is the $O(1)$ contribution of the slowly moving farfield vortices. The main result of this analysis is to show that this $O(1)$ term can be written in terms of the appropriate geometric phase for a passive particle in the flow.

4.2 The interface problem

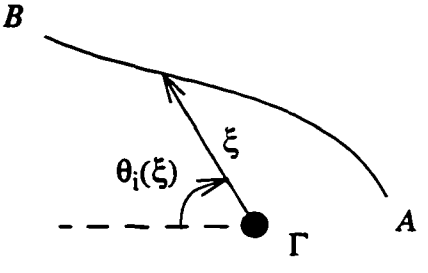

Figure 4.1: A passive interface between two particles labelled A and B in the flowfield of an isolated point vortex (filled circle) at time $t = 0$.

We view the passive interface as a smooth C^1 curve drawn in the flow domain each point of which represents a passive particle at that location. Consider such an interface in the flowfield of an isolated point vortex of strength Γ at time $t = 0$, as shown in Figure 4.1. Let the interface connect two arbitrary particles, labelled A and B. Assume that the interface is transversal at every point to the circular streamlines of the point vortex flow.[1] We choose a coordinate frame centered at the vortex location and parametrize the interface by ξ, the distance from the vortex, as shown in the figure. Consider now the evolution of an arbitrary particle $(r_0(t), \theta_0(t))$ on the

[1] We show in the next section that relaxing this assumption does not change our final result.

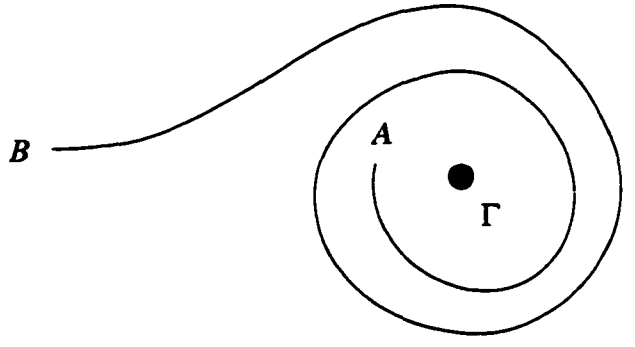

Figure 4.2: With time the interface stretches and wraps around the vortex.

interface with $r_0(0) = \xi$, $\xi_A \leq \xi \leq \xi_B$; $\theta(0) = \theta_i(\xi)$. We know that the time evolution of such a particle is governed by:

$$\begin{aligned} r_0(t) &= \xi, \\ \theta_0(t) &= \frac{\Gamma t}{2\pi\xi^2} + \theta_i(\xi). \end{aligned}$$

This implies that with time the interface stretches and wraps around the vortex in a spiral as shown in Figure 4.2.

The arclength $L_0(t)$, of the interface is given by[2]:

$$\begin{aligned} L_0(t) &= \int_{\xi_A}^{\xi_B} \sqrt{\left(r_0(t)\frac{d\theta_0(t)}{d\xi}\right)^2 + \left(\frac{dr_0(t)}{d\xi}\right)^2}\, d\xi, \qquad (4.1) \\ &= \int_{\xi_A}^{\xi_B} \sqrt{1 + \left(\xi\frac{d\theta_0}{d\xi}\right)^2}\, d\xi, \\ &= \int_{\xi_A}^{\xi_B} \sqrt{1 + \left(\xi\frac{d\theta_i}{d\xi} - \frac{\Gamma t}{\pi\xi^2}\right)^2}\, d\xi. \end{aligned}$$

Note that because of our transversality assumption $d\theta_i/d\xi$ is finite at all points of the curve. It is then straightforward to expand the above expression for long times ($t >> 1$) to get the formula:

$$\begin{aligned} L_0(t) &= \int_{\xi_A}^{\xi_B} \sqrt{\left(\frac{\Gamma t}{\pi\xi^2}\right)^2 \left[1 - 2\frac{\xi d\theta_i/d\xi}{\Gamma t/\pi\xi^2} + \frac{1 + (\xi d\theta_i/d\xi)^2}{(\Gamma t/\pi\xi^2)^2}\right]}\, d\xi, \\ &= \int_{\xi_A}^{\xi_B} \left[\frac{|\Gamma| t}{\pi\xi^2} - sgn(\Gamma)\xi\frac{d\theta_i}{d\xi} + O(\frac{1}{t})\right] d\xi, \qquad (4.2) \end{aligned}$$

[2] We assume positive square roots everywhere.

$$= \frac{|\Gamma|t}{\pi}\left(\frac{1}{\xi_A}-\frac{1}{\xi_B}\right) - sgn(\Gamma)\int_{\xi_A}^{\xi_B}\xi\frac{d\theta_i}{d\xi}d\xi + O(\frac{1}{t}). \tag{4.3}$$

In the special case where the initial interface lies on a ray, $d\theta_i/d\xi = 0$, the above formula gives:

$$L_0(t) = \frac{|\Gamma|t}{\pi}\left(\frac{1}{\xi_A}-\frac{1}{\xi_B}\right) + O(\frac{1}{t}).$$

Now consider what happens to such an interface when subjected to an additional slowly varying background field, hence allow the coordinates $(r(t,\tau),\theta(t,\tau))$ to depend on some slow timescale $\tau = \epsilon^2 t$ $(0 < \epsilon << 1)$. In addition, suppose the background field is periodic with period $T \sim 1/\epsilon^2$. In such a field, the 'perturbed' interface length is given by:

$$L_\epsilon(t) = \int_{\xi_A}^{\xi_B}\sqrt{\left(r\frac{d\theta}{d\xi}\right)^2 + \left(\frac{dr}{d\xi}\right)^2}\,d\xi. \tag{4.4}$$

At any given time, we can compute the difference between the 'unperturbed' length $L_0(t)$ and the 'perturbed' length $L_\epsilon(t)$:

$$\Delta L(t) = L_\epsilon(t) - L_0(t).$$

From this, we can derive a formula for $\Delta L(t = T \sim 1/\epsilon^2)$:

$$\Delta L(T) = L_\epsilon(T) - L_0(T). \tag{4.5}$$

We now ask the question: what is $\Delta L(T)$ in the limit as $\epsilon \to 0$ or, equivalently, as $T \to \infty$? It is not difficult to see that, in general, the interfacial growth in the presence of the background field is due to two distinct but highly coupled effects:

(i) a 'fast' wrapping of the interface in a spiral around the vortex,

(ii) a 'slow' evolution of the spiral due to the background field.

The interaction and balance of these two effects is, of course, what determines $\Delta L(T)$.

In this paper we answer the above question for the three canonical point vortex configurations of Chapter 2. Recall that in each of these configurations we tracked a phase object in the vicinity of a parent vortex. The slowly varying background field is provided by the farfield vortices. We showed that the phase object exhibits a geometric phase θ_g in its angle variable at the end of one time period T of the background field. In this chapter we take the phase object as a passive

particle and show that in all three problems for a passive interface in the vicinity of the parent vortex:

$$\Delta L := \lim_{\substack{\epsilon \to 0 \\ (T \to \infty)}} \Delta L(T) = \lim_{\substack{\epsilon \to 0 \\ (T \to \infty)}} (L_\epsilon(T) - L_0(T)) = O(1). \tag{4.6}$$

This result is due to the fact that in the three problems, as $\epsilon \to 0$ the background flow gets slower *and* weaker. This means that there is a balance between two compensating effects--the vanishing of the perturbation due to the background flow versus the increasing time period over which it acts. We will show that this balance can be directly related to the geometric or Hannay-Berry phase θ_g for a passive particle in these flows by the following simple formula:

$$\Delta L = -\int_{\xi_A}^{\xi_B} d(\xi\theta_g).$$

This formula shows two things:

(i) ΔL depends only on geometric quantities, in particular on the geometric phase for the appropriate vortex configuration. It is independent of the frequency of revolution of the vortices.

(ii) ΔL is a path independent quantity and hence depends only on the endpoints (A, B), not on the shape of the (transversal) interface connecting A and B.

We briefly describe the point vortex configurations with the interface and summarize the results we obtain for ΔL below. In all formulas, θ_i refers to the initial angle of the phase object.

Configuration 1: A restricted three vortex problem.

In Chapter 2 we considered three point vortices in an unbounded plane. Their strengths are of the same sign, but can be of arbitrary magnitude $(\Gamma_1, \Gamma_2, \Gamma_3)$. Without loss of generality, we took Γ_1 as the parent vortex, Γ_2 as the phase object, and Γ_3 as the farfield vortex. The geometric phase induced on the phase object is given by (2.17). For the purpose of this paper we take $\Gamma_2 = 0$ and the geometric phase on the passive particle is then given by:

$$\theta_g = \frac{\Gamma_3}{\Gamma_1 + \Gamma_3} 2\pi \cos 2\theta_i.$$

The appropriate configuration with interface is shown in Figure 4.3. We will show that for this flow:

$$\Delta L = -\int_{\xi_A}^{\xi_B} d(\xi\theta_g),$$

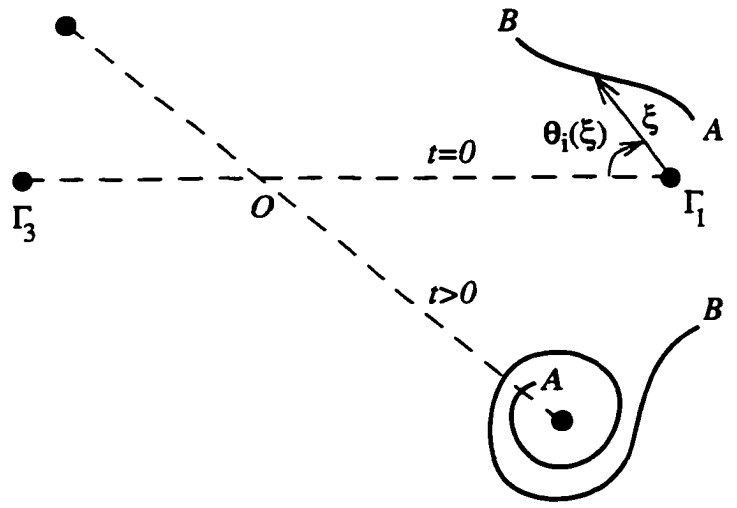

Figure 4.3: Two like-signed point vortices (filled circles) and a passive interface between two particles labelled A and B close to Γ_1. As the vortices rotate uniformly about the center of vorticity O the interface stretches and wraps around Γ_1.

$$= \left(\frac{4\pi\Gamma_3}{\Gamma_1+\Gamma_3}\right)\int_{\xi_A}^{\xi_B}\left(\xi\sin 2\theta_i\frac{d\theta_i}{d\xi}-\frac{\cos 2\theta_i}{2}\right)d\xi.$$

Configuration 2: A vortex and a particle in a circle.

In this configuration we considered a point vortex inside a circular domain. The vortex in any eccentric position moves in a closed circular path with radius R_1 and with constant frequency. We consider a passive particle orbiting this parent vortex Γ. The farfield vorticity is due to the circular boundary of radius $R_2 > R_1$. Equivalently, we can think of the farfield vortex as an image vortex $-\Gamma$ placed at its image point R_2^2/R_1 outside the circle. The flow configuration with interface is shown in Figure 4.4. The geometric phase for the particle was shown to be:

$$\theta_g = -\frac{2\pi\cos 2\theta_i}{(R_2/R_1)^2-1}.$$

We will show that for this flow:

$$\Delta L = -\int_{\xi_A}^{\xi_B} d(\xi\theta_g),$$

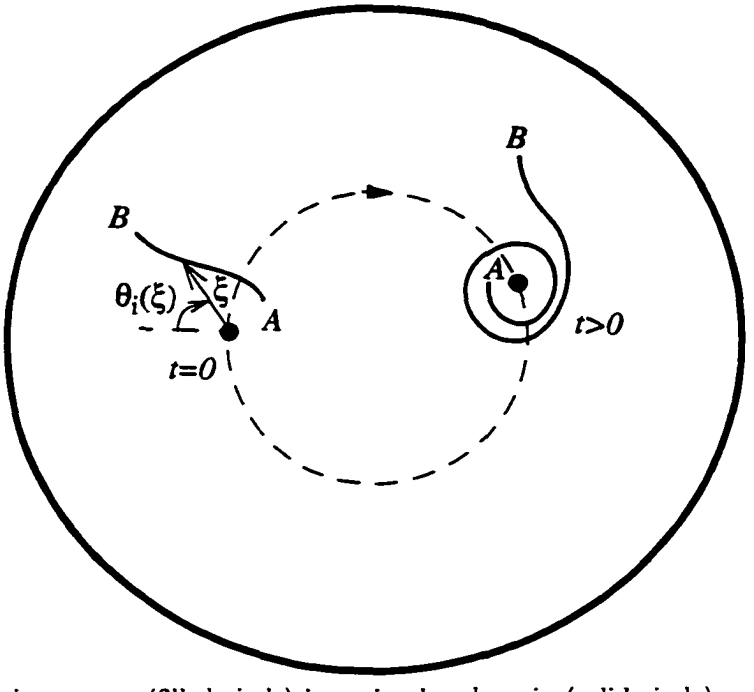

Figure 4.4: A point vortex (filled circle) in a circular domain (solid circle) and a passive inter face between two particles labelled A and B close to it. As the vortex moves in a circular orbit (dashed circle) about the center of the domain, the interface stretches and wraps around it.

$$= \left(\frac{4\pi}{(R_2/R_1)^2 - 1}\right) \int_{\xi_A}^{\xi_B} \left(-\xi \sin 2\theta_i \frac{d\theta_i}{d\xi} + \frac{\cos 2\theta_i}{2}\right) d\xi.$$

Configuration 3: A particle in a mixing layer model.

In this configuration, an infinite row of evenly spaced, equal strength vortices is given a subharmonic perturbation so that neighboring vortices pair up and undergo periodic motion. In Chapter 2 we considered a passive particle near any parent vortex, The farfield flow is due to the infinite number of other point vortices periodically spaced. For this flow the geometric phase for the particle was calculated as:

$$\theta_g = \left(\frac{2k+6}{3}\right) K \cos 2\theta_i,$$

where k is the modulus of the elliptic function solutions of the periodic vortex motion and K is the complete elliptic integral associated with these solutions and related to the time period of the vortex motion. The flow configuration with interface is shown in Figure 4.5. Here, we will prove that:

$$\begin{aligned} \Delta L &= -\int_{\xi_A}^{\xi_B} d(\xi\theta_g), \\ &= \int_{\xi_A}^{\xi_B} \left[-\left(\frac{2k+6}{3}\right) K \cos 2\theta_i + \left(\frac{4k+12}{3}\right) K\xi \sin 2\theta_i \frac{d\theta_i}{d\xi}\right] d\xi. \end{aligned}$$

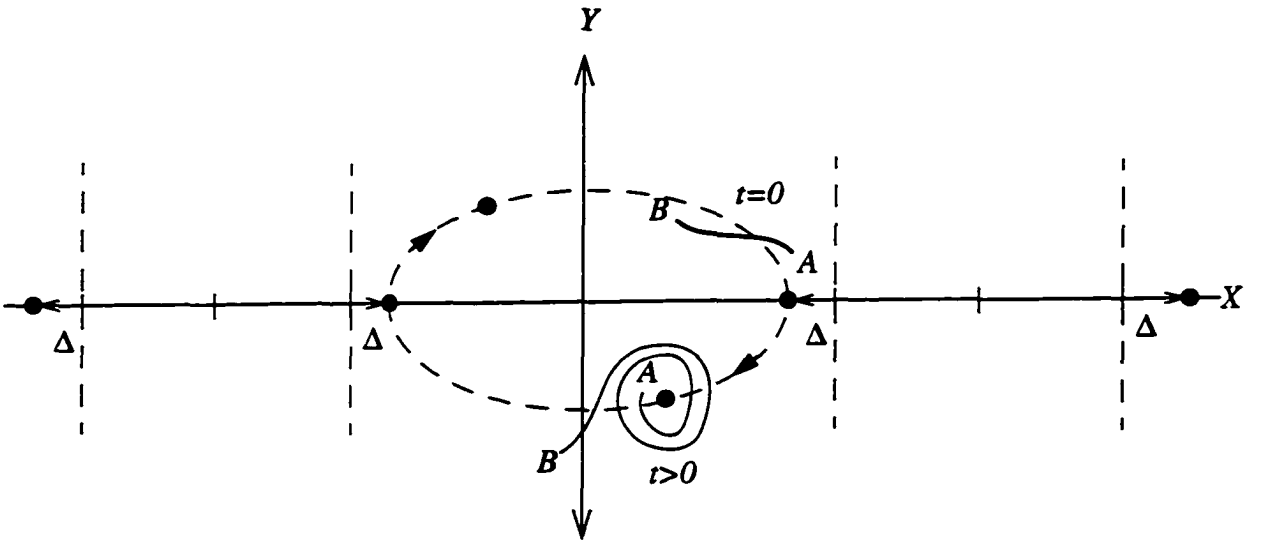

Figure 4.5: As the vortices move in closed orbits in the mixing layer model, a passive interface between two particles labelled A and B near one of the vortices gets stretched and wrapped around the vortex.

4.3 Asymptotic procedure

In this section we outline the method to compute the interface formulae for the general equations introduced in §2.2. We also highlight and summarize the main steps in the computation and mention the specific assumptions made on the behaviour of higher order terms in deriving our final result. The general form of the equations we consider are given by:

$$\begin{aligned} \frac{dr}{dt} &= \epsilon^2 f(r,\theta,D(\epsilon^2 t),\phi(\epsilon^2 t),\epsilon), \\ \frac{d\theta}{dt} &= \frac{\Omega}{r^2} + \epsilon^2 g(r,\theta,D(\epsilon^2 t),\phi(\epsilon^2 t),\epsilon), \end{aligned}$$

with initial conditions $r(0) = 1$ and $\theta(0) = \theta_i$.

Here (r,θ) denote the non-dimensional polar coordinates of the phase object with respect to the parent vortex, (D,ϕ) are non-dimensional polar variables representing the periodic vortex motion, f,g are the components of the vector field due to the farfield vortices and ϵ is the perturbation parameter. For small ϵ we introduce a slow time scale $\tau = \epsilon^2 t$ and use a multi-scale method to obtain asymptotic solutions. Subject to certain conditions on f and g we have non-dimensional asymptotic solutions of the form (see (2.6) , (2.7)):

$$r(t,\tau;\theta_i) = 1 + \epsilon^2 r_2(t,\tau;\theta_i) + O(\epsilon^3), \tag{4.7}$$

$$\theta(t,\tau;\theta_i) = \Omega t + \left(2\Omega\tau \int f_0 dt_{|t=0} + \theta_i\right) + \epsilon\tilde{\theta}_1(\tau;\theta_i) + \epsilon^2\theta_2(t,\tau;\theta_i) + O(\epsilon^3), \tag{4.8}$$

where f_0 is the leading term in the Taylor-expansion of f about $\epsilon = 0$, the integration is with respect to the fast time t and Ω is a non-dimensional constant. We have emphasized the dependence of the variables on $\theta_i(\xi)$, which need not be constant along the interface. We assume, for the present, that $d\theta_i/d\xi < \infty$ at all points of the interface i.e. the initial interface is transversal at all points to the circular streamlines of the parent vortex flow. We relax this transversality assumption at the end of the section and show that it does not alter our result.

To evaluate ΔL from the above solutions we proceed in three steps as follows:

1. Write the asymptotic expansions for $r(t,\tau;\theta_i)$, $\theta(t,\tau;\theta_i)$ in dimensional form.
2. Compute $L_\epsilon(T)$ and formulate the difference:

$$\Delta L(T) = L_\epsilon(T) - L_0(T).$$

3. Take the limit $\epsilon \to 0$ to derive the expression ΔL.

Step 1: The nondimensional variables in (4.7) and (4.8) are:

$$r = \frac{\hat{r}}{\xi}, \quad t = \omega\hat{t}, \quad \tau = \epsilon^2 t = \epsilon^2\omega\hat{t}. \tag{4.9}$$

This gives:

$$\begin{aligned}
\hat{r}(\hat{t},\xi) &= \xi\left[1 + \epsilon^2 r_2(\omega\hat{t}, \epsilon^2\omega\hat{t}, \theta_i(\xi)) + O(\epsilon^3)\right], \\
\theta(\hat{t},\xi) &= \Omega\omega\hat{t} + \left(2\Omega\omega\epsilon^2\hat{t} \int f_0 dt_{|t=0} + \theta_i\right) + \epsilon\tilde{\theta}_1(\epsilon^2\omega\hat{t}, \theta_i(\xi)) \\
&\quad + \epsilon^2\theta_2(\omega\hat{t}, \epsilon^2\omega\hat{t}, \theta_i(\xi)) + O(\epsilon^3),
\end{aligned}$$

where $\omega \propto 1/\xi^2$ and $\epsilon = a_1\xi/D$ (a_1 constant). The limit $\epsilon \to 0$ can obviously be interpreted in two different ways: (i) ξ fixed, $D \to \infty$ or (ii) D fixed, $\xi \to 0$. For calculating ΔL, however, these two limits are *not* equivalent. Indeed, the second limit process does not give a well-defined interface problem. We therefore perform our calculation using the first limit process. This corresponds to keeping the initial position of the interface fixed with respect to the parent vortex (i.e. ξ fixed) while increasing the initial separation distance between the parent vortex and the farfield vortex (i.e. $D \to \infty$).

Step 2: We rewrite the above series at the end of the time period T of the farfield vortices. Since $T = a_2 D^2$ (a_2 constant), this implies that all terms involving the slow time ($\epsilon^2 \omega \hat{t}$) appear as constants. In particular, the second term in the θ series above gives the geometric phase θ_g. The first term in the series is the angle swept out in time T of a particle about an isolated parent vortex of strength Γ in an unbounded flow. Indeed in all three problems $\Omega\omega = \Gamma/(2\pi\xi^2)$ which is the angular frequency of such a motion. Defining $c = a_1^2 a_2$, one then gets for large T:

$$\hat{r}(T,\xi) = \xi\left[1 + \frac{c\xi^2}{T} r_2\left(\frac{T}{\xi^2}, \theta_i(\xi)\right) + O\left(\frac{1}{T\sqrt{T}}\right)\right], \tag{4.10}$$

$$\theta(T,\xi) = \frac{\Gamma T}{2\pi\xi^2} + \theta_g(\theta_i(\xi)) + \theta_i(\xi) + \frac{\sqrt{c}\xi}{\sqrt{T}}\theta_1((\theta_i(\xi)) + \frac{c\xi^2}{T}\theta_2\left(\frac{T}{\xi^2}, \theta_i(\xi)\right) + O\left(\frac{1}{T\sqrt{T}}\right). \tag{4.11}$$

The functions r_j, θ_j are now viewed as functions of T/ξ^2 and ξ. We assume that all these functions (with the exception of θ_0) are bounded in T/ξ^2 and hence $O(1)$ in T. This assumption implies and follows from the assumption of boundedness in t of the formal expansions (4.7) and (4.8). Denoting T/ξ^2 by ρ we differentiate [3] the above series with respect to ξ to get the representations:

$$\frac{d\hat{r}}{d\xi}(T,\xi) = 1 - 2c\frac{\partial r_2}{\partial \rho} + O\left(\frac{1}{\sqrt{T}}\right), \tag{4.12}$$

$$\frac{d\theta}{d\xi}(T,\xi) = -\frac{\Gamma}{\pi\xi^3}T + \frac{d}{d\xi}(\theta_g + \theta_i) - \frac{2c}{\xi}\frac{\partial\theta_2}{\partial\rho} + O\left(\frac{1}{\sqrt{T}}\right). \tag{4.13}$$

We assume that these derivatives are also bounded in T/ξ^2 and hence $O(1)$ in T. We then obtain the following representations:

$$\left[\hat{r}\frac{d\theta}{d\xi}\right]^2 = \left[-\frac{\Gamma}{\pi\xi^2}T + \left\{-\frac{cr_2\Gamma}{\pi} + E\right\} + O\left(\frac{1}{\sqrt{T}}\right)\right]^2,$$

$$= \left\{\frac{\Gamma}{\pi\xi^2}\right\}^2 T^2 + 2\left\{\frac{\Gamma}{\pi\xi^2}\right\}\left\{\frac{cr_2\Gamma}{\pi} - E\right\}T + O(\sqrt{T}),$$

$$\left[\frac{d\hat{r}}{d\xi}\right]^2 = O(1),$$

where $E = \xi d(\theta_g + \theta_i)/d\xi - 2c(\partial\theta_2/\partial\rho)$. Hence:

$$\sqrt{\left[\hat{r}\frac{d\theta}{d\xi}\right]^2 + \left[\frac{d\hat{r}}{d\xi}\right]^2} = \sqrt{\left\{\frac{\Gamma}{\pi\xi^2}\right\}^2 T^2\left[1 + \frac{2\left\{\frac{cr_2\Gamma}{\pi} - E\right\}}{\left\{\frac{\Gamma}{\pi\xi^2}\right\}}\frac{1}{T} + O\left(\frac{1}{T\sqrt{T}}\right)\right]},$$

[3] Note that differentiating and integrating these functions with respect to ξ changes their order with respect to T.

$$= \left|\frac{\Gamma T}{\pi\xi^2}\right| \left[1 + \frac{\left\{\frac{cr_2\Gamma}{\pi} - E\right\}}{\left\{\frac{\Gamma}{\pi\xi^2}\right\}} \frac{1}{T} + O(\frac{1}{T\sqrt{T}})\right],$$

$$= \frac{|\Gamma| T}{\pi\xi^2} + \left\{\frac{cr_2|\Gamma|}{\pi} - sgn(\Gamma)E\right\} + O(\frac{1}{\sqrt{T}}). \tag{4.14}$$

The length integral (4.4) then assumes the form:

$$L_\epsilon(T) = \int_{\xi_A}^{\xi_B} \left[\frac{|\Gamma| T}{\pi\xi^2} + \left\{\frac{cr_2|\Gamma|}{\pi} - sgn(\Gamma)E\right\} + O(\frac{1}{\sqrt{T}})\right] d\xi.$$

Subtracting $L_0(T)$ (as given by (4.2)) from this and writing out E gives:

$$\triangle L(T) = \int_{\xi_A}^{\xi_B} \left[\frac{cr_2|\Gamma|}{\pi} + sgn(\Gamma)\left(-\xi\frac{d\theta_g}{d\xi} + 2c\frac{\partial\theta_2}{\partial\rho}\right) + O(\frac{1}{\sqrt{T}})\right] d\xi.$$

The functions $r_2(t,\tau,\theta_i)$ and $\theta_2(t,\tau,\theta_i)$ in all three problems are of the form $r_2(t,\tau,\theta_i) = r_{2F}(t,\tau,\theta_i) + \tilde{r}_2(\theta_i)$ and $\theta_2(t,\tau,\theta_i) = \theta_{2F}(t,\tau,\theta_i) + \tilde{\theta}_2(\tau,\theta_i)$ where the subscript F denotes the dependency on the fast time. This means that $r_2(T/\xi^2,\xi) = r_{2F}(T/\xi^2,\xi) + \tilde{r}_2(\xi)$ and $\theta_2(T/\xi^2,\xi) = \theta_{2F}(T/\xi^2,\xi) + \tilde{\theta}_2(\xi)$. Hence:

$$\triangle L(T) = \int_{\xi_A}^{\xi_B} \left[\frac{c\tilde{r}_2|\Gamma|}{\pi} - sgn(\Gamma)\cdot\xi\frac{d\theta_g}{d\xi} + \frac{cr_{2F}|\Gamma|}{\pi} + sgn(\Gamma)\cdot 2c\frac{\partial\theta_{2F}}{\partial\rho} + O(\frac{1}{\sqrt{T}})\right] d\xi.$$

The first term in the integrand is related to the geometric phase in the problem by the following linear relation (2.8) derived in §2.2:

$$\theta_g = -2\Omega\beta\tilde{r}_2,$$

where β is a constant related to the dimensional time period as $T = \beta/\omega\epsilon^2$. This implies that:

$$\begin{aligned}
\theta_g &= -2\Omega\omega\epsilon^2 T\tilde{r}_2, \\
&= -2\Omega\omega\xi^2 c\tilde{r}_2, \\
&= -\frac{\Gamma}{\pi\xi^2}\xi^2 c\tilde{r}_2, \\
&= -\frac{\Gamma}{\pi}c\tilde{r}_2.
\end{aligned}$$

Therefore:

$$\triangle L(T) = \int_{\xi_A}^{\xi_B} \left[-sgn(\Gamma)\left(\theta_g + \xi\frac{d\theta_g}{d\xi}\right) + \frac{cr_{2F}|\Gamma|}{\pi} + sgn(\Gamma)\cdot 2c\frac{\partial\theta_{2F}}{\partial\rho} + O(\frac{1}{\sqrt{T}})\right] d\xi.$$

Step 3: The first two terms in the integrand depend only on ξ and are clearly the contribution of the geometric phase. The third and fourth terms in all three problems are the trignometric functions Sin or Cosine with arguments of the form $CT/\xi^2 + u(\theta_i)$, where C is a constant and u is a function of $\theta_i(\xi)$ alone. A simple application of the Riemann-Lebesgue lemma then shows that:

$$\lim_{T\to\infty} \int_{\xi_A}^{\xi_B} \exp\left[i\left(CT/\xi^2 + u(\theta_i)\right)\right] d\xi \quad = \quad 0.$$

Assuming that all higher order terms in the integrand series display this behaviour, we get:

$$\Delta L = \lim_{T\to\infty} \Delta L(T) = -sgn(\Gamma) \int_{\xi_A}^{\xi_B} \left[\theta_g + \xi \frac{d\theta_g}{d\xi}\right] d\xi.$$

Noting that the geometric phase changes sign with Γ in all three problems we observe that ΔL is independent of the sign of Γ. Therefore, without loss of generality we assume that $sgn(\Gamma) = +1$ and are left with the following simple expression for ΔL:

$$\Delta L = -\int_{\xi_A}^{\xi_B} d(\xi\theta_g). \tag{4.15}$$

Thus for an interface of arbitrary shape and orientation the geometric phase causes the above additional $O(1)$ term to appear in the length evolution. For an initially linear interface coincident with a ray from the point vortex, θ_i and hence θ_g are independent of ξ and the $O(1)$ contribution takes on the simpler form:

$$\Delta L = -\theta_g \int_{\xi_A}^{\xi_B} d\xi = -\theta_g(\xi_B - \xi_A).$$

Circumferential interfaces:

We now analyse the change in length for an interface that initially coincides with a portion of a circular streamline of the parent vortex. We assume as before that the interface connects two points labelled A and B. ξ now assumes a constant value Π along the interface. The parametrization with respect to ξ breaks down and we therefore parametrize the interface with respect to θ_i. The length integral (4.4) assumes the form:

$$L_\epsilon(t) = \int_{(\theta_i)_A}^{(\theta_i)_B} \sqrt{\left(r\frac{d\theta}{d\theta_i}\right)^2 + \left(\frac{dr}{d\theta_i}\right)^2}\, d\theta_i,$$

where $(\theta_i)_A \leq \theta_i \leq (\theta_i)_B$. It is trivial to see that in the absence of the background field the interface length remains constant ($= L_i$, say) for all times. We evaluate this integral in the presence of the background field using (4.10) and (4.11) with $\xi = \Pi$. It is straightforward to see that:

$$\begin{aligned} L_\epsilon(T) &= \int_{(\theta_i)_A}^{(\theta_i)_B} \left[\Pi \frac{d}{d\theta_i}(\theta_i + \theta_g) + O(\frac{1}{\sqrt{T}})\right] d\theta_i, \\ &= L_i + \int_{(\theta_i)_A}^{(\theta_i)_B} \left[\Pi \frac{d\theta_g}{d\theta_i} + O(\frac{1}{\sqrt{T}})\right] d\theta_i. \end{aligned}$$

Hence:

$$\Delta L = \int_{(\theta_i)_A}^{(\theta_i)_B} \Pi \frac{d\theta_g}{d\theta_i} d\theta_i = \int_{(\theta_i)_A}^{(\theta_i)_B} d(\xi\theta_g) = -\int_{(\theta_i)_B}^{(\theta_i)_A} d(\xi\theta_g),$$

which is an integral formula exactly like (4.15) except that here the upper limit of the integral is the lower bound of the parameter. To calculate the length change for an interface with both transversal and circumferential portions one partitions the interface into these portions and applies (4.15) in each portion appropriately. The length change for the whole interface being the sum of the length changes over all portions.

Remarks on the derivation of (4.15):

1. The expansions (4.10), (4.11) and (4.12), (4.13) are viewed as formal in the sense that we have made assumptions about the boundedness of the higher order terms and their derivatives with respect to ξ.

2. In Step 3, use is made of the Riemann-Lebsegue lemma, which says that if a real-valued function $f(x)$ is Riemann-integrable on the real interval (a, b) then:

$$\lim_{\lambda \to \infty} \int_a^b f(x) e^{i\lambda x} dx = 0, \qquad \lambda \in \mathbf{R}.$$

   For a precise statement of the lemma see Sirovich [91].

We now give details of these calculations in each of the problems. We split the calculations into the three steps as outlined in this section. We assume that in all problems the vortex strengths are positive.

4.4 Model flows

4.4.1 Two vortices with an interface

We perform the interface calculation first in a flow in the unbounded plane due to two like-signed vortices of strengths Γ_1 and Γ_3 separated by a distance D. The vortices rotate uniformly with

constant D about the fixed center of vorticity of the configuration. As mentioned in §4.2 the geometric phase for a particle close to Γ_1 in this flow is a special case of the geometric phase for the three-vortex problem and is given by $\theta_g = 2\pi\Gamma_3 \cos 2\theta_i/(\Gamma_1+\Gamma_3)$.

Step 1: The asymptotic solutions for the particle motion are:

$$\begin{aligned} r(t,\tau,\theta_i) &= 1+\epsilon^2\left[\frac{\alpha_3}{\alpha_1}\left(\frac{\cos(2\beta(t,\tau))}{2}-\frac{\cos 2\theta_i}{2}\right)\right]+O(\epsilon^3), \\ \theta(t,\tau,\theta_i) &= \frac{\alpha_1}{2\pi}t+\frac{\alpha_3}{2\pi}\tau\cos 2\theta_i+\theta_i+\epsilon\tilde{\theta}_1(\tau) \\ &\quad +\epsilon^2\left[\frac{\alpha_3}{\alpha_1}\sin(2\beta(t,\tau))+\tilde{\theta}_2(\tau)\right]+O(\epsilon^3), \end{aligned}$$

where:

$$\beta(t,\tau,\theta_i) = [\alpha_1+\alpha_3(1-\cos 2\theta_i)]\frac{\tau}{2\pi}-\frac{\alpha_1}{2\pi}t-\theta_i.$$

r and t are defined as in (4.9) and:

$$\epsilon = \frac{\xi}{D}, \qquad \alpha_j = \frac{\Gamma_j}{\omega\xi^2} \quad (j=1,3).$$

Step 2: The (dimensional) time period of the two vortices is given by $T = 4\pi^2D^2/(\Gamma_1+\Gamma_3) = cD^2$. Converting all quantities to their dimensional form the above series at the end of T become:

$$\begin{aligned} \hat{r}(T,\xi) &= \xi+\frac{c\Gamma_3}{\Gamma_1}\frac{\xi^3}{T}\left[\frac{1}{2}\cos(2\beta(\frac{T}{\xi^2},\xi))-\frac{1}{2}\cos 2\theta_i\right]+O(\frac{1}{T\sqrt{T}}), \\ \theta(T,\xi) &= \frac{\Gamma_1}{2\pi}\frac{T}{\xi^2}+\theta_g+\theta_i+\frac{\sqrt{c}\xi}{\sqrt{T}}\theta_1(\xi) \\ &\quad +\frac{c\xi^2}{T}\left[\frac{\Gamma_3}{\Gamma_1}\sin(2\beta(\frac{T}{\xi^2},\xi))+\tilde{\theta}_2(\xi)\right]+O(\frac{1}{T\sqrt{T}}), \end{aligned}$$

where:

$$\begin{aligned} \beta(\frac{T}{\xi^2},\xi) &= [\Gamma_1+\Gamma_3(1-\cos 2\theta_i)]\frac{2\pi}{\Gamma_1+\Gamma_3}-\frac{\Gamma_1}{2\pi}\frac{T}{\xi^2}-\theta_i, \\ &= 2\pi-\frac{\Gamma_1}{2\pi}\frac{T}{\xi^2}-(\theta_g+\theta_i), \end{aligned}$$

and θ_i in general can be a function of ξ. Differentiating with respect to ξ we get the series:

$$\begin{aligned} \frac{d\hat{r}}{d\xi}(T,\xi) &= 1-\frac{c\Gamma_3}{\pi}\sin 2\beta+O(\frac{1}{\sqrt{T}}), \\ \frac{d\theta}{d\xi}(T,\xi) &= -\frac{\Gamma_1}{\pi\xi^3}T+\frac{d}{d\xi}(\theta_g+\theta_i)+\frac{2c\Gamma_3}{\pi\xi}\cos 2\beta+O(\frac{1}{\sqrt{T}}). \end{aligned}$$

Therefore:

$$\begin{aligned}\left[\hat{r}\frac{d\theta}{d\xi}\right]^2 &= \left[-\frac{\Gamma_1}{\pi\xi^2}T + E + O(\frac{1}{\sqrt{T}})\right]^2, \\ &= \left\{\frac{\Gamma_1^2}{\pi^2\xi^4}\right\}T^2 - \left\{\frac{2E\Gamma_1}{\pi\xi^2}\right\}T + O(\sqrt{T}), \\ \left[\frac{d\hat{r}}{d\xi}\right]^2 &= O(1),\end{aligned}$$

where $E = (c\Gamma_3/\pi)(3\cos 2\beta/2 + \cos 2\theta_i/2) + \xi(d/d\xi)(\theta_g + \theta_i)$. Hence:

$$\begin{aligned}\sqrt{\left[\hat{r}\frac{d\theta}{d\xi}\right]^2 + \left[\frac{d\hat{r}}{d\xi}\right]^2} &= \sqrt{\left\{\frac{\Gamma_1^2}{\pi^2\xi^4}\right\}T^2\left[1 - \left\{\frac{2E}{\Gamma_1/\pi\xi^2}\right\}\frac{1}{T} + ..\right]}, \\ &= \left|\frac{\Gamma_1 T}{\pi\xi^2}\right|\left[1 - \left\{\frac{E}{\Gamma_1/\pi\xi^2}\right\}\frac{1}{T} + ..\right], \\ &= \frac{\Gamma_1 T}{\pi\xi^2} - E + O(\frac{1}{\sqrt{T}}).\end{aligned}$$

Using (4.2) and (4.4) and writing out E we then get:

$$\Delta L(T) = -\int_{\xi_A}^{\xi_B}\left[\frac{c\Gamma_3}{\pi}\left(\frac{3}{2}\cos 2\beta + \frac{\cos 2\theta_i}{2}\right) + \xi\frac{d\theta_g}{d\xi} + O(\frac{1}{\sqrt{T}})\right]d\xi. \tag{4.16}$$

Step 3: The second and third terms in the integrand depend on ξ alone and will therefore give $O(1)$ terms after integration. We now examine the order of the first term after integration:

$$\begin{aligned}\int_{\xi_A}^{\xi_B}\cos 2\beta d\xi &= \int_{\xi_A}^{\xi_B}\cos\left(2\left\{2\pi - \frac{\Gamma_1}{2\pi}\frac{T}{\xi^2} - (\theta_g + \theta_i)\right\}\right)d\xi, \\ &= \int_{\xi_A}^{\xi_B}\cos\left(\frac{\Gamma_1}{\pi}\frac{T}{\xi^2} + 2(\theta_g + \theta_i)\right)d\xi, \\ &= \int_{\xi_A}^{\xi_B}\cos\left(\frac{\Gamma_1}{\pi}\frac{T}{\xi^2}\right)\cos 2(\theta_g + \theta_i)\,d\xi \\ &\quad - \int_{\xi_A}^{\xi_B}\sin\left(\frac{\Gamma_1}{\pi}\frac{T}{\xi^2}\right)\sin 2(\theta_g + \theta_i)\,d\xi.\end{aligned}$$

By the Riemann-Lebesgue lemma, each of the integrals in the last line vanishes in the limit $T \to \infty$. Making the further assumption that all other (higher order) terms in the integrand of (4.16) are of the same form and hence have vanishing limits leads us to the result:

$$\Delta L = \lim_{T\to\infty}\Delta L(T) = -\int_{\xi_A}^{\xi_B}\left(\xi\frac{d\theta_g}{d\xi} + \frac{c\Gamma_3\cos 2\theta_i}{2\pi}\right)d\xi,$$

$$= -\int_{\xi_A}^{\xi_B} \left(\xi \frac{d\theta_g}{d\xi} + \theta_g\right) d\xi,$$
$$= -\int_{\xi_A}^{\xi_B} d\left(\xi\theta_g\right).$$

In terms of the initial angle θ_i and the vortex strengths the result is:

$$\Delta L = \frac{4\pi\Gamma_3}{\Gamma_1+\Gamma_3}\int_{\xi_A}^{\xi_B}\left(\xi \sin 2\theta_i \frac{d\theta_i}{d\xi} - \frac{\cos 2\theta_i}{2}\right) d\xi.$$

In the particular case of an interface initially coincident with a ray from the parent vortex (Γ_1) we get:

$$\begin{aligned}\Delta L &= -\theta_g \int_{\xi_A}^{\xi_B} d\xi, \\ &= -\theta_g(\xi_B - \xi_A), \\ &= -\frac{2\pi\Gamma_3}{\Gamma_1+\Gamma_3}\cos 2\theta_i(\xi_B - \xi_A).\end{aligned}$$

The result for this case can also be found in Newton and Shashikanth [70].

4.4.2 Vortex and interface in a circular domain

We next perform the interface computation in the flow due to a point vortex in a circular domain (in the plane) of radius R_2. The point vortex moves with constant speed in a circular orbit of radius $R_1 (0 < R_1 < R_2)$. The geometric phase for a fluid particle closer to the point vortex than to the circular boundary is given by $\theta_g = -(2\pi/b)\cos 2\theta_i$, where $b = (R_2/R_1)^2 - 1$.

Step 1: The asymptotic solutions for the particle motion are:

$$\begin{aligned} r(t,\tau,\theta_i) &= 1 + \epsilon^2\left[-\frac{1}{2}\cos(2\beta(t,\tau)) + \frac{1}{2}\cos 2\theta_i\right] + O(\epsilon^3), \\ \theta(t,\tau,\theta_i) &= \frac{\alpha}{2\pi}(t - \tau\cos 2\theta_i) + \theta_i + \epsilon\tilde{\theta}_1(\tau) \\ &\quad + \epsilon^2\left[-\sin(2\beta(t,\tau)) + \tilde{\theta}_2(\tau)\right] + O(\epsilon^3),\end{aligned}$$

where:

$$\beta(t,\tau,\theta_i) = \frac{\alpha}{2\pi}\left[(b + \cos 2\theta_i)\tau - t\right] - \theta_i.$$

It can be easily shown that $D = bR_1$ is the distance between the point vortex and its image vortex in an equivalent unbounded flow. r and t are defined as in (4.9) and:

$$\epsilon = \frac{\xi}{bR_1} = \frac{\xi}{D}, \qquad \alpha = \frac{\Gamma}{\omega\xi^2}.$$

Step 2: The (dimensional) time period is given by $T = 4\pi^2 b R_1^2/\Gamma = 4\pi^2 D^2/b\Gamma = cD^2$. In dimensional form the above series at the end of T are:

$$\begin{aligned}
\hat{r}(T,\xi) &= \xi + \frac{c\xi^3}{T}\left[-\frac{1}{2}\cos(2\beta(\frac{T}{\xi^2},\xi)) + \frac{1}{2}\cos 2\theta_i\right] + O(\frac{1}{T\sqrt{T}}), \\
\theta(T,\xi) &= \frac{\Gamma}{2\pi}\frac{T}{\xi^2} + \theta_g + \theta_i + \frac{\sqrt{c}\xi}{\sqrt{T}}\theta_1(\xi) \\
&\quad + \frac{c\xi^2}{T}\left[-\sin(2\beta(\frac{T}{\xi^2},\xi)) + \tilde{\theta}_2(\xi)\right] + O(\frac{1}{T\sqrt{T}}),
\end{aligned}$$

where:

$$\begin{aligned}
\beta(\frac{T}{\xi^2},\xi) &= 2\pi\left(1 + \frac{\cos 2\theta_i}{b}\right) - \frac{\Gamma}{2\pi}\frac{T}{\xi^2} - \theta_i, \\
&= 2\pi - \frac{\Gamma}{2\pi}\frac{T}{\xi^2} - (\theta_g + \theta_i),
\end{aligned}$$

and θ_i in general can be a function of ξ. Differentiating with respect to ξ we get the series:

$$\begin{aligned}
\frac{d\hat{r}}{d\xi}(T,\xi) &= 1 + \frac{c\Gamma}{\pi}\sin 2\beta + O(\frac{1}{\sqrt{T}}), \\
\frac{d\theta}{d\xi}(T,\xi) &= -\frac{\Gamma}{\pi\xi^3}T + \frac{d}{d\xi}(\theta_g + \theta_i) - \frac{2c\Gamma}{\pi\xi}\cos 2\beta + O(\frac{1}{\sqrt{T}}).
\end{aligned}$$

Therefore:

$$\begin{aligned}
\left[\hat{r}\frac{d\theta}{d\xi}\right]^2 &= \left[-\frac{\Gamma}{\pi\xi^2}T + E + O(\frac{1}{\sqrt{T}})\right]^2, \\
&= \left\{\frac{\Gamma^2}{\pi^2\xi^4}\right\}T^2 - \left\{\frac{2E\Gamma}{\pi\xi^2}\right\}T + O(\sqrt{T}), \\
\left[\frac{d\hat{r}}{d\xi}\right]^2 &= O(1),
\end{aligned}$$

where $E = (c\Gamma/\pi)\,(-3\cos 2\beta/2 - \cos 2\theta_i/2) + \xi(d/d\xi)\,(\theta_g + \theta_i)$. Hence:

$$\begin{aligned}
\sqrt{\left[\hat{r}\frac{d\theta}{d\xi}\right]^2 + \left[\frac{d\hat{r}}{d\xi}\right]^2} &= \sqrt{\left\{\frac{\Gamma^2}{\pi^2\xi^4}\right\}T^2\left[1 - \left\{\frac{2E}{\Gamma/\pi\xi^2}\right\}\frac{1}{T} + O(\frac{1}{T\sqrt{T}})\right]}, \\
&= \left|\frac{\Gamma T}{\pi\xi^2}\right|\left[1 - \left\{\frac{E}{\Gamma/\pi\xi^2}\right\}\frac{1}{T} + O(\frac{1}{T\sqrt{T}})\right], \\
&= \frac{\Gamma T}{\pi\xi^2} - E + O(\frac{1}{\sqrt{T}}).
\end{aligned}$$

Using (4.2) and (4.4) and writing out E we then get:

$$\Delta L(T) = \int_{\xi_A}^{\xi_B} \left[\frac{c\Gamma}{\pi} \left(\frac{3}{2} \cos 2\beta + \frac{\cos 2\theta_i}{2} \right) - \xi \frac{d\theta_g}{d\xi} + O(\frac{1}{\sqrt{T}}) \right] d\xi. \tag{4.17}$$

Step 3: As in the previous problem the integral of the first term has a zero limit as $T \to \infty$. Making the further assumption that all other (higher order) terms in the integrand of (4.17) have a similiar form and hence vanishing limits leads us to the result:

$$\begin{aligned} \Delta L = \lim_{T \to \infty} \Delta L(T) &= -\int_{\xi_A}^{\xi_B} \left(\xi \frac{d\theta_g}{d\xi} - \frac{c\Gamma \cos 2\theta_i}{2\pi} \right) d\xi, \\ &= -\int_{\xi_A}^{\xi_B} \left(\xi \frac{d\theta_g}{d\xi} + \theta_g \right) d\xi, \\ &= -\int_{\xi_A}^{\xi_B} d(\xi \theta_g). \end{aligned}$$

Since the geometric phase in this problem is independent of the vortex strength so is ΔL. In terms of the initial angle θ_i the result is:

$$\Delta L = \frac{4\pi}{b} \int_{\xi_A}^{\xi_B} \left(-\xi \sin 2\theta_i \frac{d\theta_i}{d\xi} + \frac{\cos 2\theta_i}{2} \right) d\xi.$$

In the particular case of an interface initially coincident with a ray from the parent vortex we get:

$$\begin{aligned} \Delta L &= -\theta_g \int_{\xi_A}^{\xi_B} d\xi, \\ &= -\theta_g (\xi_B - \xi_A), \\ &= \frac{2\pi}{b} \cos 2\theta_i (\xi_B - \xi_A). \end{aligned}$$

4.5 Mixing layer model

In our final problem we perform the interface computation for the mixing layer model of Chapter 2. As illustrated in Figure 4.5, vortex-pairing is induced in this configuration of initially stationary vortices by a subharmonic perturbation. The geometric phase for a fluid particle in this point vortex flow is given by $\theta_g = [(2k+6)/3]K \cos 2\theta_i$ (k and K are defined below).

Step 1: The asymptotic solutions for the particle motion are:

$$\begin{aligned} r(t,\tau,\theta_i) &= 1+\epsilon^2\left[\frac{\tilde{S}_h(\tau)\tilde{S}_t(\tau)}{4L^2}\sin 2\theta_0+\left(\frac{2}{3}-\frac{\tilde{S}_h^2(\tau)-\tilde{S}_t^2(\tau)}{2L^2}\right)\cos 2\theta_0\right. \\ &\qquad \left.-\left(\frac{k+3}{24k}\right)\cos 2\theta_i\right]+O(\epsilon^3), \\ \theta(t,\tau,\theta_i) &= \theta_0(t,\tau,\theta_i)+\epsilon\tilde{\theta}_1(\tau)+\epsilon^2\left[\frac{\tilde{S}_h(\tau)\tilde{S}_t(\tau)}{2L^2}\cos 2\theta_0\right. \\ &\qquad \left.+\left(\frac{\tilde{S}_h^2(\tau)-\tilde{S}_t^2(\tau)}{4L^2}-\frac{1}{3}\right)\sin 2\theta_0+\tilde{\theta}_2(\tau)\right]+O(\epsilon^3), \end{aligned}$$

where $\theta_0(t,\tau,\theta_i)=2kt+\left(\frac{k+3}{6}\right)\tau\cos 2\theta_i+\theta_i$ and $\tilde{S}_h,\tilde{S}_t$ are functions of the vortex motion and hence vary on the slow time alone. L is an invariant of the vortex motion. These terms are therefore independent of both T/ξ^2 and ξ and do not play a role in our derivation. To simplify notation we define $F=\tilde{S}_h\tilde{S}_t/4L^2$ and $G=(\tilde{S}_h^2-\tilde{S}_t^2)/(4L^2)-1/3$. r and t are defined as in (4.9) and:

$$\epsilon=\delta\frac{\xi}{D_i}, \qquad k=\frac{\Gamma}{4\pi\omega\xi^2},$$

where $\delta=\pi D_i/a$, a is the inter-vortex spacing for the unperturbed configuration and D_i is the initial inter-vortex spacing for the perturbed configuration (see §2.5). k (which depends on δ) is the modulus of the elliptic integrals that appear in the vortex solutions.

Step 2: The (dimensional) time period of the vortex motion is given by $T=(16kK/\pi\Gamma)a^2=(16\pi kK/\Gamma\delta^2)D_i^2=a_2D_i^2$ where $K(k)$ is the complete elliptic integral of the first kind. Defining $c=\delta^2a_2$ we write the above series in dimensional form at the end of time T:

$$\begin{aligned} \hat{r}(T,\xi) &= \xi+\frac{c\xi^3}{T}\left[F\sin 2\theta_0-2G\cos 2\theta_0-\left(\frac{k+3}{24k}\right)\cos 2\theta_i\right]+O(\frac{1}{T\sqrt{T}}), \\ \hat{\theta}(T,\xi) &= \frac{\Gamma}{2\pi}\frac{T}{\xi^2}+\theta_g+\theta_i+\frac{\sqrt{c}\xi}{\sqrt{T}}\theta_1(\xi) \\ &\qquad +\frac{c\xi^2}{T}\left[2F\cos 2\theta_0+G\sin 2\theta_0+\tilde{\theta}_2\right]+O(\frac{1}{T\sqrt{T}}), \end{aligned}$$

where:

$$\theta_0(\frac{T}{\xi^2},\xi)=\frac{\Gamma}{2\pi}\frac{T}{\xi^2}+\theta_g+\theta_i.$$

Differentiating with respect to ξ we get the series:

$$\frac{d\hat{r}}{d\xi}(T,\xi) = 1+\frac{2c\Gamma}{\pi}[-F\cos 2\theta_0-2G\sin 2\theta_0]+O(\frac{1}{\sqrt{T}}),$$

$$\frac{d\theta}{d\xi}(T,\xi) = -\frac{\Gamma}{\pi\xi^3}T + \frac{d}{d\xi}(\theta_g+\theta_i) + \frac{2c\Gamma}{\pi\xi}[G\cos 2\theta_0 - 2F\sin 2\theta_0] + O(\frac{1}{\sqrt{T}}).$$

Therefore:

$$\begin{aligned}\left[\hat{r}\frac{d\theta}{d\xi}\right]^2 &= \left\{-\frac{\Gamma}{\pi\xi^2}T + E + O(\frac{1}{\sqrt{T}})\right\}^2, \\ &= \left\{\frac{\Gamma^2}{\pi^2\xi^4}\right\}T^2 - \left\{\frac{2E\Gamma}{\pi\xi^2}\right\}T + O(\sqrt{T}), \\ \left[\frac{d\hat{r}}{d\xi}\right]^2 &= O(1),\end{aligned}$$

where $E = -(c\Gamma/\pi)\,[5F\sin 2\theta_0 - 4G\cos 2\theta_0 - (k+3)\cos 2\theta_i/(24k)] + \xi(d/d\xi)(\theta_g+\theta_i)$. Hence:

$$\begin{aligned}\sqrt{\left[\hat{r}\frac{d\theta}{d\xi}\right]^2 + \left[\frac{d\hat{r}}{d\xi}\right]^2} &= \sqrt{\left\{\frac{\Gamma^2}{\pi^2\xi^4}\right\}T^2\left[1 - \left\{\frac{2E}{\Gamma/\pi\xi^2}\right\}\frac{1}{T} + O(\frac{1}{T\sqrt{T}})\right]}, \\ &= \left|\frac{\Gamma T}{\pi\xi^2}\right|\left[1 - \left\{\frac{E}{\Gamma/\pi\xi^2}\right\}\frac{1}{T} + O(\frac{1}{T\sqrt{T}})\right], \\ &= \frac{\Gamma T}{\pi\xi^2} - E + O(\frac{1}{\sqrt{T}}).\end{aligned}$$

Using (4.2) and (4.4) and writing out E we then get:

$$\Delta L(T) = \int_{\xi_A}^{\xi_B}\left\{\frac{c\Gamma}{\pi}\left[5F\sin 2\theta_0 - 4G\cos 2\theta_0 - \left(\frac{k+3}{24k}\right)\cos 2\theta_i\right] - \xi\frac{d\theta_g}{d\xi} + O(\frac{1}{\sqrt{T}})\right\}d\xi. \qquad (4.18)$$

Step 3: As in the previous problems it is easy to show that the integrals of the first and second terms vanish in the limit $T \to \infty$. Making our assumption that all other (higher order) terms in the integrand of (4.18) have a similiar form and hence vanishing limits leads us to the result:

$$\begin{aligned}\Delta L = \lim_{T\to\infty}\Delta L(T) &= -\int_{\xi_A}^{\xi_B}\left[\xi\frac{d\theta_g}{d\xi} + \frac{c\Gamma}{\pi}\left(\frac{k+3}{24k}\right)\cos 2\theta_i\right]d\xi, \\ &= -\int_{\xi_A}^{\xi_B}\left[\xi\frac{d\theta_g}{d\xi} + \theta_g\right]d\xi, \\ &= -\int_{\xi_A}^{\xi_B} d(\xi\theta_g).\end{aligned}$$

As in the previous problem, since θ_g is independent of the vortex strength so is ΔL. In terms of the initial angle θ_i the result is:

$$\Delta L = \int_{\xi_A}^{\xi_B} \left[-\left(\frac{2k+6}{3}\right) K \cos 2\theta_i + \left(\frac{4k+12}{3}\right) K\xi \sin 2\theta_i \frac{d\theta_i}{d\xi} \right] d\xi.$$

For an interface initially coincident with a ray from the parent vortex, we get:

$$\begin{aligned} \Delta L &= -\theta_g \int_{\xi_A}^{\xi_B} d\xi, \\ &= -\theta_g(\xi_B - \xi_A), \\ &= -K\left(\frac{2k+6}{3}\right) \cos 2\theta_i (\xi_B - \xi_A). \end{aligned}$$

Thus we have shown in this chapter that the geometric phase exhibited in the angle variable of a passive particle in the three 'canonical' vortex configurations considered in Chapter 2 also affects the evolution of an interface of passive particles in these flows. The interface wraps into a spiral structure around the parent vortex with a slowly varying component induced by the farfield vortices. An extra term appears in the length of the interface over long time periods which depends on the geometric phase and, like the phase, is also geometric. It is the integral over the initial interface of a perfect differential, or an exact form, of a function that is a weighted geometric phase term. We believe that from the fluid dynamics point of view this result, based on the results of Chapter 2, is a further step towards understanding the significance and implications of the geometric phase in fluid flows. From a more practical point of view, the results in these results may be useful as theoretical estimates allowing for future quantitative comparisons with numerical and experimental work.

Chapter 5

The geometric phase in an elliptical vortex patch model

In this chapter we calculate the geometric phase in a model of the motion of well-separated vortex patches in the plane. We introduce the concept of a vortex patch briefly in §5.1, the specific model in §5.2, then describe the phase calculation in §5.3.

5.1 Introduction to patches

A vortex patch is a desingularization of a point vortex in which the vorticity is a bounded function over a finite, non-zero area A of the plane. It can thus be viewed as the perpendicular section of an infinitely long rectilinear vortex tube of area A whose vorticity distribution is invariant along the length of the tube. The induced velocity field is given by integrating the contribution due to each infinitesimal vorticity element over the area of the patch. For a patch with vorticity distribution $\omega(x, y)$, the streamfunction is given by:

$$\psi(x, y) = -\frac{1}{4\pi} \int_A \omega(x', y') \log \left[(x - x')^2 + (y - y')^2\right] dA'. \tag{5.1}$$

The velocity components (u, v) at a point (x, y) are related to the streamfunction in the usual fashion $u = \partial\psi/\partial y$ and $v = -\partial\psi/\partial x$.

A patch with $\omega(x, y) =$ constant is termed a uniform patch. The simplest example of an isolated uniform vortex patch is the Rankine vortex. This is a circular patch which rotates with constant angular velocity about its center. The velocity field outside the patch is identical to that of a point vortex at the center of the patch of strength ωA while the velocity field inside the patch is like that due to solid body rotation i.e. varies linearly with distance from the center of the patch. Another example, which is the basis for the model we consider, is the Kirchhoff elliptical vortex [48]. Here the uniform vorticity is distributed over an elliptical region with aspect ratio

$\lambda = a/b$ (a major axis, b minor axis). The patch rotates about the center of the ellipse with constant angular velocity given by:

$$\Theta = \frac{\omega\lambda}{(1+\lambda)^2} = \frac{\Gamma\lambda}{A(1+\lambda)^2}, \tag{5.2}$$

where $\Gamma = \omega A$ is the strength of the patch. As shown in Lamb (section 159) a fluid particle on the patch moves in a circular orbit with *twice* this frequency. Deem and Zabusky [22] have conjectured, based on numerical computations, that the Kirchhoff vortex is a member ($m = 2$) of a class of rotating patches (constant frequency) with m-fold symmetry. Overman and Zabusky [75, 76] have computed interactions of such m-fold 'states.'

A system of N interacting patches is in general far more complicated than a system of N interacting point vortices due to the internal structure associated with each patch. There is a large body of numerical work documenting various complex processes associated with vortex patches, such as merger and filamentation. A good overview of work done on patches can be found in chapter 9 of Saffman [80].

It is well-known (see [68, 73, 58, 89] and references therein) that the Euler equations, and hence N patch systems, posses a noncanonical Hamiltonian structure. The real-valued Hamiltonian is now a functional of the vorticity field ω of the domain. The dynamics of the vorticity field can be expressed in the form:

$$\frac{dF}{dt} = \{F, H\},$$

where F is any functional of ω, and $\{\ \}$ are appropriately defined Poisson brackets. This representation is equivalent to the dynamics represented by the Euler equations in the vorticity-streamfunction form. For N patches in an unbounded domain, the Hamiltonian of the system is given by:

$$H(\omega) = \frac{1}{2}\sum_{k=1}^{N}\int_{A_k} \omega_k(x,y)\psi_k(x,y)dA,$$

where ω is the vorticity field of the whole domain and:

$$\psi_k(x,y) = -\frac{1}{4\pi}\sum_{k=1}^{N}\int_{A_k} \omega_k(x',y')\log\left[(x-x')^2+(y-y')^2\right]dA'.$$

Invariants of the N-patch system arise, as per Noether's theorem, from the invariance of the Hamiltonian (itself an invariant) to continuous transformation groups. Thus invariance to translations and rotations lead, respectively, to the conservation of:

$$\sum_{k=1}^{N}\int_{A_k} \mathbf{x}\omega_k dA, \quad \sum_{k=1}^{N}\int_{A_k} |\,\mathbf{x}\,|\,\omega_k dA,$$

where $\mathbf{x} = (x, y)$ and $| \mathbf{x} |= x^2 + y^2$. The first invariant can be used to define a global centroid analogous to the center of vorticity of N point vortices, by dividing by the sum of the patch strengths $\Gamma = \sum_{k=1}^{N} \Gamma_k$, where $\Gamma_k = \int_{A_k} \omega_k dA$ is the strength of the kth patch:

$$X_G \equiv \sum_{k=1}^{N} \int_{A_k} x\omega_k dA/\Gamma, \quad Y_G \equiv \sum_{k=1}^{N} \int_{A_k} y\omega_k dA/\Gamma.$$

The centroid (X_k, Y_k) of each patch is defined analogously.[1] The centroid of each patch has the property that its velocity is affected only by the external velocity field (u_e, v_e). The external velocity field is the total velocity field minus the velocity field of the patch. Thus in the case of N patches it is the sum of the velocity fields due to the other $N - 1$ patches. The centroid velocity is given by:

$$\frac{dX_k}{dt} = \int_{A_k} \omega_k u_e dA/\Gamma_k, \quad \frac{dY_k}{dt} = \int_{A_k} \omega_k v_e dA/\Gamma_k.$$

The noncanonical structure of the Hamiltonian system implies that the following quantity, generically termed *Casimir*, is also invariant though not explicitly arising from invariance under a group action:

$$\int_{\mathbf{R}^2} F(\omega) dA,$$

where F is any arbitrary functional of the vorticity.[2]

5.2 The MZS model

Melander, Zabusky and Styczek [61, 60] derived a system of equations (henceforth referred to as the MZS model) valid for N uniform vortex patches as long as they satisfy the following:

1. The maximum diameter of any patch is much smaller than the minimum distance between any two patch centroids.

2. The centroid of any patch is within the patch itself.

The logarithmic integrands in the streamfunction are then expanded in an infinite series about the centroids of the respective patches. This leads to an infinite system of equations in the patch

[1] Note that all invariants are generalized to the the invariants of a continuous vorticity distribution by integrating over the plane.

[2] See [73, 89] for how such Casimirs arise. Note that in the 3-D Euler eqations the Casimir does not take this form but is equal to the *helicity* [62].

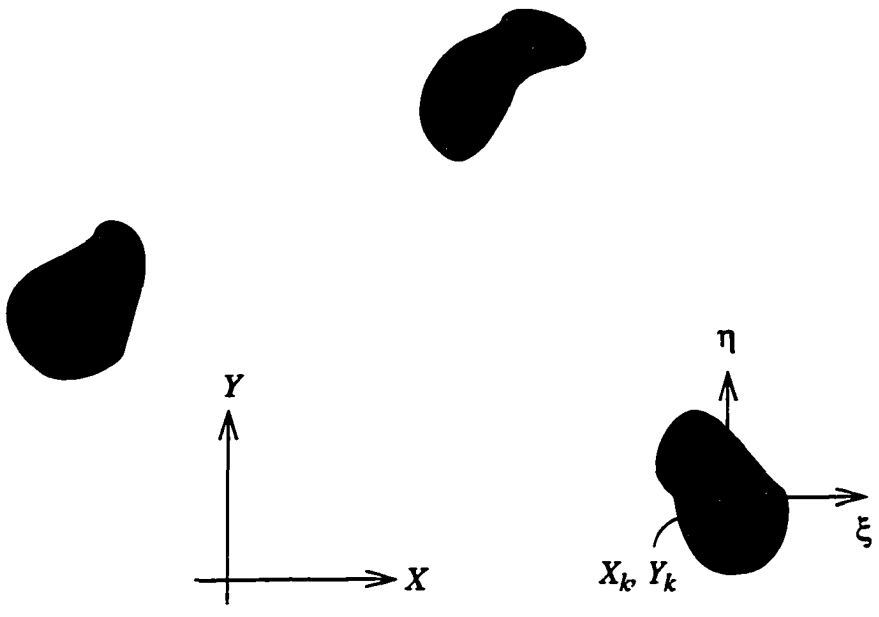

Figure 5.1: A schematic representation of well-separated vortex patches in the MZS model. The local geometric moments for each patch are measured with respect to a moving frame ξ-η fixed to the centroid of the patch. X_k,Y_k are the coordinates of the centroid of the kth patch in a fixed X-Y frame.

centroids, measured with respect to a fixed frame, and the *local* geometric moments of all orders. The local geometric moment of order $m+n$ $(m, n = 0, 1, 2....)$ for a patch is defined as:

$$J^{(m,n)} \equiv \int_A \xi^m \eta^n dA,$$

where ξ and η are local coordinates in a moving frame whose origin is at the centroid of the patch,[3] as shown in Figure 5.1. On the basis of criterion 1, a small parameter can then be introduced: $\epsilon \equiv$ maximum patch diameter / minimum intercentroid distance. Defining the initial minimum intercentroid distance as a characteristic unit length it can then be seen that:

$$J^{(m,n)} = O(\epsilon^{m+n+2}).$$

The higher order moments are thus viewed as higher order perturbation terms. Note that the zeroth order geometric moment $J^{(0,0)}$ is just the area of the patch which, as a consequence of Kelvin's circulation theorem, is conserved.

For the lowest order model all the moments of order greater than one are omitted. The local geometric moments of order one represent the centroid of the patch in local coordinates. These

[3] Such a moving frame is attached to each patch.

are zero by the choice of the local coordinate system. The truncated equations then show that the patch centroids move like a system of N point vortices.

In the next order of truncation, the three moments of second order $J^{(2,0)}$, $J^{(1,1)}$ and $J^{(0,2)}$ are included. These moments, by their definition, can also be viewed as the moments of inertia of the geometric shape of the patch. The authors, noting that the isolated Kirchhoff elliptical vortex is an exact solution of the Euler equation, then give the following reason to show that the second order model is 'mathematically consistent with an elliptical distribution of vorticity' [60]. For an ellipse, the three moments of inertia satisfy the following geometric relation:

$$\frac{A^4}{16\pi^2} = J^{(2,0)}J^{(0,2)} - J^{(1,1)}J^{(1,1)}.$$

This geometric relation is satisfied at all times by the second order model as can be verified by differentiating each side with respect to time. The time derivative of the left hand side is zero. Substituting the time derivatives of the moments as given by the model shows that the right hand side is also zero. Thus the assumption that an elliptical distribution of vorticity remains elliptical for all times does not introduce any apparent inconsistency with the second order model. As further reasons to justify an elliptical distribution, the authors [61] cite Kida's work [45] who showed that an elliptical vortex in a uniform shear flow maintains its elliptical shape, and numerical and experimental evidence of elliptical vortices (see references therein).

The second order model thus treats each patch as a uniformly rotating Kirchhoff elliptical vortex perturbed by the presence of the other patches. The perturbation keeps the patch elliptical but changes its aspect ratio and rotation rate in general. The variables $\lambda :=$ aspect ratio and $\theta :=$ tilt of major axis, are introduced in place of the second order moments. For elliptical shapes they are related by:[4]

$$\begin{aligned} J^{(2,0)} &= \frac{A^2}{4\pi\lambda}\left(\lambda^2 + (1-\lambda^2)\sin^2\theta\right), \\ J^{(0,2)} &= \frac{A^2}{4\pi\lambda}\left(\lambda^2 + (1-\lambda^2)\cos^2\theta\right), \\ J^{(1,1)} &= -\frac{A^2}{8\pi\lambda}(1-\lambda^2)\sin 2\theta. \end{aligned}$$

Thus for each patch we get a system of four variables X, Y, λ and θ, where X, Y are the coordinates of the centroid of the patch. As shown in [61], the system of N patches in the variables:

$$\left(\sqrt{\Gamma_k}X_k, \sqrt{\Gamma_k}Y_k, \frac{\Gamma_k A_k}{16\pi}\frac{(\lambda_k-1)^2}{\lambda_k}, 2\theta_k\right), \qquad k = 1, ..., N$$

then becomes a Hamiltonian system in the canonical sense.

[4] The apparent inconsistency in transforming from three variables to two is explained by the area-moments relation above.

5.3 The geometric phase in the second-order MZS model for two elliptical patches

5.3.1 Asymptotic procedure

Consider a system of two elliptical patches of arbitrary strengths but of the same sign, as shown in Figure 5.2. Each patch is a phase object while the background field is provided by the other patch. The relevant phase is the orientation of the patch as measured by the inclination of the major axis of the ellipse with respect to the horizontal axis. As in the point vortex problems the small parameter ϵ in the MZS model defines a ratio of two time periods or frequencies in the following way. As ϵ goes to zero the size of the patches goes to zero with respect to the intercentroid distance. The rotation and deformation of each patch would then be more influenced by its own velocity field than by the background field. We would thus expect the patch motion to approach the uniformly rotating, non-deforming motion of the Kirchhoff ellipse. If we assume that the strength of each patch and its initial aspect ratio is unaltered as ϵ varies, we can then, from (5.2), associate a time period $T_s \sim A$ with each patch.[5] Simultaneously, we would expect the centroid motion to approach point vortex motion as discussed in the previous section. There is also a longer time period $T_l \sim D^2$, where D is the typical distance between the centroids. Assuming for simplicity that $A_1/A_2 = C$ =constant for all ϵ, we define the small parameter explicitly as

$$\epsilon^2 = \frac{A_1 + A_2}{D_i^2},$$

where D_i is the initial intercentroid distance. We then see that $\epsilon^2 \sim T_s/T_l$. Therefore small values of ϵ define an adiabatic process just as in the point vortex problems in which there exist two timescales, one associated with the rotation of the patch and the other with the (relatively) slow revolution of the centroids. Using scaling arguments as in §2.1, one would expect that, as $\epsilon \to 0$, there is an $O(1)$ contribution to the angle change of the patches at the end of the time period T_l.

Referring to Figure 5.2, we denote by $\hat{D}$ the distance between the centroids, by ϕ the angle with the horizontal axis[6] made by the line joining the centroids, by λ_k $(k = 1, 2)$ the aspect ratio of each patch and by θ_k $(k = 1, 2)$ the angles made with the horizontal axis by the major axis of each patch. The following equations are then obtained from the second order model:

[5] This means, in particular, that if ϵ is decreased by decreasing the area of the patches then the patches rotate faster and faster.

[6] In this problem we stick to the sign convention for angles and circulations used by MZS, namely that angles are measured in a counterclockwise direction from the positive X-axis and that counterclockwise circulations are assumed to be positive. This is different from our sign convention in the point vortex problems.

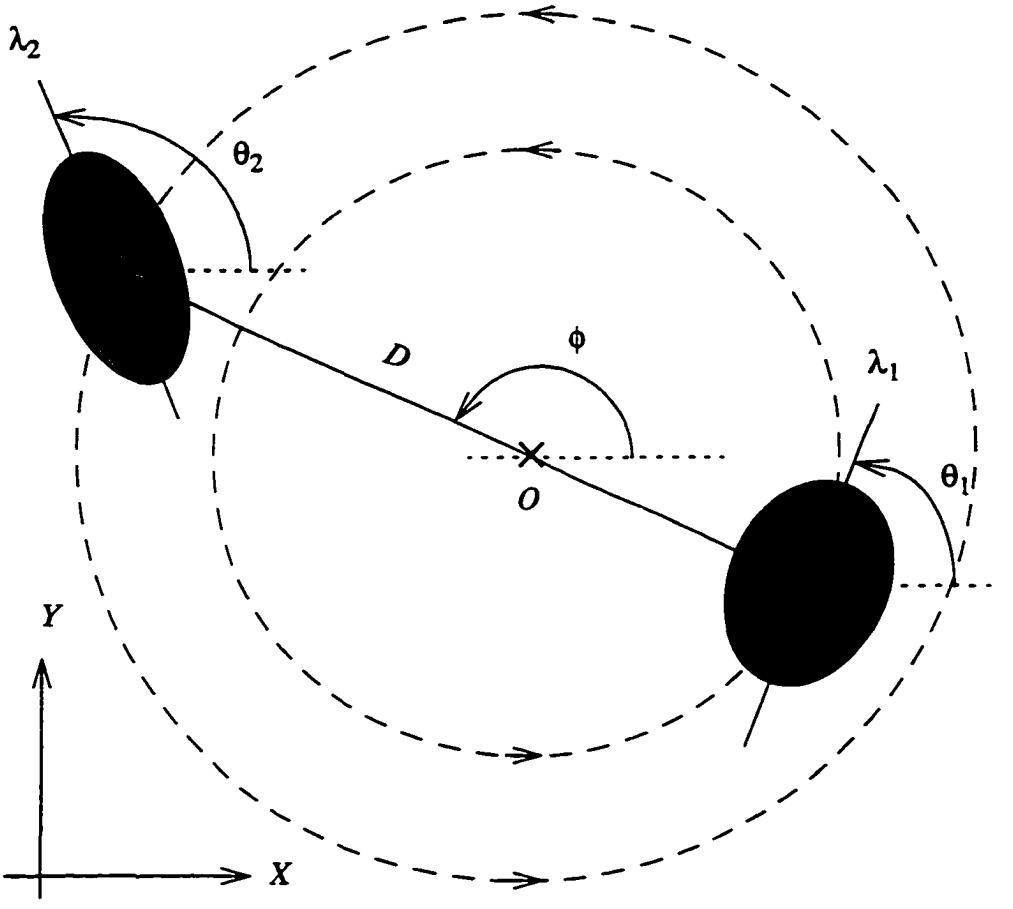

Figure 5.2: The motion of two well-separated uniform elliptical vortex patches of the same sign in the MZS model. The patches have areas A_1, A_2 and like-signed strengths Γ_1, Γ_2. The motion of the centroids of the patches (small, filled circles) is, to leading order, the same as that of two point vortices of strengths Γ_1, Γ_2. This motion, shown by the concentric dashed circles, is about the center of vorticity of the point vortices marked O.

$$
\begin{aligned}
\frac{d\hat{D}}{dt} &= \left(\frac{\Gamma_1+\Gamma_2}{8\pi^2\hat{D}^3}\right)\sum_{k=1}^{2} A_k \frac{1-\lambda_k^2}{\lambda_k}\sin(2(\phi-\theta_k)),\\
\frac{d\phi}{dt} &= \frac{\Gamma_1+\Gamma_2}{2\pi\hat{D}^2} - \left(\frac{\Gamma_1+\Gamma_2}{8\pi^2\hat{D}^4}\right)\sum_{k=1}^{2} A_k \frac{1-\lambda_k^2}{\lambda_k}\cos(2(\phi-\theta_k)),\\
\frac{d\lambda_1}{dt} &= \lambda_1 \frac{\Gamma_2}{\pi\hat{D}^2}\sin(2(\phi-\theta_1)),\\
\frac{d\theta_1}{dt} &= \frac{\omega_1\lambda_1}{(1+\lambda_1)^2} + \left(\frac{1+\lambda_1^2}{1-\lambda_1^2}\right)\frac{\Gamma_2}{2\pi\hat{D}^2}\cos(2(\phi-\theta_1)),\\
\frac{d\lambda_2}{dt} &= \lambda_2 \frac{\Gamma_1}{\pi\hat{D}^2}\sin(2(\phi-\theta_2)),\\
\frac{d\theta_2}{dt} &= \frac{\omega_2\lambda_2}{(1+\lambda_2)^2} + \left(\frac{1+\lambda_1^2}{1-\lambda_1^2}\right)\frac{\Gamma_1}{2\pi\hat{D}^2}\cos(2(\phi-\theta_2)).
\end{aligned}
$$

One checks that this system is Hamiltonian in the canonical variables:

$$
\left(\frac{\Gamma_1\Gamma_2}{\Gamma_1+\Gamma_2}\right)\frac{\hat{D}^2}{2}, \phi, \frac{\Gamma_k A_k}{8\pi}\frac{(\lambda_k-1)^2}{\lambda_k}, \theta_k \qquad (k=1,2)
$$

with the Hamiltonian:

$$
H = \sum_{k=1}^{2}\frac{\Gamma_k^2}{8\pi}\log\left[\frac{(1+\lambda_k)^2}{4\lambda_k}\right] + \frac{\Gamma_1\Gamma_2}{2\pi}\log\hat{D} + \frac{\Gamma_1\Gamma_2}{16\pi^2\hat{D}^2}\sum_{k=1}^{2} A_k\frac{(1-\lambda_k^2)}{\lambda_k}\cos(2(\phi-\theta_k)).
$$

We make the following remarks about this system of equations:

1. The first two equations give the centroid motion and are obtained from equations (3.24) in [61] (for two patches) after introducing the polar variables $\hat{D}, \phi$:

   $$
   X_2 - X_1 = \hat{D}\cos\phi, \qquad Y_2 - Y_1 = \hat{D}\sin\phi.
   $$

   These equations clearly show that for large $\hat{D}$ or small A_1, A_2 the centroids move like two point vortices of strengths Γ_1 and Γ_2 respectively.

2. The λ_k, θ_k variables represent the patch deformation and rotation, respectively. Their equations are the same as equations (3.19) and (3.20) in [61]. They show that for large $\hat{D}$ or small A_1, A_2 (equivalently large ω_1, ω_2) the patches rotate like Kirchhoff ellipses.

3. The λ_k, θ_k equations for a patch are not explicitly dependent on the λ_k, θ_k of the other patch. The mutual interdependency comes only through the $\hat{D}$ and ϕ variables. However, there is a direct dependency on the strength of the other patch.

4. The θ_1, θ_2 equations are not defined for $\lambda_k = 1$ i.e. circular patches. As pointed out in [61] this is because these variables are not defined for circles.

We now proceed to non-dimensionalize these equations and calculate the adiabatic phase in the angle variables θ_1 and θ_2 at the end of one long time period T_l of the centroid motion.

Introduce the non-dimensional variables:

$$D = \frac{\hat{D}}{D_i}, \qquad t = \Omega \hat{t},$$

where $\Omega = (\Gamma_1 + \Gamma_2)/(A_1 + A_2)$. Ω is the mean strength over the mean area of the patches and represents the timescale of the 'unperturbed' frequency of the patches. This gives the following equations in the non-dimensional variables:

$$\begin{aligned}
\frac{dD}{dt} &= \left(\frac{\epsilon^4}{8\pi^2 D^3}\right) \sum_{k=1}^{2} \sigma_k f(\lambda_k) \sin(2(\phi - \theta_k)), \\
\frac{d\phi}{dt} &= \left(\frac{\epsilon^2}{2\pi D^2}\right) - \left(\frac{\epsilon^4}{8\pi^2 D^4}\right) \sum_{k=1}^{2} \sigma_k f(\lambda_k) \cos(2(\phi - \theta_k)), \\
\frac{d\lambda_1}{dt} &= \epsilon^2 \lambda_1 \frac{\alpha_2}{\pi D^2} \sin(2(\phi - \theta_1)), \\
\frac{d\theta_1}{dt} &= \frac{\alpha_1 g(\lambda_1)}{\bar{A}_1} + \epsilon^2 \frac{\alpha_2 h(\lambda_1)}{2\pi D^2} \cos(2(\phi - \theta_1)), \\
\frac{d\lambda_2}{dt} &= \epsilon^2 \lambda_2 \frac{\alpha_1}{\pi D^2} \sin(2(\phi - \theta_2)), \\
\frac{d\theta_2}{dt} &= \frac{\alpha_2 g(\lambda_2)}{\bar{A}_2} + \epsilon^2 \frac{\alpha_1 h(\lambda_2)}{2\pi D^2} \cos(2(\phi - \theta_2)),
\end{aligned}$$

where $\sigma_k = A_k/(A_1 + A_2)$, $\alpha_k = \Gamma_k/(\Gamma_1 + \Gamma_2)$, $f(\lambda) = (1 - \lambda^2)/\lambda$, $g(\lambda) = \lambda/(1 + \lambda)^2$ and $h(\lambda) = (1 + \lambda^2)/(1 - \lambda^2)$. The initial conditions for this system are:

$$D(0) = 1, \quad \phi(0) = 0, \quad \theta_1(0), \quad \theta_2(0), \quad \lambda_1(0), \quad \lambda_2(0).$$

We now proceed to perform a multi-scale perturbation analysis on this sytem of equations. With slow timescale $\tau = \epsilon^2 t$, seek series solutions to the variables in the form:

$$\begin{aligned}
D(t,\tau) &= \sum_{j=0}^{\infty} \epsilon^{2j} D^{(2j)}(t,\tau), \qquad \phi(t,\tau) = \sum_{j=0}^{\infty} \epsilon^{2j} \phi^{(2j)}(t,\tau), \\
\theta_k(t,\tau) &= \sum_{j=0}^{\infty} \epsilon^{2j} \theta_k^{(2j)}(t,\tau), \qquad (k = 1,2) \\
\lambda_k(t,\tau) &= \sum_{j=0}^{\infty} \epsilon^{2j} \lambda_k^{(2j)}(t,\tau), \qquad (k = 1,2).
\end{aligned}$$

Note that we consider only even powers of ϵ in the series since only even powers of ϵ appear in the coefficients of the equations.[7] The leading order functions in the series ($D^{(0)}, \phi^{(0)}$ etc.) have the same initial conditions as the variables. The initial conditions for all other functions are zero.

At leading order we get:

$\underline{O(1)}$:

$$\begin{aligned}
\frac{\partial D^{(0)}}{\partial t} &= 0 \Rightarrow \quad D^{(0)} = \tilde{D}^{(0)}(\tau), \quad \tilde{D}^{(0)}(0) = 1, \\
\frac{\partial \phi^{(0)}}{\partial t} &= 0 \Rightarrow \quad \phi^{(0)} = \tilde{\phi}^{(0)}(\tau), \quad \tilde{\phi}^{(0)}(0) = \phi(0) = 0, \\
\frac{\partial \lambda_k^{(0)}}{\partial t} &= 0 \Rightarrow \quad \lambda_k^{(0)} = \tilde{\lambda}_k^{(0)}(\tau), \quad \tilde{\lambda}_k^{(0)}(0) = \lambda_k(0), \quad (k = 1, 2) \\
\frac{\partial \theta_k^{(0)}}{\partial t} &= \frac{\alpha_k}{\sigma_k} g(\tilde{\lambda}_k^{(0)}), \\
\Rightarrow \quad \theta_k^{(0)} &= \frac{\alpha_k}{\sigma_k} g(\tilde{\lambda}_k^{(0)}) t + \tilde{\theta}_k^{(0)}(\tau), \quad \tilde{\theta}_k^{(0)}(0) = \theta_k(0), \quad (k = 1, 2)
\end{aligned}$$

$\underline{O(\epsilon^2)}$:

$$\begin{aligned}
\frac{\partial D^{(2)}}{\partial t} + \frac{d\tilde{D}^{(0)}}{d\tau} &= 0, \\
\frac{\partial \phi^{(2)}}{\partial t} + \frac{d\tilde{\phi}^{(0)}}{d\tau} &= \frac{1}{2\pi(\tilde{D}^{(0)})^2} \\
\frac{\partial \lambda_k^{(2)}}{\partial t} + \frac{d\tilde{\lambda}_k^{(0)}}{d\tau} &= \frac{\alpha_{k'} \tilde{\lambda}_k^{(0)}}{\pi(\tilde{D}^{(0)})^2} \sin\left(2(\phi^{(0)} - \theta_k^{(0)})\right), \\
\frac{\partial \theta_k^{(2)}}{\partial t} + \frac{\partial \theta_k^{(0)}}{\partial \tau} &= \frac{\alpha_k}{\sigma_k} \lambda_k^{(2)} \frac{1 - \tilde{\lambda}_k^{(0)}}{\left(1 + \tilde{\lambda}_k^{(0)}\right)^3} + \frac{\alpha_{k'} h(\tilde{\lambda}_k^{(0)})}{2\pi(\tilde{D}^{(0)})^2} \cos\left(2(\phi^{(0)} - \theta_k^{(0)})\right),
\end{aligned}$$

where $k' = 1$ if $k = 2$ and $k' = 2$ if $k = 1$.

This gives the following solutions:

$$\begin{aligned}
&\tilde{D}^{(0)}(\tau) = \tilde{D}^{(0)}(0) = 1, \quad D^{(2)} = \tilde{D}^{(2)}(\tau), \quad \tilde{D}^{(2)}(0) = 0, \\
&\tilde{\phi}^{(0)}(\tau) = \frac{\tau}{2\pi}, \quad \phi^{(2)} = \tilde{\phi}^{(2)}(\tau), \quad \tilde{\phi}^{(2)}(0) = 0, \\
&\tilde{\lambda}_k^{(0)}(\tau) = \tilde{\lambda}_k^{(0)}(0) = \lambda_k(0),
\end{aligned}$$

[7] Indeed taking a series with all (positive) integral powers of ϵ leads to an incompatibility condition with the initial conditions in the equations for the λ_k s at $O(\epsilon)$.

$$\lambda_k^{(2)} = \frac{\Gamma_{k'}\sigma_k\,(1+\lambda_k(0))^2}{2\pi\Gamma_k}\cos(2(\phi^{(0)}-\theta_k^{(0)})) + \tilde{\lambda}_k^{(2)}(\tau),$$

$$\tilde{\lambda}_k^{(2)}(0) = -\frac{\Gamma_{k'}\sigma_k\,(1+\lambda_k(0))^2}{2\pi\Gamma_k}\cos 2\theta_k(0),$$

$$\theta_k^{(2)} = -\frac{\Gamma_{k'}\sigma_k}{2\pi\Gamma_k g(\lambda_k(0))}\left(\frac{1-\lambda_k(0)}{1+\lambda_k(0)} + h(\lambda_k(0))\right)\sin(2(\phi^{(0)}-\theta_k^{(0)})) + \tilde{\theta}_k^{(2)}(\tau).$$

The last equation is obtained by imposing the solvability condition which gives the equation for the adiabatic phase $\tilde{\theta}_k^{(0)}(\tau)$. Thus, corresponding to the 'slow phase' equation (in box, §2.2) in the point vortex problems, we have here:

$$\frac{d(\theta_S)_k}{d\tau} \equiv \frac{d\tilde{\theta}_k^{(0)}(\tau)}{d\tau} = \frac{\alpha_k}{\sigma_k}\frac{1-\lambda_k(0)}{(1+\lambda_k(0))^3}\tilde{\lambda}_k^{(2)}, \qquad \tilde{\theta}_k^{(0)}(0) = \theta_k(0).$$

Note the similarity to the 'slow phase' equation in the point vortex problems. We find that here too the rate of change of the adiabatic phase depends linearly on the a second order 'slow' term of the conjugate variable. To solve for $\tilde{\lambda}_k^{(2)}$ we proceed to the $\lambda_k^{(4)}$ p.d.e. at $O(\epsilon^4)$:

$\underline{O(\epsilon^4)}$:

$$\begin{aligned}\frac{\partial\lambda_k^{(4)}}{\partial t} + \frac{\partial\lambda_k^{(2)}}{\partial\tau} &= \frac{\alpha_1}{\pi}\Big[2\lambda_k(0)\left(\phi^{(2)}-\tilde{\theta}_k^{(2)}\right)\cos(2(\phi^{(0)}-\theta_k^{(0)})) \\ &\qquad + \left(\lambda_k^{(2)} - 2\lambda_k(0)D^{(2)}\right)\sin(2(\phi^{(0)}-\theta_k^{(0)}))\Big].\end{aligned}$$

This gives the solvability condition:

$$\frac{d\tilde{\lambda}_k^{(2)}}{d\tau} = 0, \qquad \tilde{\lambda}_k^{(2)}(\tau) = \tilde{\lambda}_k^{(2)}(0) = -\frac{\Gamma_{k'}\sigma_k\,(1+\lambda_k(0))^2}{2\pi\Gamma_k}\cos 2\theta_k(0).$$

Hence,

$$(\theta_S)_k \equiv \tilde{\theta}_k^{(0)}(\tau) = -\frac{\alpha_{k'}}{2\pi}\frac{1-\lambda_k(0)}{1+\lambda_k(0)}\cos 2\theta_k(0)\cdot\tau + \theta_k(0), \tag{5.3}$$

is the slow phase term. The change in $\tilde{\theta}_k^{(0)}$ is now evaluated at the end of the time period T (to leading order) of the centroid motion. This is obtained from the solution for $\tilde{\phi}^{(0)}(\tau)$ from the condition $\tilde{\phi}^{(0)}(T) - \phi(0) = 2\pi$, giving $T = 4\pi^2$. Hence, the geometric phase for each patch is:

$$\begin{aligned}(\theta_g)_k &= \tilde{\theta}_k^{(0)}(T) - \theta_k(0), \\ &= -\alpha_{k'}\frac{1-\lambda_k(0)}{1+\lambda_k(0)}2\pi\cos 2\theta_k(0), \\ &= -\frac{\Gamma_{k'}}{\Gamma_1+\Gamma_2}\frac{1-\lambda_k(0)}{1+\lambda_k(0)}2\pi\cos 2\theta_k(0).\end{aligned}$$

Proposition 2: *The geometric phase for a system of two elliptical co-rotating vortex patches evolving according to the equations of the second-order truncated MZS model is given by:*

$$\begin{aligned}(\theta_g)_1 &= -\left(\frac{\Gamma_2}{\Gamma_1+\Gamma_2}\right)\left(\frac{1-\lambda_1(0)}{1+\lambda_1(0)}\right)2\pi\cos 2\theta_1(0),\\ (\theta_g)_2 &= -\left(\frac{\Gamma_1}{\Gamma_1+\Gamma_2}\right)\left(\frac{1-\lambda_2(0)}{1+\lambda_2(0)}\right)2\pi\cos 2\theta_2(0),\end{aligned}$$

where the Γs and λs refer to the strengths and the aspect ratios of the patches respectively.

Remarks:

1. Comparing with the results of §2.3.1, we find that the geometric phase for each of the two vortex patches is the geometric phase of a corresponding pair of point vortices in a four-vortex configuration, where the sum of the strengths of the two vortices in a pair is the patch strength, *times* the factor $(1-\lambda_k(0))/(1+\lambda_k(0))$ $(k=1,2)$. This factor can be viewed as the contribution to the geometric phase of the internal structure associated with each patch.

2. Note that to calculate the phase, the multi-scale analysis does not have to proceed to orders higher than ϵ^4 which is the order of truncation, in ϵ, of the second order model.

5.3.2 Geometric interpretation

The geometric interpretation of the phases in the patches is identical to the interpretation in the point vortex problems in Chapter 3. This is not surprising since the leading order behaviour of each patch again displays the characteristic splitting into a 'fast' term and a 'slow' term in the angle variable: $\theta_0(t,\tau)=\theta_F(t)+\theta_S(\tau)$, with no change in the conjugate aspect ratio variable. The geometric phase in each is unaffected by the higher order terms of the centroid evolution. Thus, analogous to the three- and four-vortex problems of Chapter 2, we can say that the same geometric phase is obtained for each patch by approximating the centroid motion by its leading order motion. This motion is that of two point vortices of the corresponding strengths and we thus have well defined closed orbits in the plane associated with the phases.

Thus, in analogy with the interpretation of §3.1, $U \equiv \mathbf{R}^2 - \{o\}$, where o is the center of vorticity of two point vortices of strengths $\Gamma_1(\equiv \omega_1 A_1)$ and $\Gamma_2(\equiv \omega_2 A_2)$ respectively. The motion of each point vortex is defined by $\phi(\tau)=\bar{\phi}^{(0)}(\tau)=\tau/2\pi$ and hence the common angular velocity of these vortices is $\omega_l(\phi)=d\phi/d\tau=1/2\pi$ for all orbits. Hence $\omega_l=\omega$ (referring to our notation in §3.1). Noting that $(C_l)_1 \equiv d(\theta_S)_1/d\tau$ and $(C_l)_2 \equiv d(\theta_S)_2/d\tau$ are obtained from (5.3) the geometric phase for each patch can be rewritten using (3.2) as:

$$(\theta_g)_k = -\oint\left(\frac{YdX-XdY}{X^2+Y^2}\right)\frac{\Gamma_{k'}}{\Gamma_1+\Gamma_2}\frac{1-\lambda_k(0)}{1+\lambda_k(0)}\cos 2\theta_k(0),$$

where X, Y are the Cartesian coordinates of either of the two point vortices and the contour is its closed orbit. This defines the 1-form γ_u on U:

$$(\gamma_u)_k = -\left(\frac{YdX - XdY}{X^2+Y^2}\right)\frac{\Gamma_{k'}}{\Gamma_1+\Gamma_2}\frac{1-\lambda_k(0)}{1+\lambda_k(0)}\cos 2\theta_k(0).$$

In terms of the area and the circumference of the circular point vortex orbit in U, we get:

$$\begin{aligned}(\theta_g)_k &= -\frac{2A_v}{R^2}\frac{\Gamma_{k'}}{\Gamma_1+\Gamma_2}\frac{1-\lambda_k(0)}{1+\lambda_k(0)}\cos 2\theta_k(0), \\ &= -\frac{8\pi^2 A_v}{L^2}\frac{\Gamma_{k'}}{\Gamma_1+\Gamma_2}\frac{1-\lambda_k(0)}{1+\lambda_k(0)}\cos 2\theta_k(0),\end{aligned}$$

where A_v, R and L are the quantities defined in 3.1.1.

In analogy with the interpretation in §3.2, the unperturbed configuration space for each patch (i.e. the configuration space for the Kirchhoff vortex) is diffeomorphic to S^1 and so also are the closed point vortex orbits in U. The geometric interpretation in terms of connections is therefore again given by **Theorem 1a** in Chapter 3 for the four-vortex problem with some minor rephrasing:

Theorem 3: *The geometric phase in the MZS elliptical vortex patch model for two patches of arbitrary strengths but of the same sign can be viewed as the holonomy of a flat connection on the trivial principal bundle $\pi : E = S^1 \times S^1 \times S^1 \to S^1$. E (the 3-torus) is diffeomorphic to the product space of each unperturbed vortex patch configuration space (i.e. the Kirchhoff vortex configuration space) and the closed orbit (for a given initial condition) in U corresponds to the two-point-vortex motion of the patch centroids. The fiber at each point is diffeomorphic to the product of the two configuration spaces. The vector-valued connection 1-form is given by*

$$\delta = (d\theta_1 - v_1(\phi)d\phi, d\theta_2 - v_2(\phi)d\phi),$$

where $(\theta_1, \theta_2, \phi)$ are the torus coordinates and $v_k(\phi)$ is the ratio of the constant slow phase 'angular velocity,' $d(\theta_S)_k/d\tau$, induced on patch k by the other patch, and the angular velocity, $\omega(\phi)$, of the point vortex in the closed orbit.

The extension of this to the bundle with base space U is obvious. As in the point vortex problems the connection on this bundle has non-zero curvature in general.

Reference List

[1] Y. Aharonov and J. Anandan. Phase change during a cyclic quantum evolution. *Phys. Rev. Lett.*, 58(16):1593–1596, 1987.

[2] M. S. Alber and J. E. Marsden. On geometric phases for soliton equations. *Comm. Math. Phys.* 149, 2, 1992.

[3] J. Anandan and L. Stodolsky. Some geometric considerations of Berry's phase. *Phys. Rev. D*, 35(8):2597–2600, 1987.

[4] H. Aref. Motion of three vortices. *Phys. Fluids*, 22:393–400, 1979.

[5] H. Aref. Integrable, chaotic, and turbulent vortex motion in two-dimensional flows. *Ann. Rev. Fluid Mech.* 15, 345-389, 1983.

[6] H. Aref. Chaos in the dynamics of a few vortices -fundamentals and applications. In F. I. Niordson and N. Olhoff, editors, *Theoretical and Applied Mechanics*, pages 43–68. Elsevier(North–Holland), 1985.

[7] H. Aref and N. Pomphrey. Integrable and chaotic motions of four vortices. *Phys. Lett. A*, 78:297–300, 1980.

[8] H. Aref and N. Pomphrey. Integrable and chaotic motions of four vortices.I.The case of identical vortices. *Proc. R. Soc. Lond. A*, 380:359–387, 1982.

[9] V. I. Arnold. *Dynamical Systems III, Encyclopedia of Mathematics, vol.3.* Springer-Verlag, 1988.

[10] V. I. Arnold. *Mathematical Methods of Classical Mechanics.* Springer-Verlag, second edition, 1989.

[11] M. V. Berry. Quantal phase factors accompanying adiabatic changes. *Proceedings of the Royal Society London A*, 392:45–57, 1984.

[12] M. V. Berry. Classical adiabatic angles and quantal adiabatic phase. *Journal of Physics A: Math. Gen*, 18:15–27, 1985.

[13] M. V. Berry. Quantum phase corrections from adiabatic iteration. *Proc. Roy. Soc. Lond. A*, 414:31–46, 1987.

[14] M. V. Berry. The geometric phase. *Scientific American*, December 1988.

[15] M. V. Berry. Anticipations of the geometric phase. *Physics Today*, pages 34–40, December 1990.

[16] M. V. Berry and J. H. Hannay. Classical non-adiabatic angles. *J. Phys. A:Math. Gen.*, 21:L325–L331, 1988.

[17] A. Bhattacharjee and T. Sen. Geometric angles in cyclic evolutions of a classical system. *Phys. Rev. A*, 38:4389–4394, 1988.

[18] R. Breidenthal. Structure in turbulent mixing layers and wakes using a chemical reaction. *J. Fluid Mech.*, 109:1–24, 1981.

[19] P. F. Byrd and M. D. Friedman. *Handbook of Elliptic Integrals for Engineers and Scientists.* Springer-Verlag, second (revised) edition, 1971.

[20] Y. Choquet-Bruhat, C. DeWitt-Morette and M. Dillard-Bleick. *Analysis, Manifolds and Physics.* North-Holland, 1977.

[21] G. M. Corcos and F. S. Sherman. The mixing layer : deterministic models of a turbulent flow. Part I. Introduction and the two-dimensional flow. *J. Fluid Mech.*, 139:29–65, 1984.

[22] G. S. Deem and N. J. Zabusky. Vortex waves: stationary "V states," interactions, recurrence, and breaking. *Phys. Rev. Lett.*, 40(13):859–862, 1978.

[23] M. P. do Carmo. *Differential Forms and Applications.* Universitext, Springer-Verlag, 1994.

[24] R. M. Everson and K. R. Sreenivasan. Accumulation rates of spiral-like structures in fluid flows. *Proc. R. Soc. Lond. A*, 437:391–401, 1992.

[25] J. C. Garrison. Adiabatic perturbation theory and Berry's phase. *Lawrence Livermore National Lab.,preprint*, (UCRL-94267), March 1986.

[26] A. Gilbert. Spiral structures and spectra in two-dimensional turbulence. *J. Fluid Mech.*, 193:475–497, 1988.

[27] H. Goldstein. *Classical Mechanics.* Addison-Wesley, Reading, Mass., 1980.

[28] S. Golin. Existense of the Hannay angle for single-frequency systems. *J. Phys. A : Math. Gen.*, 21:4535–4547, 1988.

[29] S. Golin. Can one measure Hannay angles? *J. Phys. A:Math. Gen.*, pages 4573–4580, 1989.

[30] S. Golin, A. Knauf and S. Marmi. The Hannay angles : geometry, adiabaticity and an example. *Comm. Math. Phys.*, 123:95–122, 1989.

[31] S. Golin, A. Knauf and S. Marmi. Hannay angles and classical perturbation theory. In J. M. Luck, P. Moussa, and M. Waldschmidt, editors, *Number Theory and Physics*, Lecture Notes in Physics. Springer : Berlin, 1990.

[32] S. Golin and S. Marmi. Symmetries,Hannay angles and precession of orbits. *Europhysics Letters*, 8:399–404, 1989.

[33] S. Golin and S. Marmi. A class of systems with measurable Hannay angles. *Nonlinearity*, 3:507–518, 1990.

[34] E. Gozzi and W. D. Thacker. Classical adiabatic holonomy and its canonical structure. *Phys. Rev. D*, 35(8):2398–2406, 1987.

[35] H. W. Guggenheimer. *Differential Geometry.* Dover Publications, New York, 1977.

[36] A. Guichardet. On rotation and vibration motions of molecules. *Ann. Inst. Henri Poincare*, 40(3):329–342, 1984

[37] J. Hannay. Angle variable holonomy in adiabatic excursion of an integrable Hamiltonian. *J. Phys. A:Math.Gen.*, 18:221–230, 1985.

[38] C. M. Ho and P. Huerre. Perturbed free shear layers. *Ann. Rev. Fluid Mech.*, 16:365–424, 1984.

[39] T. Iwai. A gauge theory for the quantum planar three-body problem. *J. Math. Phys.*, 28(4):964–974, 1987.

[40] J. Jimenez. On the visual growth of a turbulent mixing layer. *J. Fluid Mech.*, 96:447–460, 1980.

[41] T. Kato. On the adiabatic theorem of quantum mechanics. *Phys. Soc. Japan*, 5, 1950.

[42] J. Kevorkian and J. D. Cole. *Multiple Scale and Singular Perturbation Methods.* Appl. Math Sci 114, Springer Verlag 1996.

[43] K. M. Khanin. Quasi-periodic motions of vortex systems. *Physica D*, 4:261–269, 1982.

[44] A. Khein and D. F. Nelson. Hannay angle study of the Foucault pendulum in action-angle variables. *Am. J. Phys.*, 61(2):170–174, 1993.

[45] S. Kida. Motion of an elliptical vortex in a uniform shear flow. *J. Phys. Soc. Japan*, 50(10), 3517–3520, 1981.

[46] P. S. Krishnaprasad. Eulerian many-body problems. *Cont. Math. AMS*, 97:187–208, 1989.

[47] I. A. Kunin, F. Hussain, X. Zhou and S. J. Prishepionok. Centroidal frames in dynamical sytems. Part 1: Point vortices. *Proc. R. Soc. Lond. A*, 439(1907):441–463, 1992.

[48] H. Lamb. *Hydrodynamics.* Dover, New York, sixth edition, 1932.

[49] M. Levi. Geometric phases in the motion of rigid bodies. *Arch. Rational Mech. Anal.*, 122:213–219, 1993.

[50] T. S. Lundgren. Strained spiral vortex model for turbulent fine structure. *Phys. Fluids*, 25 (12):2193–2203, 1982.

[51] B. Marcu, E. Meiburg and P. K. Newton. Dynamics of heavy particles in a Burgers vortex. *Phys. Fluids*, 7(2):400–410, 1995.

[52] J. E. Marsden, R. Montgomery and T. S. Ratiu. Cartan-Hannay-Berry phases and symmetry. *Cont. Math. AMS*, 97:279–295, 1989.

[53] J. E. Marsden, R. Montgomery and T. S. Ratiu. Reduction, symmetry and phases in mechanics. *AMS Memoirs*, 436, 1990.

[54] J. E. Marsden, O. M. O'Reilly, F. J. Wicklin and B. W. Zombro. Symmetry, stability, geometric phases and mechanical integrators (Part II). *Nonlinear Science Today*, Vol. 1, No. 1, 1991.

[55] J. E. Marsden and T. S. Ratiu. *Introduction to Mechanics and Symmetry.* Springer-Verlag, 1994.

[56] J. E. Marsden and J. Scheurle. Pattern evocation and geometric phases in mechanical systems with symmetry. *Dyn. and Stab. of Systems*, 10:315–338, 1995.

[57] J. E. Marsden, J. Scheurle and J. Wendlandt. Visualization of orbits and pattern evocation for the double spherical pendulum. *ICIAM 95: Mathematical Research, Academie Verlag, Ed. by K. Kirchgässner, O. Mahrenholtz and R. Mennicken*, 87:213–232, 1996.

[58] J. Marsden and A. Weinstein. Coadjoint orbits, vortices, and Clebsch variables for incompressible fluids. *Physica D*, 7:305–323, 1983.

[59] E. Meiburg, P. K. Newton, N. Raju and G. Reutsch. Unsteady models for the nonlinear evolution of the mixing layer. *Phys. Rev. E*, 52:1639–1657, August 1995.

[60] M. V. Melander, A. S. Styczek and N. J. Zabusky. Elliptically desingularized model for the two-dimensional Euler equations. *Phys. Rev. Lett.*, 53(13):1222–1225, 1984.

[61] M. V. Melander, N. J. Zabusky and A. S. Styczek. Moment model for vortex interactions. Part I. *J. Fluid Mech.*, 167:95–115, 1986.

[62] H. K. Moffat. The degree of knottedness of tangled vortex lines. *J. Fluid Mech*, 35:117–129, 1969.

[63] H. K. Moffat. Spiral structures in turbulent flow. In T. Dracos and A. Tsinobar, editors, *New Approaches and Concepts in Turbulence*, 121–131, 1993.

[64] R. Montgomery. The connection whose holonomy is the classical adiabatic angles of Hannay and Berry and its generalization to the non-integrable case. *Comm. Math. Phys.*, 120:269–294, 1988.

[65] R. Montgomery. Optimal control of deformable bodies and its relation to gauge theory. *The Geometry of Hamiltonian Systems*, proceedings of a workshop held in June 1988 at MSRI, Berkeley. T. S. Ratiu ed., Springer-Verlag, 1990

[66] R. Montgomery How much does the rigid body rotate? A Berry's phase from the 18th century. *Am. J. Phys.*, 59(5):394-398, 1991

[67] R. Montgomery. The geometric phase of the three-body problem. *Nonlinearity*, 9:1341–1360, 1996.

[68] P. J. Morrison and J. M. Greene. Noncanonical Hamiltonian density formulation of hydrodynamics and ideal magnetohydrodynamics. *Phys. Rev. Lett.*, 45(10):790–794, 1980; 48(8):569, 1982.

[69] P. K. Newton. Hannay-Berry phase and the restricted three-vortex problem. *Physica D*, 79:416–423, 1994.

[70] P. K. Newton and B. N. Shashikanth. Vortex problems, rotating spiral structure and the Hannay-Berry phase. *Second International Workshop on Vortex Flows and Related Numerical Methods, Montreal, Canada, 1995. ESAIM Proceedings, Soc. Math. Appl. Indust., Inst. Henri Poincare, 1996.*

[71] R. G. Newton. S matrix as geometric phase factor. *Phys. Rev. Lett.* 72,9, 1994.

[72] E . A. Novikov and Y. B. Sedov. Stochastic properties of a four-vortex system. *Sov. Phys. JETP*, 48:440–444, 1978.

[73] P. J. Olver. A nonlinear Hamiltonian structure for the Euler equations. *J. Math. Anal. Appl.*, 89:233–250, 1982.

[74] J. Oprea. Geometry and the Foucault pendulum. *American Mathematical Monthly*, 102(6):515–522, June-July 1995.

[75] E. A. Overman and N. J. Zabusky. Coaxial scattering of Euler-equation translating V states via contour dynamics. *J. Fluid Mech.*, 125:187–202, 1982.

[76] E. A. Overman II and N. J. Zabusky. Evolution and merger of isolated vortex structures. *Phys. Fluids*, 25(8):1297–1305, 1982.

[77] C. Pozrikidis and J. J. L. Higdon. Nonlinear Kelvin-Helmholtz instability of a finite vortex layer. *J. Fluid Mech.*, 157:225–263, 1985

[78] J. M. Robbins and M. V. Berry. The geometric phase for chaotic sytems. *Proc. R. Soc. Lond. A*, 436:631–661, 1992.

[79] F. A. Roberts. *Effects of a periodic disturbance on structure and mixing in turbulent shear layers and wakes.* PhD thesis, Caltech., GALCIT, 1985.

[80] P. G. Saffman. *Vortex Dynamics.* Cambridge Monographs on Mechanics and Applied Mathematics. Cambridge University Press, 1992.

[81] J. A. Sanders and F. Verhulst. *Averaging Methods in Nonlinear Dynamical Systems*, volume 59 of *Applied Mathematical Sciences.* Springer-Verlag, 1985.

[82] C. G. Schroer. Geometric 'tempus' for a class of ergodic classical systems. *J. Phys. A: Math. Gen.*, 29:3289–3297, 1996.

[83] B. F. Schutz. *Geometrical Methods of Mathematical Physics.* Cambridge University Press, 1980.

[84] A. Shapere and F. Wilczek. Self-propulsion at low Reynolds number. *Phys. Rev. Lett.*, 58:2051–2054, 1987.

[85] A. Shapere and F. Wilczek. Geometry of self-propulsion at low Reynolds number. *J. Fluid Mech.*, 198:557–585, 1989.

[86] A. Shapere and F. Wilczek, editors. *Geometric Phases in Physics.* World Scientific,Singapore, 1989.

[87] B. N. Shashikanth and P. K. Newton. Vortex motion and the geometric phase. Part I: Basic configurations and asymptotics. *(to appear) J. Nonlinear Science*, 1998.

[88] B. N. Shashikanth and P. K. Newton. Vortex motion and the geometric phase. Part II: Slowly varying spiral structures. *(to appear) J. Nonlinear Science*, 1998.

[89] T. G. Sheperd. Symmetries, conservation laws and Hamiltonian structure in geophysical fluid dynamics. *Advances in Geophysics*, 32:287–338, 1990.

[90] B. Simon. Holonomy, the quantum adiabatic theorem, and Berry's phase. *Phys. Rev. Lett.*, 51(24):2167–2170, 1983.

[91] L. Sirovich. *Techniques of Asymptotic Analysis.* Applied Mathematical Sciences, Vol.2, Springer-Verlag 1971.

[92] J. L. Synge. On the motion of three vortices. *Can. J. Math.*, 1:257–270, 1949.

[93] J. Synge and B. Griffith. *Principles of Mechanics.* McGraw-Hill, New York, 1959.

[94] C. von Westenholz. *Differential forms in Mathematical Physics.* North-Holland, 1981.

[95] F. Wilczek and A. Shapere. Efficiencies of self-propulsion at low Reynolds number. *J. Fluid Mech.*, 198:587–599, 1989.

[96] C. D. Winant and F. K. Browand. Vortex pairing : the mechanism of turbulent mixing layer growth at moderate Reynolds number. *J. Fluid. Mech.*, 63:237–255, 1974.

[97] Y. Wu. On the quantization of the planar N-point vortex problem. *J. Math. Phys.*, 34(6):2342–2352, 1993.

[98] R. Yang and P. S. Krishnaprasad. On the dynamics of floating four bar linkages. *Proc. 28th IEEE Conf. on Decision and Control*, 1990.

[99] L. Zannetti and P. Franzese. Advection by a point vortex in a closed domain. *Eur. J. Mech. B/Fluids*, 12, no. 1, 43-67, 1993.

[100] L. Zannetti and P. Franzese. The non-integrability of the restricted problem of two vortices in closed domains. *Physica D 76*, 99-109, 1994.

[101] S. L. Ziglin. Nonintegrability of a problem on the motion of four point vortices. *Sov. Math. Dokl.*, pages 296–299, 1980.

[102] J. W. Zwanziger, M. Koenig and A. Pines. Berry's phase. *Ann.Rev. Phys. Chem.*, 41:601, 1990.

IMAGE EVALUATION TEST TARGET (QA-3)

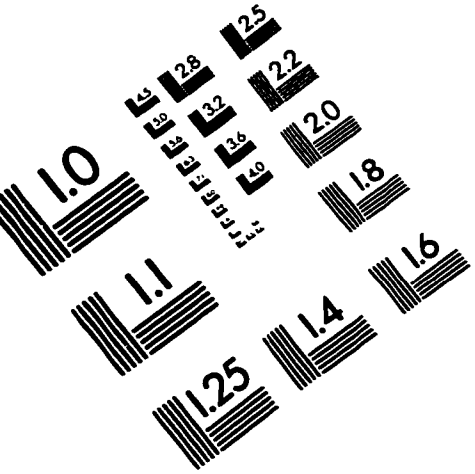

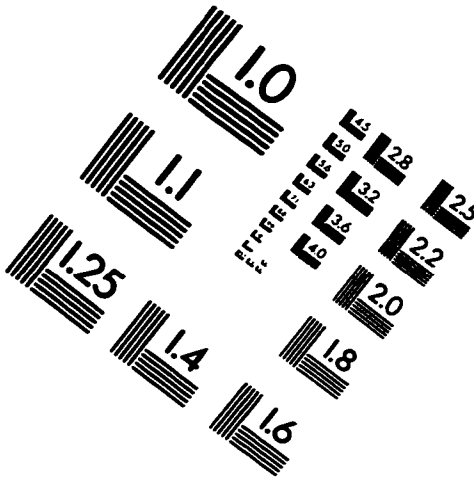

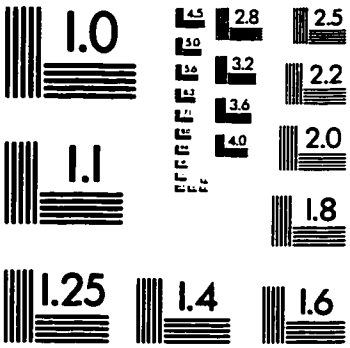

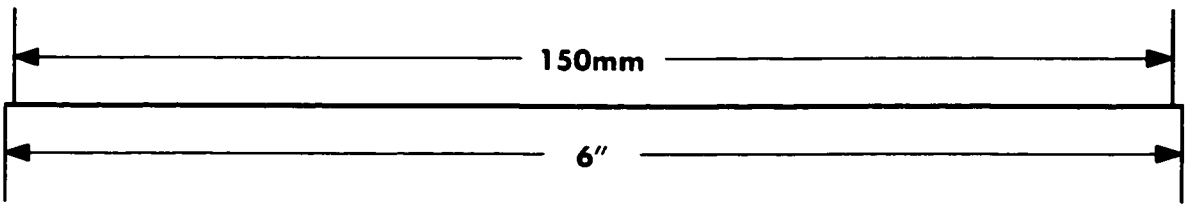

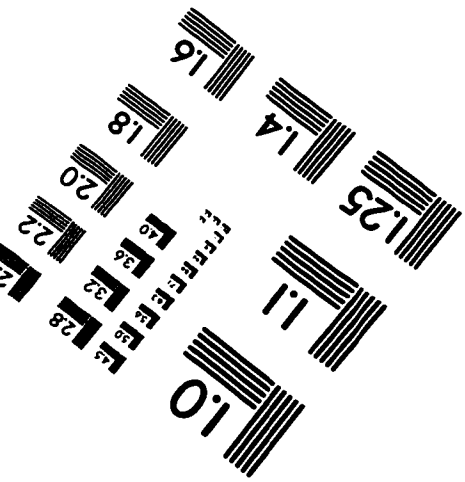

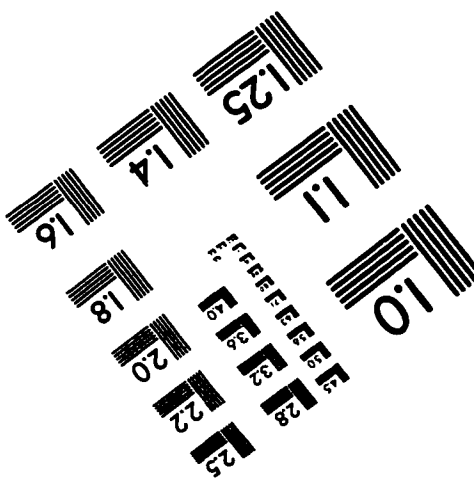

APPLIED IMAGE, Inc
1653 East Main Street
Rochester, NY 14609 USA
Phone: 716/482-0300
Fax: 716/288-5989